PERFORMANCE ANALYSIS OF PRECODING SCHEMES FOR MASSIVE MULTIPLE-INPUT MULTIPLE-OUTPUT (MIMO) SYSTEMS

by

Nompumelelo Innocentia Chili

(20512079)

Submitted in fulfilment of the requirements for the degree of:

MASTER OF ENGINEERING

in the

DEPARTMENT OF ELECTRONIC AND COMPUTER ENGINEERING,

FACULTY OF ENGINEERING AND THE BUILT ENVIRONMENT

at the

DURBAN UNIVERSITY OF TECHNOLOGY

March 2024

Supervisor: Dr. E. Mukubwa

Co-Supervisor: Dr. N. Pillay

PREFACE

My name is Nompumelelo Innocentia Chili, and I am delighted to present this thesis entitled "Performance Analysis of Precoding Schemes for Massive Multiple-Input Multiple-Output (MIMO) Systems." This work represents the culmination of my academic journey at the Electronic and Computer Engineering (ECE) Department, Durban University of Technology (DUT), reflecting the extensive research, dedication, and passion invested in exploring the intricate facets of pilot contamination in massive MIMO systems.

This work aims to study various precoding schemes to analyse the effect of pilot contamination on the performance of a massive MIMO system. Throughout this endeavour, I have received invaluable guidance, encouragement, and support from my supervisors. Supervisors Dr. E. Mukubwa and Dr. N. Pillay, whose expertise and mentorship have been instrumental in shaping this research. I am also grateful for the assistance and mentorship of Mr. Christopher Mcineka, whose insights have profoundly influenced the development of this work. Furthermore, I acknowledge the financial support from the DSI-Space Science Centre that enabled the execution of this study.

The thesis is organized into five chapters, each contributing distinctly to the overall argument and research objectives. Chapter 1 provides the preliminaries to the study. Chapter 2 focuses on the literature review, while subsequent chapters delve into the research methodology, the results and discussion, and finally the conclusion. Each chapter's progression contributes to the cohesive narrative of the thesis, advancing the argument and validating the research objectives.

As readers embark on this journey through "Performance Analysis of Precoding Schemes for Massive Multiple-Input Multiple-Output (MIMO) Systems," I anticipate their engagement with an open mind and shared enthusiasm for exploration. I invite readers to delve into this work, fostering a sense of shared inquiry and discovery.

Thank you for joining me on this intellectual expedition, and I hope the insights within these pages resonate and contribute to our collective knowledge.

Nompumelelo Innocentia Chili

Durban University of Technology

March 2024

DECLARATION 1: SUPERVISORS

According to the contents of this thesis, as the candidate's supervisor, I agree to the submission of the thesis.

Dr. E. Mukubwa

(Main supervisor)

Date: 19 March 2024

Dr. N. Pillay

(Co-supervisor)

Date: 19 March 2024

DECLARATION 2: PLAGIARISM

I, Nompumelelo Innocentia Chili, student number 20512079, the undersigned, declare that:

1. The Research presented in this thesis is my original work except where otherwise indicated.
2. This thesis has not been submitted for degree or examination at any other university.
3. This thesis does not contain other persons' data, images, graphs, or other information unless specifically acknowledged as being sourced from other persons.
4. This thesis does not contain other persons' writing unless specifically acknowledged as being sourced from other researchers. Where other written sources have been quoted, then:
    a) Their words have been re-written, but the general information attributed to them has been referenced.
    b) Where their exact words have been used, their writing has been placed inside quotation marks and referenced.
5. Where I have reproduced a publication of which I am an author, co-author or editor, I have indicated in detail which part of the publication was actually written by myself alone and have fully referenced such publications.
6. This thesis does not contain text, graphics, or tables copied and pasted from the Internet unless expressly acknowledged, and the source is detailed in the dissertation and the reference sections.

[redacted]
Nompumelelo Innocentia Chili

March 2024

DECLARATION 3: PUBLICATIONS

I, Nompumelelo Innocentia Chili, student number 20512079, declare that the following publication came of this thesis.

1) Nompumelelo Chili, Emmanuel Mukubwa and Nelendran Pillay, "Performance comparison of Linear and Nonlinear Precoding for massive MIMO." 3rd International Conference on Electrical, Computer and Energy Technologies (ICECET2023), November 16-17, 2023, Cape Town, South Africa. DOI: 10.1109/ICECET58911.2023.1038932

DEDICATION

This work is dedicated to my family, my husband, Judge Nkosinathi Chili, and my kids Ziphelele and Skhathisakhe. My sisters Nelisiwe, Nomfundo and Amahle Ngcobo and Samkelisiwe Chili.

ACKNOWLEDGEMENTS

I express my heartfelt gratitude to all whose support and guidance contributed to the successful completion of this project. First and foremost, I am deeply indebted to Mr. Christopher Mcineka, whose mentorship, encouragement, and invaluable insights have been instrumental in shaping my research journey. Your guidance and unwavering support have immensely enriched this project.

I sincerely thank Dr. E. Mukubwa for his expertise, guidance, and continuous support throughout this endeavour. Your invaluable feedback and constructive criticism significantly contributed to the refinement of this work. I am also grateful to Dr. N. Pillay for his guidance and valuable input, which greatly enriched the depth and quality of this project.

I am indebted to my family for their unwavering love, encouragement, and understanding during this research. Their constant support and belief in my endeavours have been a source of strength. My heartfelt thanks go to my friends and colleagues for their encouragement, stimulating discussions, and unwavering support throughout this project.

I would like to acknowledge the financial support received from the DSI-Space Science Centre at Durban University of Technology. Their support provided the necessary resources and opportunities to conduct this research.

I would like to acknowledge the affiliation with Durban University of Technology, the Department of Electronic and Computer Engineering (ECE), and the Department of Electrical Power Engineering (EPE) for providing the conducive environment and resources essential for the successful completion of this project.

Lastly, I express my heartfelt gratitude to God Almighty. It is by His will that I have managed to produce this work.

ABSTRACT

The transformative impact of Multiple-Input Multiple-Output (MIMO) technology on terrestrial wireless networks is indisputable, revolutionizing applications ranging from social media (WhatsApp, Twitter, Instagram, Facebook) to video streaming and online gaming. Massive MIMO (M-MIMO), an advanced system scaling up MIMO with hundreds of antennas, has emerged to meet escalating demands for capacity and data throughput. This technology serves multiple user equipment (UEs) concurrently, encompassing mobile phones, tablets, smart cars, smartwatches, smart homes, and intelligent industries, utilising the same time-frequency resources. Despite its superior performance, M-MIMO faces challenges, notably pilot contamination (PiC). PiC occurs when identical pilot sequences interfere across home and adjacent cells, leading to channel estimation errors and degraded system performance.

This study investigates the performance of linear and non-linear precoding schemes for mitigation of pilot contamination. The main focus is assessing the efficacy of various precoding strategies in the presence of channel interference errors and explore their impact on critical performance metrics. The recommendation in terms of performance comparison of M-MIMO by this research may be used to further optimise the performance of the M-MIMO systems. Theoretical analyses and simulations are employed to unravel the complexities of precoding schemes, providing a nuanced understanding of their strengths, limitations, and practical implications in wireless communication scenarios.

The research confronts challenges encompassing computational complexity, realistic channel modelling, imperfect channel state information (CSI), trade-offs, practical validations, interference management, and standardisation. These challenges necessitate interdisciplinary collaboration, advanced modelling techniques, and realistic simulations in the context of analysing the performance of M-MIMO precoding schemes.

The study employs precoding structures such as Zero-Forcing (ZF), Minimum Mean Square Error (MMSE), Neumann Series Approximation (NSA), Lattice Reduction-Lenstra-Lenstra-Lovász (LR-LLL), and Tomlinson-Harashima Precoding (THP) for simulation, comparison, and analysis in the context of M-MIMO. The chosen metrics for evaluation are the bit-error

rate (BER), spectral efficiency (SE), signal-to-noise ratio (SNR) and Achievable Sum Rate (ASR).

The outcomes of this research unequivocally demonstrate the superior performance of nonlinear precoding over linear precoding in the context of M-MIMO systems. The analysis, conducted using MATLAB® simulations, reveals that nonlinear precoding strategies outperform their linear counterparts in mitigating pilot contamination, addressing channel estimation errors, and enhancing overall system performance.

TABLE OF CONTENTS

LIST OF FIGURES

LIST OF ABBREVIATIONS

4IR	fourth industrial revolution
5G	fifth generation
3GPP	3rd generation partnership project
AI	artificial intelligent
AOA	angle of arrival
ASR	achievable sum rate
AP	access point
AWGN	additive white Gaussian noise
BER	bit error rate
BF	beamforming
BS	base station
BSs	base stations
CAGR	compound annual growth rate
CC	channel capacity
CFs	correlation functions
CSI	channel state information
CSM	Cholesky and Sherman-Morrison
dB	decibel
DoF	degree of freedom
DL	downlink
DPC	dirty paper coding
EE	energy efficiency
FDD	frequency division duplex
GBSM	geometric-based stochastic models
GSCM	geometric-based stochastic channel model
Gbps	gigabit per second
GHz	gigahertz
HL-THP	hybrid-linear Tomlinson-Harashima precoding
i.i.d	independent and identically distributed
IoT	internet-of-things
IRS	intelligent reflecting surface

KBSM	Kronecker based stochastic model
LOS	line of sight
LTE	long-term evolution
M2M	machine–to–machine
MF	matched filter
MIMO	multiple-input multiple-output
MMSE	minimum mean square error
mmWave	millimetre wave
MS	Microsoft
MSE	mean square error
MRT	maximum ration transmission
NLOS	non-line of sight
NMSE	normalized mean square error
PZF	phased zero forcing
QAM	quadrature amplitude modulation
QoS	quality of service
RF	radio frequency
RZF	regularized zero-forcing
SDMA	space division multiple access
SE	spectral efficiency
SINR	signal-to-interference-and-noise ratio
SNR	signal-to-noise ratio
SVD	single-value decomposition
TDD	time division duplex
THP	Tomlinson-Harashima precoding
TPE	truncated polynomial estimation
UL	uplink
UE	user equipment
VP	vector perturbation
ZF	zero forcing

LIST OF NOTATIONS

$\mathbf{X}$	Capital bold letter represent matrix
$\boldsymbol{x}$	Small bold letter represents vector
$\boldsymbol{x}_i$	ith entry of vector $\boldsymbol{x}$
x	Small italic letter represents scalar
$\mathbf{h}_{i,j}$	$(i,j)th$ entry of matrix
$(\cdot)^T$	The transpose operator
$(\cdot)^H$	The Hermitian transpose operator
$(\cdot)^*$	Complex conjugate operator
$(\cdot)^{-1}$	The inverse matrix
$tr(\cdot)$	Trace function
$d\text{iag}(\cdot)$	Diagonal elements of a matrix
$\lvert\cdot\rvert$	Absolute
$\lVert\cdot\rVert$	Denotes the Euclidean norm
$\Re\{\cdot\}$	Real part of a complex number
$\Im\{\cdot\}$	Imaginary part of a complex number
$\mathbb{T}$	Channel coherent time
$\mathcal{O}(K)$	Big-O notation
$\mathbb{E}[\cdot]$	Denote expectation operator
t	Number of iterations
$\sim$	Approximate
$\cong$	Approximately equal to
$\sum(\cdot)$	Summation
I	The identity matrix
$\mathbb{C}^{M\times K}$	The set of complex matrices with M rows and K columns.

1 Introduction

1.1 Introduction

Fifth-generation (5G) wireless systems is one of the emerging drivers in the fourth industrial revolution (4IR), including robotics, quantum computing, artificial intelligence, and the Internet of Things (IoT). The 4IR is characterised by a combination of technologies collectively called cyber-physical systems, where the currently human-dominated wireless communication is extended to the state-of-the-connected world of humans and objects. The 4IR building components, such as 5G networks, had to be swiftly adopted as the high demand for data rates and reliable links increased rapidly.

The high demand for 5G implementation surged during and post the global COVID-19 pandemic [1]. The pandemic introduced the new normal, wherein most private, government and public business sectors had to operate remotely, relying on virtual communication. Platforms like MS Teams, ZOOM, Skype, Moodle, and video calling, to mention a few, were daily tools for communication; meanwhile, the quality of service (QoS) in real-time was essential.

Cisco® [2] had anticipated that the initial deployment of 5G networks would be completed by approximately 2021, boasting an impressive peak data rate of 10 Gbps. High data rates offer users a seamless connectivity experience similar to fibre-optic connections. Fifth-generation wireless networks aim to increase the data rate, reduce latency, reduce energy and costs, have higher system capacity, and have massive device connectivity. Multiple-Input Multiple-Output (MIMO) is a foundational methodology that makes 5G possible [3].

MIMO has been crucial in revolutionising terrestrial wireless networks. MIMO systems typically utilise a small number of antennas. Massive MIMO (M-MIMO) is a rapidly growing technology that expands upon MIMO but faces challenges such as pilot contamination. Therefore, this study focuses on analysing the influence of pilot contamination on the efficacy of M-MIMO system. Various precoding schemes are

examined through MATLAB simulations to achieve precise results using metrics for evaluation such as the bit-error rate (BER), spectral efficiency (SE), signal-to-noise ratio (SNR) and Achievable Sum Rate (ASR).

1.2 Background and Motivation

Over the last few years, there has been a substantial rise in the count of wireless users, leading to a considerable volume of data that requires efficient and highly reliable management [4]. The vast number of Internet of Things (IoT) gadgets, which enable advanced healthcare, automated homes, and efficient energy systems, also affect data flow. Cisco® [2] predictions were 50 billion linked devices by 2020, over 70% of the world equipped with mobile connectivity by 2023 and mobile users projected to increase from 5.1

Figure 1.1 Expected growth of global Internet usage [2]

billion in 2018 to 5.7 billion in 2023. Figure 1.1 depicts the number of people with internet access over the 2018-2023 range. The author predicts 66%, which is 5.3 billion internet users worldwide by 2023, up from 3.9 billion in 2018.

By 2023, IP-connected devices will outnumber people three times over. Networked devices were expected to reach 29.3 billion by 2023, up from 18.4 billion in 2018. Machine-to-Machine (M2M) applications, including smart metres, healthcare monitoring, video

surveillance, transportation, package or asset tracking, drive device and connection growth. According to Figure 1.2, the percentage of M2M connections is projected to increase from 33% in 2018 to 50%, resulting in 14.7 billion M2M connections. Connected home applications are projected to hold almost half, or 48%, of the M2M share.

Additionally, connected car applications are anticipated to experience the fastest growth, with a compound annual growth rate (CAGR) of 30% over the forecast cycle from 2018 to 2023 [2]. Global mobile devices were predicted to rise from 8.8 billion in 2018 to 13.1 billion in 2023. Roughly 1.4 billion devices will be 5G capable. The existing MIMO technologies used in 4G/LTE (Long Term Evolution) networks strain to handle the massive data traffic surge, compromising speed and consistency. Hence, the 5G network is exploring the implementation of M-MIMO technology as a prospective strategy to tackle the obstacles presented by the increasing data transfer and user demands [2].

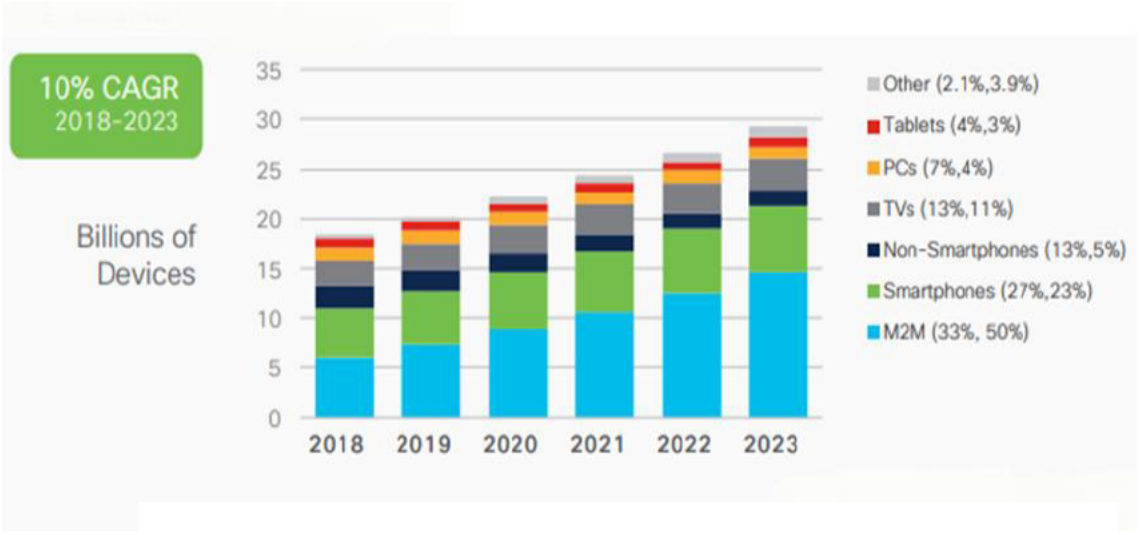

Figure 1.2 Expected growth for global devices and connection [2]

M-MIMO encounters challenges, particularly pilot contamination (PiC), despite its exceptional performance [5, 6]. This phenomenon arises when identical pilot sequences cause interference between home and adjacent cells, resulting in errors in channel estimation and a decline in system performance. This dissertation conducts a performance comparison of linear and non-linear precoding, which is an integral part of M-MIMO interference reduction, using MATLAB simulation platform.

1.3 Research problem statement

The growing need for extensive fixed broadband and wireless communication services, along with their availability, has led to the rapid expansion of satellite networks. This expansion is driven by the crucial need to provide ubiquitous connectivity, especially in remote and underserved areas where traditional terrestrial infrastructure may be impractical. Despite significant advancements, challenges persist in optimising the performance and efficiency of satellite networks. Key issues include seamless integration with terrestrial networks, scalability, and effective management of network resources. Satellite networks offer built-in multicast capabilities, robust support for terrestrial backhaul networks, and seamless radio coverage for mobile (3G to 5G), LTE, Wi-Fi, portable, and stationary receivers. MIMO systems have played an integral role in transforming terrestrial wireless networks.

M-MIMO is the technique used to upscale MIMO, however its experience challenges such as PiC due to estimation error [4]. The propagated signal is often impaired by known and unknown interferences, with intra-cell and inter-cell interference being common channel impairments. Pilot contamination occurs when the transmitted signal from the intended user equipment (UE) encounters interference from other pilot signals transmitted by different UEs at each access point (AP). This results in a decline in the accuracy of the estimated channel, thereby affecting the system's effectiveness. Figure 1.3 depicts the uplink system in a Massive MIMO (M-MIMO) setup and highlights the effects of pilot contamination

within such a system. The dotted lines indicate various pilot signals from different users directed towards the base station.

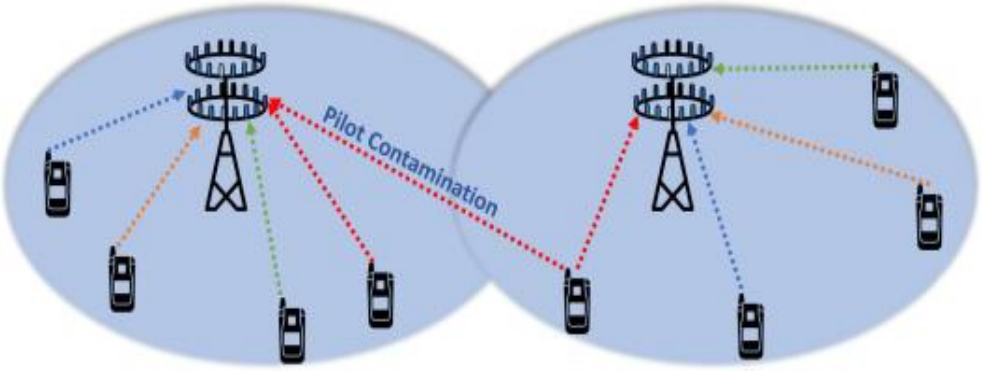

Figure 1.3 Pilot contamination in a massive MIMO system [4]

One of the most critical components in addressing interference within a channel in M-MIMO systems is precoding, which plays a key role in various performance aspects and designs [7]. Precoding at the Base Station (BS) is essential to ensure reliable communication. PiC is detailed in section 2.4

1.4 The aims and objectives of research

This work aims to study various precoding schemes to analyse the influence of pilot contamination on the performance of a M-MIMO approach, employing MATLAB® simulations. The study aims to achieve the following objectives:

1. To compare and analyse both linear and nonlinear precoding schemes.
2. Modelling channels using the Rayleigh fading model at time division duplex (TDD) within similar time-frequency resources.
3. Perform a comparison of precoding schemes based on the bit-error rate and spectral effectiveness.
4. Combine the model to conduct the analysis based on chosen precoding schemes for the perfect and imperfect channel state information (CSI).
5. Compare spectral efficiency (SE) and bit-error rate (BER) of the studied models.

1.5 Research questions

The study aims to answer the following questions:

1. What is the effectiveness of linear and nonlinear precoding schemes when comparing their Bit Error Rate (BER) and Spectral Efficiency (SE) in M-MIMO systems?
2. How can various precoding schemes be strategically integrated with channel estimation techniques to address the issue of pilot contamination?

1.6 Research contributions

The following is a list of contributions made to the research area:

1. Analysis of precoding schemes will be investigated, and the impact of PiC on the operation of massive MIMO systems will be investigated.
2. MATLAB® simulations examining the effects of precoding schemes will be provided, detailing a comprehensive and coherent evaluation.
3. The 5G network's performance results will be evaluated by comparing its behaviour with perfect and imperfect CSI, providing an understanding of the network's capabilities.

1.7 Limitations

Following are other limitations that may affect the practical implementations of this work:

1. Real-world systems often face challenges obtaining accurate CSI due to channel estimation errors, quantization, and feedback limitations. The study may not fully capture the impact of these imperfections on precoding performance.

2. Using theoretical channel models may not fully capture the complexities of practical hardware wireless environments.

1.8 Structure of the dissertation

This thesis is organised into five chapters:

- Chapter 1 introduces the work to be undertaken, providing background and motivation for the study. The research problem statement, as well as the aims and objectives of the research, are highlighted. The research question, contributions, and limitations are also thoroughly examined and addressed.

- Chapter 2 focuses on the literature survey. This section examines the evolution of wireless networks, explores the evolution of M-MIMO, discusses pilot contamination and precoding schemes, analyses various channel models, evaluates performance metrics, and presents the conclusion.

- Chapter 3 presents the methodology through the utilisation of specific precoding schemes. The simulation models the algorithms for both optimal and impaired channels. Combining the modelled channel to perform the analysis of perfect and imperfect CSI.

- Chapter 4 discusses the findings and subsequent conversations.

- Chapter 5 concludes the thesis. This chapter includes a synopsis of all the preceding chapters, the comprehensive findings of the entire work and the possible future research extension.

2 Literature Review

2.1 Introduction

This chapter reviews the literature on wireless network evolution, massive MIMO technology, pilot contamination, precoding schemes, channel modelling, and accuracy validation methods. It discusses the development of 1G to 5G technologies, M-MIMO's potential, mitigation techniques for pilot contamination, implementation strategies in linear and nonlinear systems, and evaluation of precoding schemes' effectiveness using metrics like signal-to- interference-plus-noise ratio (SINR), SE, BER, and channel capacity (CC). The synthesis provides a comprehensive summary of the current state of knowledge and potential innovative contributions.

2.2 Evolution of wireless network

Developing wireless communication systems has been fascinating, demonstrating significant technological breakthroughs. The growing need for enhanced data rates, expanded network capacity, and an improved user experience have propelled the development of wireless networks. Several studies and research manuscripts have extensively examined the progression of wireless communication from single-input single-output (SISO) to M-MIMO, which have highlighted the advantages and challenges linked to this shift [4], [8-12]. Wireless communication systems have progressed through different stages of development, with each stage building upon the accomplishments and obstacles encountered in the previous technologies.

The critical challenges in the progression of wireless communication from (SISO) 1G to (M-MIMO) 5G and beyond include the necessity to maximise transmission rate to meet the growing demand for multimedia and safety applications [13]. Additionally, there is a need for expandable technology, inexpensive low-power components, and the task of guaranteeing the cohesive operation of numerous economical, low-accuracy functionalities. Other challenges encompass the procurement and coordination for recently added terminals,

the utilisation of surplus service antennas to leverage additional freedom levels, the minimisation of internal power usage to attain overall energy efficiency (EE) enhancements, and the exploration of novel deployment scenarios [5].

SISO, the first generation of wireless network, is described as an uncomplicated configuration within the radio communication network [8]. According to the author, SISO utilised a single transmitter and a single receiver. Hence it lacked diversity. This technology was therefore recommended for transmiting signals over the short distance [14] thus they possessed weak channel capacity in the presence of interference and fading [9]. As the demand of wireless communication increased the SISO system was restricted under massive demand, therefore it was necessary to further develop robust systems.

The improved first generation of wireless communication was single-input multiple-output (SIMO) [11]. SIMO technology was characterised by having one antenna for transmission and multiple antennas for reception, hence the receiver diversity was better than that of a SISO. In [15], uathors noted that employing multiple antennas at the receiving end improved signal reception, reduced interference and increased the overall performance of wireless communication systems. However the system required an additionl signal processing at the receiver. Conversely, the demand for more efficacious and authentic wireless communication systems increased, which prompted the development of multiple-input single-output (MISO) technology.

MISO systems were developed to mitigate the challenges presented by the SIMO system including having to add an additional signal processing at the receiver [15]. Authors in [8], explored MISO as a form of transmit diversity rather than receiver diversity. Meanwhile [16] suggested that the advancement in wireless communication allowed for greater capacity and improved reliability. The authors described the latter as achieved by exploiting spatial diversity and employing signal processing techniques such as beamforming. This technology enabled the simultaneous distribution of multiple data streams, thus increased the wireless communication system, data rate, and spectral efficiency (SE). According to [9] many transmitter antennas redundantly communicated the data, allowing the receiver to efficiently extract the most pertinent information from the received signal.

An inherent benefit of MISO systems relied in the relocation of code processing tasks to the transmitter terminal. Therefore, by optimising various aspects, such as size, cost, and battery life, the efficiency of communication systems can be significantly improved. While MISO has the capability to utilise multiple transmitter antennas, however MISO does not provide support for multipath propagation.With only one receiver antenna, MISO systems cannot exploit the spatial diversity that comes from multiple paths, limiting the ability to combine signals arriving from different paths to improve signal quality. MISO systems cannot fully leverage on the diversity gain due to single receiver antenna.

The second generation of wireless network was a multiple-input multiple-output (MIMO). The introduction of MIMO marked a significant milestone in the context of wireless systems. MIMO involves using a large number of antennas in the process of both transmitting and receiving signals, enabling higher data rates, improved spectral efficiency (SE), and enhanced link reliability. Author in [17] compared MIMO to SISO technology, gaining widespread attention and research interest in recent years due to its potential for improved systems. Author in [18], agreed with [17] that MIMO benefits are higher data rates, improved SE, and enhanced link reliability. The authors further suggest that MIMO has also shown the capability to increase the robustness of wireless communication systems to ambient interference and channel fluctuations.

Aurthors in [10] reviewed a MIMO system with antenna selection, discussing the importance of MIMO systems in wireless communication and the different formats and configurations used to enhance system performance. The authors highlighted that MIMO systems require multiple antennas, which can be challenging to implement, especially in compact devices. Additionally, the equipment needed for MIMO systems is generally more expensive compared to traditional systems and often limited support for open drivers, which can hinder development and integration. Furthermore, MIMO systems are more complex and require more sophisticated hardware and algorithms to manage the multiple data streams. As a result the authors recommended antenna selection as a solution, suggested that the MIMO system used multiple transceivers to facilitate multipath propagation. In literature the advantages of MIMO systems were discussed, highlighting the enhancement of SE at a minimal expense and the proportional increase in system capacity with the number of antennas. The authors

subsequently concluded that the MIMO system improves the signal-to-noise ratio (SNR), increases data capacity, enhances link reliability, and boosts data throughput with no additional bandwidth or transmission power [9], [11]. Author in [19] studied the performance estimation of SISO and MIMO Radio-over-Free-Space Optics (Ro-FSO) links under atmospheric turbulence conditions. The analysis proved that MIMO systems significantly outperform SISO systems in terms of bit error rate (BER) under various turbulence conditions. Additionally, authors used machine learning techniques, such as artificial neural networks (ANN) to estimate received signal quality, providing a robust model for predicting BER. The paper [20] reviewed the BER performance of MIMO systems using the Alamouti Space-Time Block Code, comparing simulated results with theoretical expectations. This comparison contributed in understanding the advantages of MIMO over other configurations like SISO, SIMO, and MISO.

MIMO systems are integral to wireless transmission standards, including IEEE 802.11n (Wi-Fi), 4G, LTE, WiMAX, and HSPA+ [21]. Multiple studies have also concurred that MIMO technology has progressed to include single-user MIMO (SU-MIMO) [22] and multiuser MIMO (MU-MIMO) [8]. Nevertheless, these technologies cannot meet the growing demand for greater capacity, enhanced link dependability, increased data transfer, better SE, and reduced delays. In the following section, we delve deeper into various wireless network systems based on M-MIMO technology.

2.3 Massive MIMO (M-MIMO)

The demand for higher data rates, improved link reliability, expanded coverage, energy efficiency, and enhanced spectral efficiency (SE) has driven the rise of Massive MIMO (M-MIMO) technology in today's wireless communication systems. Known also as Large-Scale MIMO, Very Large MIMO, hyper MIMO, or full-dimension MIMO, M-MIMO is recognized as a key technology for future wireless networks. This system expands on conventional Multi-User MIMO (MU-MIMO) [23],[24] by utilizing a large number of antennas, which significantly enhances performance in spectrum efficiency, power savings, and link reliability [25],[26],[27]. Multiple studies have demonstrated the effectiveness of M-MIMO in future wireless networks [6], [28], [29],[30], [31].

M-MIMO system plays a crucial role in enabling high-performance requirements of 5G networks and beyond (5GaB). Xie et al. [32], agree that M-MIMO's vast antenna arrays support a revolutionary leap in data transmission and reception capabilities, allowing substantial gains in capacity, security, and SE. However, these improvements depend heavily on precise channel state information (CSI) at the base station. Studies have emphasized the need for accurate CSI, nevertheless, the deploying of numerous antennas at the BS also increases the feedback load in frequency division duplex (FDD) mode, presenting a key implementation challenge [33],[32].

Authors in [6] and [9] prove the M-MIMO's potential to achieve higher SE and capacity compared to traditional intelligent antenna technologies. Another study in [8], highlight M-MIMO's advantages in energy efficiency and single-carrier transmission through the Degrees of Freedom (DoF) offered by its extensive antenna arrays. Marzetta in [28] and Lu et al. [34], have shown that these large antenna arrays push spatial multiplexing and DoF to their limits, maximizing data rate through adaptive transmissions based on each user's reported CSI [35].

Researchers in [4],[12] provide a comprehensive view of M-MIMO's principles, current research, challenges, and future directions. The technology's effectiveness has been repeatedly demonstrated in enhancing the capacity, robustness, and reliability of wireless networks. However, implementing M-MIMO also poses several challenges, including high computational demands for signal processing tasks such as channel estimation and precoding, accuratetely identify the transmitted signals in the presence of noise and interference and allocating resources to multiple users to maximize network performance while minimizing interference. Furthermore, dealing with the interference caused by the reuse of pilot signals in adjacent cells, which can significantly impact the accuracy of channel estimation was discussed [36]. Pilot contamination and precoding, in particular, remain performance-limiting factors, while channel estimation, antenna design, resource allocation, and SE and EE control add further complexity to M-MIMO's adoption [11].

2.4 Pilot Contamination

Pilot contamination poses a significant challenge in M-MIMO systems, significantly affecting the architectures overall performance [37, 38]. Pilot contamination occurs in M-MIMO systems when the pilot signals transmitted by adjacent base stations overlap or when pilot signals transmitted by neighbouring users lead to interference and reduced system performance [39]. This interference greatly degrades the efficacy of M-MIMO systems and decreases the possible data rate [40], [41].

Pilot signals are predefined reference signals that are transmitted to estimate the channel through which they travel. Within time-division-duplex (TDD) M-MIMO systems, the process of channel estimation occurs specifically during the uplink (UL) training phase. In a comprehensive review [31], pilot contamination in massive MIMO systems is thoroughly examined, with a focus on identifying various prospective traces of pilot contamination such as non-reciprocal transceivers and hardware impairments. Furthermore, the assessment explores established theories that have been applied to evaluate the influence of pilot contamination on the overall efficiency of large-scale MIMO systems, specifically concerning attainable data rates.

Several investigations have been carried out to tackle and alleviate the issue of pilot contamination in M-MIMO systems. They are categorising various mitigation procedures for pilot contamination using the pilot-based and subspace-based taxonomies. Moreover, some open issues related to pilot contamination are highlighted, and not limited to computational complexity, deployment scenarios, training overheads, and the utilization of channel reciprocity.

2.5 Mitigating Pilot Contamination Techniques

Mitigating pilot contamination plays a fundamental role in enhancing the performance of M-MIMO systems. In a study by Moghadam [42], various strategies were introduced to mitigate pilot contamination and enhance the performance of M-MIMO systems. These strategies can be categorized into distinct groups. One strategy entails the utilization of different pilot

phases along with diverse pilot sequences to mitigate pilot contamination without depending on statistical information. Yin et al.[4] presented a dual methodology to address pilot contamination in massive MIMO systems. The initial methodology involves establishing an appropriate criterion on the second-order statistics of desired and interference signals to achieve the asymptotic elimination of pilot contamination for increasing antenna usage.

The second approach focuses on devising a synchronized user-to-pilot assignment architecture to fulfil practical network conditions. The authors also discuss the utilization of covariance matrices for encapsulating structural details pertaining to the distribution of multipath angles of arrival at the BS. They analysed the restrictive nature of covariance-based approximations for large-scale antenna arrays in the presence of noise.

According to [43], one approach is to carefully design the pilot allocation strategy carefully, ensuring that pilots are assigned in a way that minimises interference. The research conducted by [4] and [6] applies multiple pilot phases with different pilot sequences, where the total length of the pilot is equal to or greater than the total number of users. The approach allows for estimating individual user channels without interference from other users' pilot signals. In [44], various methods of pilot contamination mitigation in M-MIMO systems were reviewed and categorised. The authors categorised the proposed methods into four distinct clusters and compared their benefits and drawbacks. They concluded that the “frequency-reuse-based” method has the minimum channel estimation error. In contrast, when statistical information is available, the MMSE channel estimator presents the best performance for minimising channel state estimation errors. The methodology showed decreased channel estimation error by a factor of 2.

Authors in [45] presented a model that utilises a matrix's Singular Value Decomposition (SVD) to solve a specific complication of a joint pilot sequence and analogue combiner design in M-MIMO systems. The authors focused on lessening pilot contamination by jointly optimising pilot sequences and analogue combiner design, aiming to lower the number of RF chains while preserving high channel estimation accuracy. The authors optimised pilot allocation and transmit power but did not design the pilot sequences.

Meanwhile, [46] proposed a pilot sequence allocation strategy to alleviate pilot contamination in TDD M-MIMO systems. The technique involves using identical pilot sequences for centre users and jointly orthogonal pilot sequences for edge users in unique cells. The proposed strategy achieves improved system capacity than conventional strategies with a one in three reuse rate for pilot sequences. Furthermore, researchers have also explored integrating machine learning techniques in M-MIMO systems to improve their performance.

Integrating machine learning techniques in M-MIMO systems has shown promise in improving their performance. Authors in [47], studied the effectiveness of employing artificial neural networks in mitigating pilot contamination in M-MIMO systems. The researchers found that by leveraging the capabilities of artificial neural networks, it is possible to optimise beamforming, channel estimation, and interference mitigation in M-MIMO systems. Additionally, precoding techniques have been proposed to suppress pilot contamination effects in many pieces of literature, including Hoydis et al. [48] and [42]. The precoding technique involves utilising joint transmission and reception across the network to eliminate interference caused by pilot contamination.

2.6 Precoding

Precoding refers to manipulating the transmitted signals at the BS to alleviate interference and enhance system performance. Precoding can be categorized into two main types: linear precoding and nonlinear precoding [49]. Linear precoding is a technique that applies a linear transformation to the transmitted signals before transmission. Nonlinear precoding, on the other hand, involves using a nonlinear conversion to the transmitted signals. The choice between linear and nonlinear precoding depends on several variables, including the system's complexity, the intended level of interference suppression, and the channel conditions [50].

Authors in [51] provided an overview of the contemporary and potential directions of interference exploitation techniques through Symbol-Level Precoding (SLP) in multi-antenna wireless communication systems. The authors classified constructive interference and destructive interference and explored optimisation-based precoding techniques. Authors

inferred that the interference exploitation techniques through SLP could improve system performance in wireless communication systems by manipulating interfering signals to add up constructively at the receiver side. Several studies have focused on addressing the challenge of precoding in M-MIMO systems [47], [52],[53], [54].

The authors in [53] provide an overview of precoding techniques for M MIMO systems in the context of 5G and 5GaB communication systems. The study focused on linear precoding schemes based on approximate matrix inversion techniques, fixed-point iteration-based linear precoding algorithms, and direct matrix decomposition-based linear precoding algorithms. Additionally, the authors discussed nonlinear precoders such as dirty-paper coding, Tomlinson-Harashima (THP), Vector Perturbation (VP), and Lattice Reduction (LR) aided algorithms. The paper included a particular subsection on peak-to-average power ratio precoding algorithms. Additionally, the paper explored the role of machine learning in precoding techniques and presents a case study of a small-scale MIMO precoding method for M-MIMO networks.

The paper also discussed precoding schemes in multiple antenna technologies like cell-free M-MIMO, beam space M-MIMO, and intelligent reflecting surfaces. The authors highlights that most research efforts in M-MIMO have focused on linear precoding algorithms. Still, there is potential for increased efficiency and higher performing nonlinear precoders with comparable complexity to be developed. Machine learning and Deep Neural Networks (DNN), can be utilized to design highly effective and low-complexity precoders. Artificial Intelligence (AI) can optimise nonlinear precoders like vector perturbation and minimise issues such as “one-bit problems”.

2.6.1 Linear precoding

In recent years, linear precoding techniques have gained significant attention in communication systems. As defined in Section 2.6, linear precoding employs linear transformations at the transmitter to mitigate interference and improve system performance. Authors in [55] discussed the optimisation problem of precoder design for wireless communication systems based on different performance criteria. Also, they provided

insights into the design criteria for precoding, considering both fundamental and practical measures. The authors also introduce different formulations and algorithms for solving the precoder optimisation problem.

Multiple linear precoding techniques have been developed and studied, each with advantages and limitations. In [53], the classification of linear precoding algorithms is presented. Linear precoders classified based on matrix inversion approximation methods are Truncated Polynomial Expansion (TPE) and Neumann Series Approximation (NSA). Furthermore, the classes are defined by the fixed-point iteration-based linear precoding algorithms such as the Successive Over-Relaxation (SOR) algorithm, and the Conjugate Gradient (CG) algorithm.

The QR decomposition and Cholesky Decomposition (CD) are direct matrix decomposition-based linear precoding algorithms. Basic linear precoders are discussed, such as Zero-Forcing (ZF) and Minimum Mean Square Error (MMSE). A comparative study of these techniques provides insights into their strengths and weaknesses in the context of M-MIMO systems. Based on the comparative analysis, it can be observed that each linear precoding technique has its advantages and drawbacks in terms of computational complexity and performance. The different types of linear precoding are discussed in Sections 2.6.1.1 to 2.6.1.7.

2.6.1.1 Zero-forcing (ZF)

Zero-forcing (ZF) precoding is one of the basic precoding techniques mentioned in Section 2.6.1. These widely studied linear precoding techniques aim to eliminate inter-user interference at the receiver for each user by broadcasting the signal towards the projected target user while nulling interference in the directions of other users [56]. Decoupling multiuser channels into multiple independent sub-channels reduces the design problem to a power allocation issue. According to[53],[57], exploiting the interference components in linear precoding systems results in a total transmit power reduction compared to conventional precoding techniques, such as Maximum Ratio Transmission (MRT).

Several research papers have highlighted the effectiveness of zero-forcing precoding in improving spectral efficiency and reducing inter-cell interference [58], [59]. Israr et al. [60], suggested that zero-forcing precoding achieves optimal performance when the number of antennas is larger than the number of users for imperfect CSI. Furthermore, it has been shown that zero-forcing precoding can achieve the total multiplexing gain when precise channel state information is accessible at the transmitter section [55]. Zero-forcing precoding eliminates user interference but may suffer from noise amplification and instability in specific scenarios. Authors in [61] concluded that the simulated results show that the equaliser-based zero-forcing receiver is effective for noise-free channels and successfully removes ISI. However, MMSE is an optimal choice regarding BER characteristics, while high SNR for ZF is achieved in [62].

2.6.1.2 Conventional Regularized Zero-Forcing Precoding

Regularized-Zero Forcing (RZF) precoding is one of the optimal linear precoding schemes in M-MIMO downlink systems. RZF precoding enhances processing to contemplate the effect of the background noise and unknown user interference. Channel inversion is regularised by adding a scaled identity matrix before taking the inverse. RZF precoding and minimum mean square error (MMSE) detection assist in exploiting the full potential of M-MIMO in practice. These require the computation of matrix inverses of $K \times K$ matrices.
In contrast, the frequently used RZF precoder is most favorable when the ratio between the SINR requirement and the average channel attenuation is shared by all users. Principally, the RZF precoder is acquired by minimising the Mean Square Error (MSE) between the transmitted and received codes, which is also defined as the Minimum MSE (MMSE) precoder [63], [64, 65]. Calculation of the RZF precoding matrix involves matrix inversion with substantial dimensions, specifically for increased values of M and K [52].

2.6.1.3 Matched Filter Precoding

The matched filter (MF) precoder is defined as the conjugate transpose of the downlink channel matrix, also referred to as a Maximum Ratio Transmission (MRT), strengthening the signal gain at the projected UE or conjugate beamforming. Transmit matched filter maximises Signal-to-Interference Ratio (SIR) at the receiver and is optimal for high SNR

region. It is derived by maximising the ratio between the power of the desired signal portion in the received signal and the signal power under the transmit power constraint [48].

2.6.1.4 Conventional Minimum Mean Square Error (MMSE)

The conventional MMSE precoding technique is another widely studied basic linear precoding technique. The MMSE is an optimal linear precoding technique in massive MIMO downlink systems. It uses the mean square error (MSE) and the Lagrangian optimisation method to ensure high-quality transmission while satisfying power constraints [63]. The MMSE technique in wireless communication offers numerous benefits. It establishes a scalar channel for each terminal, treats interference as additive noise, enhances performance with additional antennas, and averages small-scale fading across the array. The MMSE algorithm demonstrates a moderate achievable rate, providing optimal outcomes at high and low transmission powers. The linear capacity expands proportionally with the increase in the number of antennas. In addition, it demonstrates excellent performance even in situations with a low signal-to-noise ratio by utilising the estimated channel matrix's Mean Squared Error (MSE).

In [64], the technique minimises the mean square error between the received and desired signals caused by interference and noise. Peng et al. [66] proved that MMSE considers both signals to reduce their impact on the receiver. The latter is achieved by applying a weight matrix to the transmitted signal to minimise the mean squared error at the receiver. Conventional minimum mean square error precoding offers improved signal quality by minimising the mean square error, but it requires a higher computational complexity than zero-forcing precoding [67].

2.6.1.5 Cholesky-Sherman-Morrison Precoder

Another linear precoding technique that has gained attention is the Cholesky-Sherman-Morrison precoder. The Cholesky-Sherman-Morrison precoder is a linear precoding scheme that aims to reduce the complexity of precoding design while achieving good performance [68]. The reduction in complexity and performance improvements is achieved by employing a matrix decomposition method that implements a Cholesky factorisation and Sherman-

Morrison equations. The channel matrix is decomposed into two components to implement the Cholesky-Sherman-Morrison precoder: an upper triangular matrix and its Hermitian transpose. These two matrices are then used to calculate the precoding matrix, which is applied to the transmitted signal to mitigate interference and improve performance. Cholesky-Sherman-Morrison precoding is efficient in matrix inversion and performs well in interference suppression and signal quality. However, it may still suffer from some interference and may not be as effective in highly dense or interference-limited environments.

2.6.1.6 Truncated Polynomial Precoder

Truncated Polynomial precoding aims to strike a balance between the low-complexity MF precoder and the high-performance ZF precoder by approximating the inverse of the channel matrix using a polynomial function [69]. Using a low-order polynomial function in truncated polynomial precoding allows for a smooth transition between MF and ZF precoders, reducing computational complexity while performing well in interference mitigation and signal quality. Truncated Polynomial precoding provides a good compromise between low-complexity MF precoding and high-performance ZF precoding, and offers reduced computational complexity while achieving good interference suppression and signal quality.

2.6.1.7 Neumann Series Approximation Precoding

Neumann Series approximation precoding is a linear system that strives to reduce the computational complexity of precoding algorithms while maintaining good execution. This technique is based on the Neumann series, a mathematical series used to approximate the inverse of a matrix [65]. To implement Neumann Series precoding, the channel matrix is iteratively multiplied by a power of itself. The resulting matrix sequence converges to an inverse approximation, which can then be used as the precoding matrix. On the other hand, Neumann Series precoding offers a unique approach to reducing computational complexity by approximating the inverse of the channel matrix using the Neumann series. This approximation technique efficiently computes the precoding matrix, reducing the computational burden associated with M-MIMO systems. Neumann Series precoding provides an efficient approach to reducing computational complexity by approximating the inverse of the channel matrix using the Neumann series. This approach allows for efficient

computation of the precoding matrix, reducing the computational burden associated with M-MIMO systems.

2.6.2 Nonlinear precoding

Nonlinear precoding techniques are another approach to alleviate interference and improve the performance of M-MIMO systems. These techniques involve advanced signal processing methods and are advantageous for performance improvements. Nonlinear precoding techniques are a promising opportunity to explore for overcoming interference and improving the overall execution of M-MIMO systems.

2.6.2.1 Dirty paper coding

Dirty paper coding (DPC) is the approach that possesses the ability to nullify the known interference with no penalty of radio resources if the optimal precoding scheme can be performed at transmission [70], [71]. The receiver does not have knowledge of this interference. Hence, full CSI of all users and other user data is required to achieve the weighted sum capacity. DPC maximise channel capacity with minimum power penalty. The thorough review indicates the challenges associated with designing precoders, where technological capabilities are usually impaired by practical implementation problems [72], [73]. The design of a DPC-based system should incorporate a strategy to feed side information to the transmitters [11]. This suboptimal approximation includes Costa precoding. However, more advanced approaches, such as Tomlinson-Harashima and vector precoding, achieve superior performance at the expense of more complexity. Although these schemes consider the computational complexity of the precoding algorithms, they do not consider limitations imposed on the system by hardware restrictions. For example, as mentioned earlier, the precoders consider the whole complex plane as the set of possible transmits constellation points; the assumption in practice does not hold due to power amplifiers' limited Peak-to-Average Power Ratio (PAPR).

2.6.2.2 Tomlinson-Harashima Precoding

Tomlinson-Harashima precoding is a nonlinear precoding technique that has shown promise in improving the performance of M-MIMO systems [74]. This technique aims to mitigate the impact of inter-user interference and pilot contamination, which are common challenges

in M-MIMO systems. A shared transmission system based on interference association and soft-space reuse has been proposed to address inter-user interference [75]. Additionally, it is

shown that Tomlinson-Harashima precoding depends heavily on the sequence of precoded symbols for optimal performance and interference mitigation [75]. Furthermore, channel estimation plays a crucial role in the performance of Tomlinson-Harashima precoding in M-MIMO systems. Authors of [76] discussed the importance of accurate channel state information for efficient interference management and proposed a channel estimation method utilising the second-order statistics of the user equipment channels. In addition to Tomlinson-Harashima precoding, other precoding techniques have also been explored for M-MIMO systems. The author [77], provided an overview of different precoding techniques, including zero-forcing precoding, regularised zero-forcing precoding, and dirty paper coding, and their applications in M-MIMO systems.

Tomlinson-Harashima precoding, as a nonlinear precoding scheme, has achieved widespread interest due to its capability to achieve near-capacity performance in massive MIMO systems. In particular, the precoding scheme has been recognised for its potential to mitigate inter-user interference and pilot contamination, critical challenges in massive MIMO systems. A cooperative transmission arrangement based on interference configuration and soft space reuse has been introduced to address inter-user interference, presenting a promising approach to assist cell-edge user equipment in mitigating interference from neighbouring cells. Furthermore, channel estimation is of paramount importance in determining the effectiveness of the Tomlinson-Harashima precoding scheme.

2.6.2.3 Vector Perturbation (VP)

Traditional linear precoding schemes, for instance Tomlinson-Harashima precoder, are not preferred in M-MIMO systems attributable to their high computational complexity and suboptimal performance in terms of interference management. Vector perturbation precoding has emerged as a promising approach for M-MIMO systems to address this challenge. Vector perturbation precoding is a nonlinear technique that introduces controlled perturbations to the transmit signal vectors to manipulate the system's interference properties. Vector perturbation precoding has been shown to mitigate inter-user interference and improve system effectiveness in M-MIMO systems.

One of the significant benefits of vector perturbation precoding is its ability to realize near-optimal performance with significantly small computational complexity compared to other advanced nonlinear precoding techniques in M-MIMO systems. Several studies have focused on the performance and implementation aspects of vector perturbation precoding in M-MIMO systems. For example, in a study conducted by Yang et al. [78], the authors proposed a low-complexity vector perturbation precoding scheme that achieved significant performance gains in terms of sum and error rates compared to traditional precoding techniques.

Another study in [79] focused on optimising vector perturbation precoding in M-MIMO systems and demonstrated its effectiveness in mitigating interference and improving system capacity. Another study by Barrenechea [80] explored the implementation aspects of vector perturbation precoding in practical M-MIMO systems. The authors implemented a vector perturbation precoder using a simplified hardware architecture and showed that it can achieve good performance with low complexity. In summary, vector perturbation precoding is a promising technique for managing inter-user interference and improving performance in M-MIMO systems.

2.6.2.4 Lattice Reduction-Lenstra-Lenstra- Lovász

One of the mitigation techniques that has been studied is lattice reduction. Lattice reduction is a mathematical technique that can be used to enhance the performance of M-MIMO systems when pilot contamination is evident. Lattice reduction algorithms like the Lenstra-Lenstra-Lovász algorithm have been applied to reduce pilot contamination in M-MIMO systems. Pilot contamination in M-MIMO systems and its mitigation using lattice reduction is a well-researched topic [81]. Lattice reduction algorithms, notably the Lenstra-Lenstra-Lovász algorithm, have emerged as potential tools to alleviate pilot contamination in M-MIMO systems.

These algorithms aim to reduce the interference triggered by pilot contamination by optimising the orthogonality of the pilots in neighbouring cells. The complexity and inter-cell interference caused by pilot contamination in M-MIMO systems have led to extensive

research on mitigation techniques. The lattice reduction algorithms, such as the Lenstra-Lenstra-Lovász algorithm, have been highlighted as a promising approach to address this challenge. These algorithms optimise the orthogonality of the pilots used in adjacent cells, thereby reducing the interference caused by pilot contamination.

In [82], the authors propose a joint pilot allocation and pilot sequences optimisation method for massive MIMO systems using a lattice reduction approach. The technique aims to reduce pilot contamination and improve the channel estimation accuracy in M-MIMO systems. The paper provides an in-depth analysis of pilot contamination in M-MIMO systems. It proposes using lattice reduction algorithms, precisely the Lenstra-Lenstra-Lovász algorithm, to mitigate pilot contamination. The authors conducted simulations to validate the effectiveness of lattice reduction for decreased pilot contamination, thereby improving system performance.

The results showed that lattice reduction can significantly reduce pilot contamination and improve the achievable throughput in M-MIMO systems. The use of lattice reduction in mitigating pilot contamination in M-MIMO systems is effective in improving system performance and achieving higher throughput. Lattice reduction techniques have been studied and proposed as a mitigation strategy for pilot contamination in M-MIMO systems. Recent advancements in M-MIMO technology have brought about significant improvements in system performance. Pilot contamination, a primary concern in M-MIMO systems, has been extensively researched, and numerous mitigation methodologies have been recommended to address its effects.

In addition to lattice reduction, other efficient schemes have been proposed to alleviate the effects of inter-cell interference triggered by pilot contamination in M-MIMO systems. These schemes include interference alignment, adaptive power allocation, and user scheduling strategies. These techniques aim to improve the channel estimation accuracy and reduce the influence of pilot contamination on system operation, thereby increasing realistic throughput in M-MIMO systems.

2.6.3 Hybrid Precoding

Hybrid precoding for M-MIMO systems has gained significant attention in recent years. M-MIMO technology, which utilises many antennas at the base station, can provide substantial gains in spectral efficiency and system capacity. Traditional all-digital precoding approaches, however, are impractical due to the high hardware and energy consumption associated with many antennas. Hybrid precoding has emerged as a promising solution to address these challenges [83]. Hybrid precoding combines analogue and digital precoding techniques to decrease the number of radio-frequency chains required while maintaining performance close to that of fully digital precoding [84].

Numerous hybrid precoding architectures have been suggested in the literature [85], [86]. One such architecture is phased-zero forcing precoding, which combines a set of phase shifters with zero-forcing digital precoding. Hybrid precoding is a technique that combines analogue and digital precoding in M-MIMO systems to overcome high signal attenuation at millimetre-wave frequencies and improve the overall system performance. It has been shown that hybrid precoding can achieve significant performance gains while reducing complexity in M-MIMO systems. For example, uathors in [87], suggested a hybrid precoding design that utilises consecutive interference cancellation to optimise each antenna array's achievable capacity. Using a non-complex sub-array, the system combines analogue and digital precoding to alleviate high signal attenuation at millimetre-wave frequencies.

Based on [88], hybrid precoding for M-MIMO systems has been extensively studied and proposed as a solution to overcome challenges such as high signal attenuation at millimetre-wave frequencies and reduced hardware complexity in M-MIMO systems. These hybrid precoding techniques have proven effective in improving M-MIMO systems' performance while reducing complexity. One study conducted by [89] proposed a precoding algorithm based on deep learning techniques to enhance the operation of M-MIMO systems. The researchers trained a deep neural network to map the unique relationships between the CSI and the precoding matrix, thereby enabling the network to adjust the precoding matrix adaptively based on the current channel conditions.

2.6.3.1 Phased Zero Forcing (PZF)

Phased-zero forcing precoding has achieved near-optimal performance with reduced hardware complexity [90]. In [91], a detailed study on hybrid precoding for M-MIMO systems was conducted. They suggested a hybrid precoding approach combining analogue and digital precoding to alleviate the influences of high signal attenuation at millimetre-wave frequencies. Tomlinson-Harashima precoding is another approach widely studied for hybrid precoding in M-MIMO systems. Furthermore, the phased-zero forcing technique has been introduced as a hybrid precoding approach for M-MIMO systems. Phased-zero forcing is a reduced complexity hybrid precoding approach that aims to achieve the performance of full-complexity zero-forcing precoding, which may not be feasible due to the requirements of dedicated RF chains for each antenna.

2.6.3.2 Hybrid Linear-Tomlinson-Harashima precoder (HL-THP)

Tomlinson-Harashima precoding is a widespread technique in the context of hybrid precoding for M-MIMO systems. Tomlinson-Harashima precoding involves mapping the transmitted symbols onto a lattice structure and then applying digital precoding to simplify the signal transmission [92]. Hybrid linear-Tomlinson-Harashima precoding is a variant of Tomlinson-Harashima precoding that further reduces complexity by incorporating linear precoding techniques. Hybrid linear-Tomlinson-Harashima precoding has achieved significant performance gains while reducing complexity in M-MIMO systems [93]. Hybrid precoding is a promising technique for reducing M-MIMO systems' hardware complexity and energy consumption. Both FDD and TDD systems have been investigated in the domain of channel estimation for hybrid precoding. In the context of FDD systems, the reference proposed a channel estimation scheme for hybrid precoding in M-MIMO arrangements.

This scheme utilises a compressed sensing-based approach to approximate the sparse channel coefficients while considering the hardware constraints of the hybrid precoding architecture [94]. The hybrid precoding for M-MIMO systems has been extensively studied and suggested as a solution to overcome challenges such as high signal attenuation at millimetre-wave frequencies and reduced hardware complexity in M-MIMO systems.

These hybrid precoding techniques have proven effective in improving M-MIMO systems' performance while reducing complexity. Moreover, Tomlinson-Harashima precoding has been extended to spatial interference equalisation for MIMO systems, leading to the spatial Tomlinson-Harashima precoding architecture. Another benefit of hybrid precoding is the reduction in complexity compared to full-complexity zero-forcing precoding. One of the challenges in hybrid precoding is accurate channel estimation. Precise channel approximation is essential in hybrid precoding for massive MIMO systems. Accurate channel estimation allows for optimal beamforming and precoding designs, improving system performance. Numerous hybrid precoding methods have been proposed in the literature to address the challenges of high signal attenuation and hardware complexity in millimetre-wave M-MIMO systems [95]. These schemes utilise a combination of analogue and digital precoding techniques to optimise the achievable capacity of each antenna array [91].

2.7 Channel models

Channel modelling plays a crucial role in developing and deploying M-MIMO systems. In M-MIMO systems, channel modelling is critical for accurately analysing precoding schemes' performance and understanding how signals behave as they propagate through the wireless channel. M-MIMO, which involves deploying many antennas at the transmitter and receiver, has emerged as a promising method to satisfy the increasing requirement for high data rates and reliable communication in future wireless networks [96]. Channel modelling is essential for evaluating the efficacy of precoding schemes in M-MIMO systems [97]. Several types of channel modelling methods have been proposed to capture the characteristics of the M-MIMO channel.

2.7.1 Types of Channel Modelling in M-MIMO

Two channel modelling techniques used in M-MIMO systems are geometrical-based stochastic models and the correlation-based stochastic models. The geometric channel model considers the system's physical layout and placement of antennas and users[98], [99]. This model finds path loss, shadowing, and multipath reflections to calculate channel gains and

delays accurately. The stochastic channel model uses statistical methods to capture the randomness and variability of the wireless channel. The stochastic channel model considers fading effects, such as Rayleigh or Rician fading, to simulate the fluctuations in the channel response. There are also hybrid channel models that merge elements of both geometric and stochastic models to provide a more comprehensive understanding of the channel behaviour.

The advantages of the geometric channel model in M-MIMO include its ability to capture the wireless environment's physical characteristics accurately. This model considers antenna placement, path loss, and multipath reflections, providing a realistic channel representation. Furthermore, the geometric channel model allows for precise calculations of the channel gains and delays, which can aid in optimising system performance and designing efficient communication schemes [100].

However, the geometric channel model may be computationally complex, especially in scenarios with many antennas and users. In contrast, stochastic channel modelling techniques offer the advantage of simplicity and efficiency. These models use statistical methods to capture the randomness and variability of the channel, allowing for faster computations. However, stochastic models may not accurately represent the physical characteristics of the wireless environment. For example, they may not account for specific path loss or multipath reflections that can significantly impact channel performance.

When considering millimeter Waves (mmWave), the CSI is greatly subjected to the geometrical and physical properties of the environment, limiting the usefulness of mathematical models. Therefore, while stochastic channel models may be computationally efficient, they may not provide the accuracy required for mmWave communication systems. In summary, the advantages of geometric channel modelling in M-MIMO systems include its ability to accurately capture the physical characteristics of the wireless environment and provide precise calculations of channel gains and delays. Additionally, it allows for optimised system performance and efficient communication scheme design.

2.7.2 Correlation-based stochastic channel models

One such channel model classified under stochastic systems is the Rayleigh channel model. In the context of M-MIMO systems, the Rayleigh fading channel model is often used to illustrate the wireless communication channel between the BS and the user equipment [101]. The Rayleigh fading channel model assumes that the channel experiences multipath propagation. Upon reaching the receiver, the sent signal may be received in many duplicates, each exhibiting different time delays and amplitudes.

Initial theoretical studies have assumed the Rayleigh fading channel has a sufficiently rich multipath, which leads to an ideal uncorrelated MIMO channel matrix with independent and identically distributed complex Gaussian entries [102]. However, in realistic scenarios, multipath fading tends to produce correlated channels. In the context of M-MIMO, the Rayleigh fading channel model is commonly employed to describe the channel between a BS and multiple-user equipment. In the Rayleigh fading model for M-MIMO, the channel matrix H is characterised by independent and identically distributed (i.i.d.) zero-mean complex Gaussian random variables.

The Rayleigh fading model is commonly used to describe the channel in M-MIMO systems. The Rayleigh fading model assumes that the entries of the channel matrix in an M-MIMO scenario, denoted as H, follow i.i.d. zero-mean complex Gaussian random variables. This means that each entry of the channel matrix H, representing the difficult channel gain from one antenna to another, is a random variable that follows a Gaussian distribution with zero mean. The Rayleigh fading channel in M-MIMO can be represented as a complex Gaussian random variable with zero mean and i.i.d. entries.

Another channel model classified as correlation-based stochastic is the Gaussian i.i.d model. From the hypothetical perspective, it proves advantageous to view the constituents of the narrowband MIMO channel matrix as i.i.d circularly-symmetric complex Gaussian random variables, characterized by zero mean and unit variance $\mathcal{CN}(0,1)$. This particular representation is associated with a complex scattering propagation surroundings and

significant distance between the elements within the transmit antenna array. While exploring this model can offer insights, it fails to capture the nuances of limited scattering conditions and minor antenna separations commonly found in practical systems.

The Kronecker model, which is also categorized as geometric, incorporates the impact of correlation within the channel model. This system accepts that the spatial covariance matrix can be expressed as the Kronecker product covariance matrices at the transmitter and receiver terminals. Previous research has demonstrated that the utilization of the Kronecker model leads to suboptimal capacity estimations.

2.7.3 Geometry-based stochastic channel models

Authors in [103] discussed that the geometry-based stochastic modelling approach is highly regarded and widely used. Its flexibility allows for both simple models that are valuable for theoretical analysis of channels and more complex models that accurately simulate real channels. Regardless of the objective, whether conducting theoretical investigations of channels or accurately replicating real channels, the approach focuses on scatterers and is therefore able to capture the fundamental aspects of the channels.

The approach of stochastic modelling based on geometry falls under the "scattering modelling" category, which also encompasses deterministic modelling based on geometry. The geometry-based stochastic modelling approach is often preferred over its deterministic equivalent due to its simplicity and generality. It does not require a detailed description of the fundamental communication environment, making it a popular choice in academic and technical fields. The overall modelling procedure is summarised and comprises the following steps:

1. Fundamental establishment of communication environment: this encompasses the placement, trajectory, and speed of the transmitter/receiver, along with categorising relevant scatterers, such as mobile and stationary scatterers.
2. Placement of scatterers: position scatterers within the designated scattering region according to a Probability Density Function (PDF). Depending on the distribution of

scatterers in this region, the approach can be classified as regular or irregular-shaped. Traditional shapes include one/two-ring, ellipse, and other similar forms, while a random distribution characterises irregular shapes.

3. Parameterisation: scatterers can be parameterised in two ways during this step. An initial analysis involves a limited set of scatterers, with fading characteristics assigned to each based on empirical data. The second premise considers an unlimited number of scatterers, resulting in the channel properties being governed solely by their probability density function (PDF). This allows for the determination of channel properties without the need to assign fading properties to each scatterer. Given the circumstances, the channel model derived is not feasible for practical implementation and is commonly known as the reference model. This information is valuable for conducting theoretical analyses of the channel characteristics.
4. Sum up the contributions of all scatterers at the received side to achieve the channel impulse response. It is essential to consider that the reference model contains infinite scatterers. To ensure the model's practicality and feasibility obtaining a simulation model that includes a finite number of scatterers in this step is necessary.

Dang et al. [104] developed a geometry-based stochastic channel mode (GSCM) for Intelligent Reflecting Surface (IRS). The IRS-assisted communication, capable of accurately characterising the path loss and correlations among various sub-channels on a large scale. Based on the proposed channel model, the authors examined multiple characteristics of the channels, including spatial correlation functions (CFs) and the ergodic capacity of the system. A spatial CF-based algorithm was provided for optimising reflection coefficients. Based on numerical simulations, it has been observed that including an IRS can enhance the system's capacity. It is recommended that the IRS be positioned near either the transmitter or the receiver. Despite the limitations of the GSCM presented, For example, in the vicinity of the object, the model lacks precision. To enhance the accuracy of our models, we must incorporate a more comprehensive near-field electromagnetic radiation model in future research. Furthermore, it is worthwhile to investigate the expansion of the model to encompass a broader scope, including multiple users and the incorporation of wideband and non-stationary channel characteristics.

The author in [105] discusses the importance of analysing new M-MIMO channel attributes and developing corresponding channel models for the Internet of Things (IoT). It mentions that various channel models have been suggested and classified using several distinct methods, which can be confusing. To address this, the document presents a unified classification framework that combines artificial intelligence (AI) based predictive channel models and conventional non-productive channel representations. It also reviews massive MIMO channel measurement campaigns and surveys recent advances in channel modelling. The document elaborates on deterministic and stochastic models, including the correlation-based stochastic model (CBSM), geometry-based stochastic model (GBSM), and beam-domain channel model (BDCM). Finally, it highlights forthcoming challenges in massive MIMO channel modelling.

2.8 Performance metrics

M-MIMO is a promising technology for future wireless communication systems. It presents several advantages, such as improved signal-to-noise ratio, increased data rate, enhanced spectral efficiency, and higher system reliability at a lower cost [106], However, the accuracy of M-MIMO systems heavily relies on the validation methods used to assess their performance. Several methods are commonly used to validate the accuracy of M-MIMO systems, including signal-to-interference-plus noise ratio, spectral efficiency, and bit-error ratio [107], [108]. Additionally, the choice of modulation schemes, such as Quadrature Amplitude Modulation (QAM) plays a crucial role in determining these performance metrics. Higher-order modulation schemes can increase data rates and spectral efficiency but may also require a higher signal-to-noise ratio to maintain low bit-error rates[109].

2.8.1 Modulation schemes

Modulation schemes such as 16-QAM and 64-QAM enable higher data rates by transmitting a greater number of bits per symbol than simpler techniques like Binary Phase Shift Keying (BPSK) and Quadrature Phase Shift Keying (QPSK). In [109], 16-QAM transmits 4 bits per symbol, whereas 64-QAM accommodates 6 bits per symbol. QAM modulation demonstrates

bandwidth efficiency, scalability and are extensively utilised in communication standards such as Wi-Fi, LTE, and 5G, enabling high data throughput and efficient spectrum utilisation[110]. However, higher-order QAM schemes, such as 64-QAM, exhibit increased sensitivity to noise and interference, demanding better signal quality and higher SNR for reliable communication. A quick overview of how different modulation schemes compare in terms of their key characteristics and typical uses in wireless networks is depicted in Table 2.1:

Table 2.1: Common digital modulation schemes used in wireless networks

Modulation Scheme	Bits per Symbol	Symbol Rate	Bandwidth Efficiency	Noise Immunity	Common Applications
BPSK	1	1 x bit rate	Low	High	Satellite communication, low-data-rate wireless
QPSK	2	1/2 x bit rate	Moderate	Moderate	Wi-Fi, LTE, satellite communication
8-PSK	3	1/3 x bit rate	Moderate	Lower than QPSK	Satellite communication, GSM
16-QAM	4	1/4 x bit rate	High	Lower than 8-PSK	Wi-Fi, LTE, digital TV
64-QAM	6	1/6 x bit rate	Very High	Lower than 16-QAM	Wi-Fi, LTE, 5G, digital cable TV
256-QAM	8	1/8 x bit rate	Extremely High	Lower than 64-QAM	5G, high-speed data links, digital cable TV

Different modulation schemes are used based on the requirements of the application[110], such as transmit more data per symbol within the same bandwidth. Choosing a modulation scheme in wireless networks involves balancing several trade-offs. These include data rate versus noise immunity, where higher data rates often come at the cost of reduced noise resistance. Bandwidth efficiency versus complexity is another consideration, as more efficient schemes typically require more complex hardware and algorithms. Power efficiency versus spectral efficiency must also be weighed, with power-efficient schemes being less spectrally efficient and vice versa. Additionally, error performance versus data throughput is a key trade-off, as improving one can negatively impact the other. Finally, application-specific requirements play a crucial role, as different applications may prioritize different aspects of performance, such as low latency or high reliability. These trade-offs depicted in Table 2.2 highlight the importance of selecting the appropriate modulation scheme based on the specific requirements and constraints of the wireless communication system.

Table 2.2: Modulation schemes trade-offs

Modulation Scheme	Data Rate	Noise Immunity	Bandwidth Efficiency	Power Efficiency	Complexity
BPSK	Low	High	Low	High	Low
QPSK	Moderate	Moderate	Moderate	Moderate	Moderate
16-QAM	High	Lower than QPSK	High	Lower than QPSK	High
64-QAM	Very High	Lower than 16-QAM	Very High	Lower than 16-QAM	Very High
256-QAM	Extremely High	Lower than 64-QAM	Extremely High	Lower than 64-QAM	Extremely High

2.8.2 Bit-Error Ratio (BER)

Bit-Error Ratio (BER) is a commonly used metric for accuracy validation in M-MIMO systems. It measures the probability of error in the received bits [111]. A low BER indicates a higher level of accuracy and system performance. On the contrary, some researchers argue

that BER may not be an adequate metric for assessing the accuracy of M-MIMO systems. They claim that BER only considers the error rate at the bit level and neglects other factors such as interference, channel conditions, and modulation scheme [111], [112, 113]. Further, they suggest that BER should be used with other metrics, such as SINR and spectral efficiency, to evaluate the system's accuracy and performance comprehensively.

2.8.3 Spectral Efficiency (SE).

Spectral Efficiency (SE) measures the amount of data transmitted through a given bandwidth. A high SE indicates a higher data capacity and improved system performance [114]. In contrast, some researchers argue that SE alone may not provide a comprehensive representation of system accuracy. While higher SE is desirable, it does not necessarily guarantee accurate transmission and reception of data [115],[116]. One study suggests that SE may not fully capture the effects of interference on the system's accuracy [108].

Another study supports the importance of considering other factors, such as channel estimation and precoding techniques alongside SE to assess system performance accurately [117],[118]. They argue that SE does not consider interference, channel conditions, and user density. These factors can significantly impact the overall system performance and accuracy. Further studies conducted by [119], [120] highlights the limitations of SE as a validation method for M-MIMO systems, stating that it may overestimate system performance in scenarios with high interference levels or poor channel conditions.

2.8.4 Signal-to-Interference Noise Ratio (SINR)

The signal-to-interference noise ratio (SINR) is a commonly used metric for validating the accuracy of M-MIMO systems [121]. It measures the received signal power ratio to the combined interference and noise power. A high SINR indicates good system performance and a low level of interference [122]. On the other hand, there are concerns about the limitations of SINR as an accuracy validation method for M-MIMO systems. Some researchers argue that SINR does not comprehensively assess system performance as it only considers the power aspect and neglects other factors such as spatial correlation and channel

quality [119], [123]. In the studies conducted by [124], [125], they state that the SINR is limited in capturing the full complexities of M-MIMO systems, particularly in scenarios with high spatial correlation and user density. Furthermore, another study suggests that SINR may not accurately reflect the system's performance in dynamic environments where interference levels can vary rapidly[126].

2.9 Performance Comparison

Comparing various precoding techniques in terms of BER, SE, achievable sum rate, and SINR involves understanding the trade-offs and performance characteristics of each precoder type [42, 53]. The BER measures the accuracy of data transmission and represents the probability of errors in transmitted bits. SE measures how efficiently the available spectrum is used to transmit data. The achievable sum rate measures the total data rate that can be achieved in a system. In comparison, the SINR measures the quality of the received signal in the presence of interference and noise. The performance of precoding techniques can vary depending on factors such as computational complexity, accuracy of channel estimation, and the specific communication scenario [60, 62].

Linear precoding techniques, such as zero-forcing, regularized zero-forcing, matched filter, minimum mean square error, Cholesky-Sherman-Morrison, truncated polynomial-based precoding, and Neumann series approximation precoding, have different performance characteristics in terms of these metrics[53, 69]. Various sources in the literature suggest that while offering lower complexity, linear precoding techniques may not achieve optimal performance.

Nonlinear precoding techniques, such as Dirty Paper Coding, Tomlinson-Harashima Precoder, Vector Perturbation Precoder, and Lattice Reduction-Lenstra-Lenstra-Lovász, offer the potential for optimal performance but with higher computational complexity [53]. Nonlinear precoding techniques have been shown to provide near-optimal performance in terms of bit-error ratio spectral efficiency, achievable sum rate, and signal-to-interference noise ratio. Hybrid precoding techniques, such as phased zero-forcing and HL-THP,

combine the advantages of linear and nonlinear precoders by leveraging the benefits of both approaches [75]. By comparing the performance of these precoding techniques, we can evaluate their suitability for different communication scenarios and the trade-offs between complexity and performance.

2.10 Computational complexity

Computational complexity plays a crucial role in determining the feasibility and efficiency of various precoding techniques. The increased number of antennas in M-MIMO system leads to higher computational demands. Basic linear techniques like ZF and MMSE precoders are effective in mitigating interference, have a computational complexity of $\mathcal{O}(K^3)$ [9], [48, 53]. Making them challenging to implement in real-time for large-scale systems. While NSA has low complexitycompared to the basic linear precoder [53] and THP offer high performance but come with even higher computational costs [69, 127] and implementation complexity. The LR-LLL improves the performance of linear precoders by reducing the lattice, but this also adds to computational burden [128]. Table 2.3 below summarises the computational complexity and the trade-offs for ZF, MMSE, NSA, THP and LR-LLL. Balancing these trade-offs is essential for optimizing massive MIMO systems, ensuring they can deliver the promised gains in throughput and efficiency without prohibitive computational overhead. The t in the number of the required iterations.

Table 2.3: Summary of computational complexity and trade-offs

Ref(s)	Precoder(s)	Complexity order	Computational complexity	Trade-offs
[9, 48]	ZF	$\mathcal{O}(K^3)$	$M + MK + 2MK^2 + K^3$	Simple implementation, but poor performance at low SNR and high computational cost for large systems.
[129], [48]	MMSE	$\mathcal{O}(K^3)$	$M + MK^2 + KM^2 + 2K^2 + 3K^3$	Balances noise and interference, better performance than ZF, but higher complexity.
[127], [69, 130, 131]	NSA	$\mathcal{O}(K^2)$ for $t \leq 2$	$K^3(t-2) + MK^2 + K^2 + 2MK + M$	High performance, reduces complexity, but may have convergence issues.
[69, 127],[53]	THP		$8\left(\frac{K}{M} + \frac{2}{3}\right)K^3 + 2\left(2\mathbb{T}\left(1 + 2\frac{K}{M}\right) - 1\right)K^2 + 2\left(\mathbb{T}\left(2 - \frac{K}{M}\right) + 2\right)K - 8\mathbb{T}$	Reduces intersymbol interference, good performance, but requires complex ordering algorithms at the receiver.
[128], [132,				Improves BER performance of

133]	LR-LLL	$\mathcal{O}(K^4)$	-	linear precoders, but with additional complexity from lattice reduction.

2.11 Conclusion

M-MIMO systems have emerged as a favourable technology for achieving higher SE and improved system performance in today's rapidly evolving wireless network landscape. M-MIMO refers to a wireless communication system that incorporates many antennas at the BS to serve numerous users simultaneously. The increase in antennas allows for spatial multiplexing, leading to improved SE and increased capacity. The configuration of M-MIMO systems and the evolution of wireless networks are essential aspects to consider when analysing the performance of precoding schemes. Each precoding technique exhibits distinct trade-offs regarding BER, SE, Achievable sum rate, and SINR. The choice of precoding technique depends on system requirements, channel conditions, computational complexity, and implementation constraints in a specific communication scenario. Conducting simulations or real-world experiments can further validate these trade-offs and assist in choosing the most suitable precoding technique for a given system.

ZF precoding aims to eliminate inter-user interference, leading to reduced BER. However, it can suffer from noise amplification and exhibit higher BER when noise dominates. Regularized Zero-Forcing Precoding balances interference reduction and noise amplification through regularization, offering improved BER compared to ZF. MMSE precoding counteracts interference suppression and signal enhancement, potentially resulting in improved BER compared to ZF. It can provide high SE by optimizing the trade-off between interference suppression and noise amplification and can perform better than ZF in non-ideal channel conditions.

The accuracy validation methods for M-MIMO systems, such as SINR, SE, and BER, have their strengths and limitations. While SE provides a measure of data capacity, it may not fully account for interference and channel conditions. On the other hand, SINR considers the

signal-to-interference and noise ratio, which considers the presence of interference and noise in the system. SINR provides a more comprehensive assessment of the system's performance. The preferred precoding schemes, chosen based on the accuracy validation methods discussed in this chapter to address pilot contamination in massive MIMO, will be thoroughly examined in the methodology chapter.

3 Methodology

3.1 Introduction

The aim of the study outlined in Chapter One sought to investigate various precoding schemes and their influence on mitigating pilot contamination in massive MIMO systems through MATLAB® simulations. The research questions strive to address the effectiveness of linear and nonlinear precoding schemes in terms of performance validation metrics in M-MIMO systems and whether different precoding schemes can be integrated with channel estimation techniques to tackle the issue of pilot contamination. The proposed objectives included comparing and analysing both linear and nonlinear precoding schemes, model channels using the Rayleigh fading model and performing a comparative analysis of precoding schemes. Chapter 2 explores the concept of massive MIMO (M-MIMO) and the evolution of wireless network technologies. It reviews the progression of wireless networks and the transmitter-receiver relationship aimed at maximizing user data rates. The chapter also addresses the issue of pilot contamination and discusses various techniques for its mitigation. Precoding techniques, a key method to mitigate pilot contamination, are thoroughly examined, highlighting the strengths and weaknesses of each approach as identified in the surveyed literature. Additionally, the chapter investigates different channel models used to simulate M-MIMO environmental scenarios, applying various performance indices to validate the accuracy of M-MIMO systems.

In this chapter, the massive MIMO system will be evaluated and modelled for the perfect and imperfect CSI. Furthermore, it will delve into the mathematical description of chosen sub-optimal precoding techniques used in M-MIMO systems. The analysis techniques encompass a range of linear precoding schemes including Zero-Forcing (ZF), Minimum Mean Square Error (MMSE), Neumann Series Approximation (NSA) and nonlinear precoders for instance Vector Perturbation (VP), Tomlinson-Harashima Precoder (THP), and Lattice Reduction (LR) algorithm, and the Lenstra-Lenstra-Lovász (LLL) precoder. The comparison will be executed using Achievable Sum Rate (ASR), BER and SNR performance metrics. These precoding techniques will also be analysed in the presence of imperfect CSIT.

The performance will be analysed using the same performance metrics in the MATLAB® environment.

3.2 System model

Let's consider a M-MIMO downlink transmission system with cells numbered $1, 2, \ldots, L$. Each cell consists of a based station (BS) equipped with $\mathcal{M} \geq \mathrm{K}$ antennas to support the $\mathrm{K} \geq 1$, single-antenna user-equipment (UE) with the same time-frequency resources through Rayleigh flat fading channels as illustrated in Figure 3.1. The antennas are considered omnidirectional. The system operates using a time division duplex (TDD) protocol, allowing the BS to obtain real-time CSI from the uplink (UL) exploiting the channel reciprocity. It is assumed that the CSI is accurately known at the BS and is shared among all users in M-MIMO systems with the assistance of the pilot signal [127].

Eq. (1) depicts the received signal as:

$$y = \mathbf{H}x + n \tag{1}$$

Where $x = [x_1, x_2, \ldots\ldots, x_K]^T$ is the $x \in \mathbb{C}^{(Kx1)}$ transmitted signal vector, $y = [y_1, y_2, \ldots\ldots, y_{\mathcal{M}}]^T$ is the $y \in \mathbb{C}^{(\mathcal{M}x1)}$ received signal vector, and $n = N \times 1$ is the received additive white Gaussian noise (AWGN) vector. The assumption is that the noise sample follows a circularly symmetric complex Gaussian distribution with zero mean and variance σ^2. If the noise vector equals zero, the reception of the transmitted signal is flawless.

The representation of the channel matrix in Eq. (1) is characterized by the M-MIMO channel, indicating the channel's complex gain connecting the receiving and transmitting antenna. The channel matrix (**H**) in Eq. (2) is expressed as[53]:

$$\mathbf{H} = \begin{bmatrix} h_{11} & h_{12} & \cdots & h_{1\mathrm{j}} \\ h_{21} & h_{22} & \cdots & h_{2\mathrm{j}} \\ \vdots & \vdots & \ddots & \vdots \\ h_{i1} & h_{i,2} & \cdots & \mathrm{h}_{ij} \end{bmatrix} \tag{2}$$

Where h_{ij} is the channel gain from the jth transmit antenna to the ith receive antenna. The elements of the channel matrix $\mathbf{H} \in \mathbb{C}^{(MxK)}$ often assumed to be independent and identically distributed (i.i.d) Gaussian random variables with zero mean and unit variance. Where $i = 1,2, \ldots, K$ and $j = 1,2, \ldots, M$. The base station M will be up to 256 antennas and the number

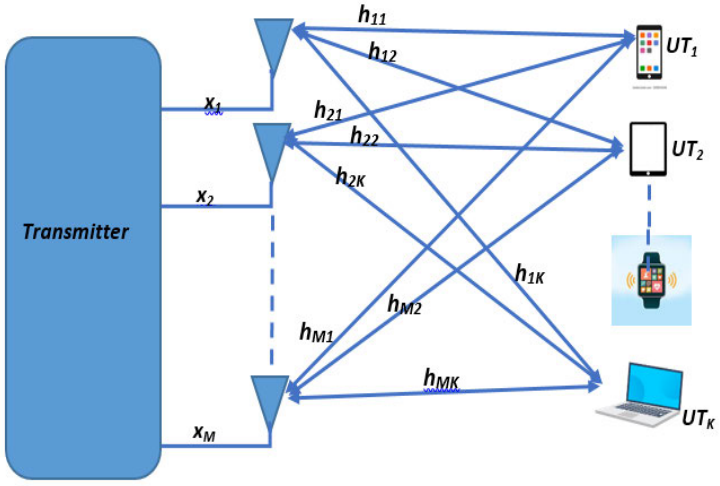

Figure 3.1 Massive MIMO Communication system

of users will vary up to 32 [~~134~~]. For the multicell (MC) system, the number of cell $L > 1$, replicating a single cell scenario in [56]. The received complex baseband signal $y_{j,m} = \sum_{l=1}^{L} h_{l,j,m}^{T} x_{l,k} + n_{j,m}$. Where $x_l \in \mathbb{C}^{M \times 1}$ is the transmit signal vector from the lth BS, $h_{l,j,m} \in \mathbb{C}^{M \times 1}$ is the channel vector from the lth BS to the mth user in the jth cell and $n_{j,m} \sim \mathcal{CN}(0, \sigma^2)$ is the zero-mean AWGN with variance σ^2. The transmit data symbols in MC are precoded as $x_l = \mathbf{W}_l s_l$.The $\boldsymbol{W}_l \in \mathbb{C}^{M \times K}$ is the precoding matrix for the lth cell, and the transmitted symbol vector is $s_l \in \mathbb{C}^{K \times 1}$.

Massive MIMO downlink system is the thesis's focus due to the higher data demand, as users typically download more data than they upload. BSs have greater power capabilities than user devices, making downlink management more feasible. Additionally, downlink scenarios present unique interference challenges and optimization opportunities, crucial for system performance. Advanced beamforming techniques can significantly enhance downlink signal quality and spectral efficiency. Improving downlink performance directly impacts user experience by enhancing the quality and speed of data services[56, 134].

3.3 Channel Model

The basic premise is that the elements exhibit uncorrelated Rayleigh flat fading, meaning that they are i.i.d. zero-mean unit-variance complex Gaussian variables. Notably for the TDD mode, the downlink has the same channel matrix **H** as the uplink if the transmission duration is within the channel coherence time, due to channel reciprocity.

3.4 Analysis of selected Precoding schemes

Several linear and nonlinear precoding techniques as described in Chapter 2 can be used in M-MIMO systems to improve performance and mitigate interference. Each method has its advantages and disadvantages regarding computational complexity and performance. Each precoding technique exhibits distinct trade-offs regarding BER, SE, ASR, and SNR. The choice of precoding technique depends on system requirements, channel conditions, computational complexity, and implementation constraints in a specific communication scenario. Linear precoding techniques, such as zero-forcing precoding, can effectively reduce inter-user interference and improve system performance. While, nonlinear precoding techniques offer promising approaches to address interference and enhance performance but experience higher computational complexity. Overall, the choice of precoding technique depends on the M-MIMO system's specific requirements and constraints. In the next section, a discussion of the chosen precoding approach is given.

3.4.1 Zero-Forcing Precoding

The ZF uses a precoding matrix $\mathbf{W} \in \mathbb{C}^{\mathbf{M}\times\mathbf{K}}$ to acquire a pseudo-inverse of the **H** matrix resulting in the combined channel **HW** for interference-free reception. The pseudo-inverse is utilised due to the fact that **H** is not necessarily a square matrix, meaning the quantity of UE does not always match the quantity of antennas at the BS. P_{tr} is the average transmission power restricted by $\mathbb{E}[\|s\|^2] = tr(\mathbf{W}^{\boldsymbol{H}}\mathbf{W}) = P_{tr}$ and s is the transmitted source of information before precoding . The precoding matrix $\mathbf{W}$ is given by [131], [135]:

$$\mathbf{W} = \mathbf{H}^{\mathrm{H}}(\mathbf{H}^{\mathrm{H}}\mathbf{H})^{-1}, \tag{3}$$

where $\mathbf{W}$ is the Moore-Penrose pseudo-inverse of a matrix. As $\mathrm{P}_{tr} \rightarrow \infty$, $\mathbf{W}_{ZF}$ can be expressed as:

$$\mathbf{W}_{\mathrm{ZF}} = \frac{1}{\beta}\mathbf{H}^{*}(\mathbf{H}^{\mathrm{T}}\mathbf{H}^{*})^{-1}, \tag{4}$$

Where,

$$\beta = \sqrt{\frac{tr(\mathbf{B}\mathbf{B}^{\mathrm{H}})}{\mathrm{P}_{tr}}} \tag{5}$$

Where β is being the scalar of Wiener Filter and,

$$\mathbf{B} = \mathbf{H}^{*}(\mathbf{H}^{\mathrm{T}}\mathbf{H}^{*})^{-1} \tag{6}$$

The ZF precoder is obtained by:

$$\mathbf{W}_{\mathrm{ZF}} = \sqrt{\alpha}\mathbf{H}^{*}(\mathbf{H}^{\mathrm{T}}\,\mathbf{H}^{*})^{-1} \tag{7}$$

Therefore the corresponding received signal vector is defined as:

$$\mathrm{y}_{\mathrm{ZF}} = \sqrt{\rho\alpha}\mathbf{H}^{\mathrm{T}}\mathbf{H}^{*}(\mathbf{H}^{\mathrm{T}}\mathbf{H}^{*})^{-1}s + n \tag{8}$$

Where $(\mathbf{H}^{\boldsymbol{H}}\,\mathbf{H})$ in [136] forms a Gram matrix, whereby the diagonal elements denote power imbalances among the channels. ρ represents the average received power, n is the vector of i.i.d $\mathcal{CN}$ $(0, \sigma_n^2)$ noise. The off-diagonal elements are characterized by the mutual correlations between the channels.

3.4.2 Conventional MMSE precoding

MMSE precoding represents the most efficient linear precoding technique within a massive MIMO downlink framework. The mean square error (MSE) serves as the foundation for this approach. Employing the Lagrangian methodology is essential for the optimization of this precoding scheme, with the average power of individual transmitting antennas serving as a key constraint. The conventional MMSE precoding can be written as:

$$\mathbf{W}_{MMSE} = \rho_{MMSE}\mathbf{H}^{\mathrm{H}}(\mathbf{H}\mathbf{H}^{\mathrm{H}} + (\sigma_n^2.n_t).\mathrm{I_K})^{-1} \quad (9)$$

$$= \rho_{MMSE}\mathbf{H}^{\mathrm{H}}.\mathbf{W}_{MMSE}^{-1}, \quad (10)$$

where $\mathbf{W_{MMSE}} = (\mathbf{H}\mathbf{H}^{\mathbf{H}} + (\boldsymbol{\sigma_n^2}.\boldsymbol{n_t})\mathbf{I_K})$, n_t is the number of transmitting antennas and $\boldsymbol{\sigma_n^2}$ is the noise power. The power normalization factor, denoted as ρ_{MMSE} is essential for ensuring power limitation adherence by MMSE precoding and it can be calculated as:

$$\rho_{MMSE} = \sqrt{\frac{K}{tr(\mathbf{W}_{MMSE}\mathbf{W}_{MMSE}^{H})}} \quad (11)$$

Hence, the vector$\boldsymbol{x}$ of the signal that is sent can be expressed as:

$$x = \mathbf{W}_{MMSE}.s = \mathbf{W}_{MMSE}\mathbf{H}^{\mathrm{H}}.\mathbf{W}_{MMSE}^{-1}.s \quad (12)$$

We can see from (10) that a matrix $\mathbf{W_{MMSE}}$ inversion of $K \times K$ size is essential, which indicates an unexpected high computational complexity and is not desirable. The hardware resource would be significantly wasted if we compute the inversion directly. Therefore, merging the property of matrix $\mathbf{W_{MMSE}}$ with known Sherman-Morrison lemma [4] and Cholesky-Decomposition [63], a less complicated precoding scheme to solve this difficulty[127] can be designed. The advantages of MMSE are covered in [6]. Linear

precoding at a fundamental level may also utilize matrix inversion approximation to reduce computational complexity.

3.4.3 Neumann Series Approximation

A methodology introduced by [69] employs a linear precoder that utilizes Neumann series expansion-based precoding to address the computational demands of inverting large complex matrices. This approach leverages matrix principles to streamline operations and reduce hardware costs. The initial matrix in the Neumann series is a diagonal matrix $\mathbf{W}$. When dealing with non-diagonal matrices, the NSA technique divides matrix into a diagonal element matrix $\mathbf{X}$ and a non-diagonal element $\mathbf{E}$. As indicated by [69, 130], this decomposition process necessitates additional iterations to achieve the desired level of performance. The Gram matrix $\mathbf{W} \in \mathbb{C}^{K\times K}$ to be inverted is approximated as a sum of matrix polynomial described as:

$$\mathbf{W}^{-1} \approx \sum_{t=0}^{\infty} (\mathbf{I}_{\mathrm{K}} - \mathbf{X}^{-1}\mathbf{W})^{t}\, \mathbf{X}^{-1}, \tag{13}$$

where $\mathbf{X}^{-1} \in \mathbb{C}^{K\times K}$ is the matrix of the initial estimate of $\mathbf{W}^{-1}$ and $\mathbf{I}_{\mathrm{K}}$ is the identity matrix $K \times K$. The matrix $\mathbf{X}^{-1}$ must satisfy the condition in Eq. (14).

$$\lim_{t\to\infty} (\mathbf{I}_{K} - \mathbf{X}^{-1}\mathbf{W})^{t} \cong 0 \tag{14}$$

The bounds of convergence in Eq. (14) and the accuracy of the approximation for a given number of terms (t) depends on the size of the eigenvalues of ($\mathbf{I}_{K} - \mathbf{X}^{-1}\mathbf{W}$). Smaller eigenvalues lead to faster convergence. The derivation and discussion follow [131]. The series converges faster when the eigenvalues of the matrix (13) are close to 1. For practical systems with finite dimensions (M) and (K), eigenvalues may lie outside the ideal range.

A modification is introduced to improve convergence by pre-conditioning the matrix $\mathbf{W}$ with a diagonal matrix $\boldsymbol{D}$, optimizing $\boldsymbol{D}$ to minimize the eigenvalues' magnitudes. For practical implementation of matrix inversion using the Neumann series, the number of iterations (T) should be finite or kept small.

$$\mathbf{W}^{-1} \approx \sum_{t=0}^{T} (-\boldsymbol{D}^{-1}\boldsymbol{E})^{t}\, \boldsymbol{D}^{-1} \tag{15}$$

The polynomial expansion in (15) converges to the matrix inverse $\mathbf{W}^{-1}$ if

$$\lim_{t\to\infty} (-\boldsymbol{D}^{-1}\boldsymbol{E})^{t} \cong 0 \tag{16}$$

In practical applications, a limited number of terms is used, leading to a set number of iterations of equation (15). As the number of iterations (t) increases, the accuracy of the matrix inverse improves, but this comes with the trade-off of increased computational complexity. Essentially, more iterations result in higher precision but require more computational resources.

3.4.4 Tomlinson-Harashima Precoding

Tomlinson-Harashima Precoding (THP) [137] is a pre-equalization method that was initially introduced for channels afflicted by inter-symbol interference (ISI). Despite THP exhibiting a degradation in performance when compared to DPC, as evidenced in previous studies [138], it can serve as a cost-efficient alternative to DPC in practical applications [92]. As revealed in [23], the configuration of THP has been likened to the reciprocal of the SIC method employed during reception. There are two fundamental THP configurations according to the positions of the diagonally weighted filter.

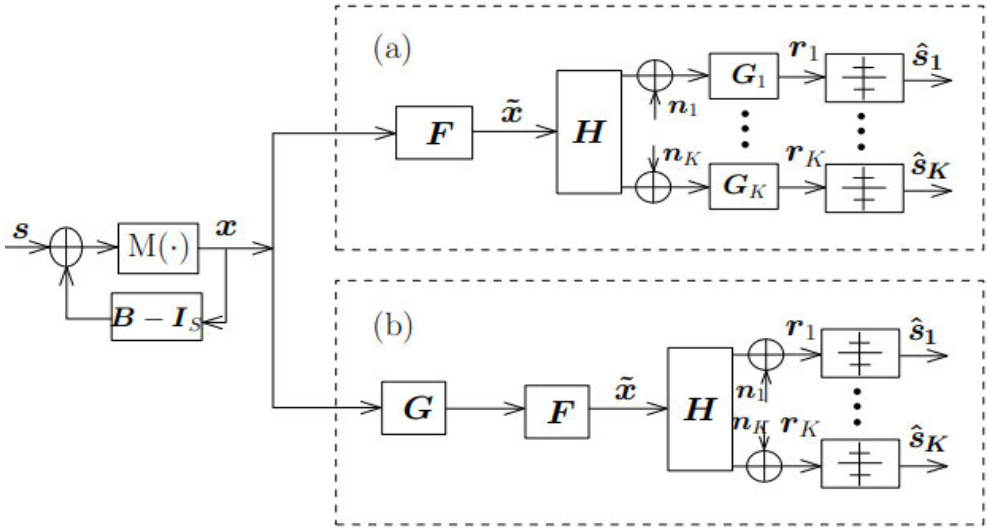

Figure 3.2 Two basic THP Structures, (a) Decentralised THP and (b) Centralised THP

These configurations consist of decentralized filters positioned at the receivers and centralized filters situated at the transmitter, known as dTHP or cTHP, respectively [42],[139].

Typically, the THP algorithm combines three filters, namely the feedback filter $\mathbf{B} \in \mathbb{C}^{S\times S}$, the feedforward filter $\mathbf{F} \in \mathbb{C}^{S\times S}$, and finally the scaling matrix $\mathbf{G} \in \mathbb{C}^{S\times S}$. Where s represents the total number of transmitted streams. Figure 3.2 delineates the two primary THP structures based on the placement of $\mathbf{G}$. The decentralized THP (dTHP) utilizes $\mathbf{G}$ (or its submatrices) at the receivers, while the centralized THP (cTHP) employs $\mathbf{G}$ at the transmitter.

The feedback filter **B** is employed to consecutively eliminate the interference generated by the preceding streams from the present stream. Therefore, the feedback filter Matrix **B** is characterized as a lower triangular matrix wherein the main diagonal elements are all equal to one [23]. The scaling filter **G** includes the subsequent weighted coefficient for each stream, thereby having a diagonal structure. The variable x represents the channel symbol after the precoding, where $x = \boldsymbol{F}x$ for dTHP and $x = \boldsymbol{FG}x$ for cTHP. The received signal after the **B**, **F**, and the **G** for the dTHP and cTHP is represented respectively by:

$$r^{dTHP} = \mathbf{G}(\mathbf{HF}x + n) \tag{17}$$

$$r^{cTHP} = \beta\left(\mathbf{H} \cdot \frac{1}{\beta}\mathbf{FG}x + n\right) \tag{18}$$

Where, $\boldsymbol{x} \in \mathbb{C}^{\boldsymbol{s}\times\mathbf{1}}$ is the merged transmit channel signal, and $n = [n_1^T, n_2^t \cdots, n_K^T]^T \in \mathbb{C}^{\boldsymbol{S}\times\mathbf{1}}$ is the Gaussian noise vector combined with i.i.d. entries of zero mean and variance σ_n^2. The factor β is used to implement the power restriction $\mathbf{E} \parallel \tilde{\boldsymbol{x}} \parallel^{\mathbf{2}} = \boldsymbol{\xi}$, whereby $\boldsymbol{\xi}$ is the average transmitted power.

In literature [140], a **QR** decomposition can efficiently implement SIC detection. Whereas an **LQ** decomposition can implement THP. By applying an **LQ** decomposition on the channel matrix **H**, we have:

$$\mathbf{H} = \mathbf{LQ} \tag{19}$$

Where, $\mathbf{Q}$ is a unitary matrix (by unitary, $\mathbf{Q^H Q} = \mathbf{QQ^H} = \boldsymbol{I}$) and $\mathbf{L}$ is a lower triangular matrix. Consequently, the filters for the THP algorithm are defined as:

$$\mathbf{F} = \mathbf{Q}^{\mathrm{H}} \tag{20}$$

$$\mathbf{G} = diag\left[l_{1,1}, l_{2,2}, \cdots, l_{S,S}\right]^{-1} \tag{21}$$

$$\mathbf{B}^{dTHP} = \mathbf{GL}, \mathbf{B}^{cTHP} = \mathbf{LG} \tag{22}$$

where $\boldsymbol{l_{i,i}}$ is the ith diagonal element of the matrix **L**. As depicted in Figure 3.2, the transmitting symbols, x_i , are consecutively produced as:

$$x_i = s_i - \sum_{j=1}^{i-1} b_{i,j}x_j\,, i = 1, \cdots, S \tag{23}$$

Where, s_i is the ith transmit data with variance $\boldsymbol{\sigma_s^2}$ and $\boldsymbol{b_{i,j}}$ are the elements of **B** in row $\boldsymbol{i}$ and column $\boldsymbol{j}$. From Eq. (23), the transmission power will experience a notable rise when the amplitude of $\boldsymbol{x_i}$ surpasses the modulation boundary through consecutive cancellation. To limit the amplitude of the channel symbol x_i within the modulation alphabet boundaries, a modulo operation $\mathbf{M}(\cdot)$ must be employed, which is represented as:

$$\mathbf{M}(x_i) = x_i - \left\lfloor \frac{\Re(x_i)}{\tau} + \frac{1}{2} \right\rfloor \tau - j \left\lfloor \frac{\Im(x_i)}{\tau} + \frac{1}{2} \right\rfloor \tau \qquad (24)$$

Where, τ is a constant utilized for the cyclic expansion of the constellation, with its precise magnitude of τ determined by the selected modulation alphabet. Conventional preferences for τ are $\tau = 2\sqrt{2}$ for QPSK symbols and $\tau = 8\sqrt{10}$ for rectangular 16-QAM when the symbol variance is one [4]. The modulo operation can be interpreted as the addition of a perturbation vector $\boldsymbol{d}$ to the transmitted data $\boldsymbol{s}$, to ensure the modified transmit data is given as:

$$v = s + d \qquad (25)$$

Hence, the original signal representation is recurrently expanded, leading to the selection of transmit data symbols v_k from the enlarged collection.

The utilization of the modulo function is applied to confine the amplitude of $\boldsymbol{x}$ within a similar scale as that of $\boldsymbol{s}$ (a power loss is caused by the nonlinear processing of THP), which can be quantified by $\boldsymbol{\alpha} = \mathbf{M}/(\mathbf{M}-\mathbf{1})$ for the M-QAM constellations [141]. Although the power deficit is considerable for small modulation sizes, it becomes insignificant for moderate sizes of when approaches infinity. Furthermore, a modulo loss is induced by THP due to potential misinterpretation of received symbols at the boundary of a constellation as symbols at the opposite boundary [138]. Particularly, the modulo loss is notably more pronounced for the small constellations. The power and modulo loss are disregarded in our study as we utilize moderate sizes of **M**. Consequently, we obtain the expression $\mathbf{E} \parallel \mathbf{x} \parallel \approx \mathbf{E} \parallel \mathbf{s} \parallel$. The multiplication of the unitary matrix $\boldsymbol{F}$ does not alter the norm of $\boldsymbol{x}$, hence the

normalization factor β is deemed unnecessary for dTHP. In the case of cTHP, where the power and modulo loss are negligible, the normalization factor can be approximated as:

$$\beta = \frac{\mathbf{E} \parallel \mathbf{FG}\mathrm{x} \parallel}{\mathrm{E} \parallel \mathrm{s} \parallel} \approx \sqrt{\sum_{i=1}^{S} \left(1/l_{i,i}^{2}\right)} \tag{26}$$

The feedback processing corresponds to an inversion operation given by $\boldsymbol{B} - \mathbf{1}$. Therefore, the transmitted symbol x can be defined by:

$$x = B^{-1}v = \mathbf{B}^{-1}(s + d) \tag{27}$$

Subsequently, the signal received for dTHP and cTHP can be individually represented as:

$$r(dTHP) = v + \mathrm{G}n, \tag{28}$$

$$r(cTHP) = v + \beta n. \tag{29}$$

From Eq. (28) and Eq. (29), it is observable that the THP has the capability to transmit the MU-MIMO channel into a correspondent parallel SISO channel as Block Diagonal or BD-type precoding. The pseudo code to implement THP is shown in Appendix C.

3.4.5 Lattice Reduction (LR)

The concept of lattice has found application across various mathematical disciplines including algebra, geometry, and group theory, as well as in engineering domains like image processing and wireless communications signal processing [132]. The significance of lattice reduction has notably increased in numerous engineering sectors, particularly in the realm of communication signal processing.

LR involves the identification of a lattice bases characterized by vectors that exhibit greater orthogonality and shorter lengths in comparison to the original vectors, based on the Euclidean norm. The most effective techniques for reduction include Minkowski or Hermite-Korkine-Zolotareff reductions, despite their drawback of higher computational expenses.

Both approaches necessitate the computation of the shortest lattice vector [133]. In order to simplify LR methods, Lenstra-Lenstra and Lovász (LLL) algorithm introduced a polynomial time algorithm for computation. This algorithm serves as an expansion of Gauss reduction or a lessening of Hermite-Korkine-Zolotareff conditions, achieving the reduced basis through the application of two distinct operations on the original foundation: size-reduction (an arrangement of linear combination between columns) and column interchange. Despite the subsequent introduction of various other reduction techniques, the LLL algorithm remains the most commonly utilized due to its exceptional balance between performance and computational intricacy [142].

3.4.5.1 LLL algorithm

The lattice structure is represented by a set of linearly independent vectors, $\boldsymbol{b_1}, \cdots\cdots, \boldsymbol{b_m} \in \boldsymbol{\mathcal{L}}$ as:

$$\mathcal{L}(\mathbf{B}) = \{\mathbf{B}_z,\ \ z \in \mathbb{Z}^{\boldsymbol{m}}\} \tag{30}$$

where $\mathbf{B} = [b_1, \cdots\cdots, b_m]$ is the basis matrix of the lattice. For the LLL algorithm, we let $\mathbf{B}^* = (b_1^*, \cdots\cdots, b_m^*) \in \mathbb{R}^{n\times m}$ represents the related orthogonal basis of B. This is calculated by the Gram-Schmidt Orthogonalisation (GSO) and is represented by:

$$b_1^* = b_1 \tag{31}$$

$$b_1^* = b_i - \sum_{j=1}^{i-1} \mu_{i,j} b_j^* \quad \text{for } 2 \le i \le m, \tag{32}$$

Where,

$$\mu_{i,j} = \frac{b_i, b_j^*}{\left\|b_j^*\right\|^2} \qquad \text{for } 1 \le j < i \le n \tag{33}$$

Thus, matrix **B** can be defined as:

$$\mathbf{B} = \boldsymbol{B}^{*}.\mathbb{U}^{T} \tag{34}$$

Where matrix $\mathbb{U} = [\mu_{i,j}] \in \mathbb{R}^{\boldsymbol{m}\times\boldsymbol{m}}$ is lower triangular with unit diagonal.

B is called LLL-reduced if a lattice $\boldsymbol{\mathcal{L}}$ with basis $\boldsymbol{B} \in \mathbb{C}^{\boldsymbol{n}\times\boldsymbol{m}}$, associated orthogonal basis $\mathbf{B}^{*} \in \mathbb{C}^{\boldsymbol{n}\times\boldsymbol{m}}$ and Gram-Schmidt coefficients $\mu_{i,j}$, satisfy the following conditions:

$$|\mu_{i,j}| \leq \frac{1}{2} \qquad \text{for } 1 \leq \mathrm{j} < \mathrm{i} \leq \mathrm{n} \tag{35}$$

$$\left\|b_i^{*} + \mu_{i,i-1}b_{i-1}^{*}\right\|^2 \geq \delta\|b_{i-1}^{*}\|^2 \quad \text{for } 1 < i \leq \mathrm{n}, \frac{1}{4} < \delta < 1 \tag{36}$$

The condition in Eq. (36) can be represented as:

$$\|b_i^{*}\|^2 \geq \left(\delta - \mu^2{}_{i,i-1}\right)\|b_{i-1}^{*}\|^2 \qquad \text{for } 1 < i \leq \mathrm{n}, \frac{1}{4} < \delta < 1 \tag{37}$$

The value of delta is typically given as $\delta = ¾$, which may affect the quality and associated computational complexity of the LLL algorithm. Although a delta value of $\delta = 1$ results in a lattice with the best orthogonal properties, it is not often employed since the algorithm might not execute in polynomial time.

Appendix A shows the original LLL algorithm. Inputs to the algorithm is a matrix containing the basis vectors, $\mathbf{B} = [\mathrm{b}_1, \cdots\cdots, \mathrm{b}_m]$, and the reduction parameter δ. The original basis B is overwritten by the reduced basis $\widetilde{\mathbf{B}}$ in the transformed algorithm Mathematical transformations performed on matrix $\boldsymbol{B}$ are registered in matrix T.

$$\widetilde{\mathbf{B}} = \mathbf{TB} \tag{38}$$

Whereby, **T** define as an unimodular matrix with integer elements, $|\boldsymbol{det}(\boldsymbol{T})| = 1$.

The LLL algorithm utilises two distinct procedures: SizeReduction(*k,l*) and Swap(*k*). The SizeReduction*(k,l)* procedure establishes the absolute value of $\mu_{i,j} \leq 0.5$. If the condition is met, the procedure halts. Alternatively, the design decreases b_k by subtracting an integer μ times b_l. To ensure that the new value of b_k remains within the lattice, it is necessary to round $\mu_{k,l}$ to the nearest integer, denoted as μ. Next, the GSC undergoes an update. The

Swap(*k*) procedure performs a vector swap between b_k and b_{k-1} while also updating the orthogonal basis and the GSC.

During the primary iteration of the procedure, *size reductions* implemented on consecutive vectors. If the condition specified in (37) is satisfied, ***size reductions*** will occur between the current and previous vectors. This results in an increment of the index k. If this condition is not satisfied then a vector swap is performed, and k is decreased. The termination of the algorithm is not trivial, however it has been proven to execute in polynomial time [143],[144].

3.5 Model of imperfect CSI

Complete interference suppression can be achieved by employing precoding techniques at the transmitter, provided that accurate Channel State Information at the Transmitter (CSIT) is accessible. Nevertheless, it is unattainable in real-world scenarios. In real-world situations, the accuracy of CSI is frequently compromised by various factors, including errors in channel estimation, quantization, delays in feedback, and limited feedback capacity. Channel estimation requires the precise estimation of the channel matrix that exists between the source and receiver. In practice, estimation errors can arise from noise, interference, and the constraints of limited training resources. Creating a CSI model with imperfections requires incorporating practical deviations into the channel understanding. ZF, MMSE, NSA, THP, and LR-LLL techniques have been extensively researched in the context of perfect CSIT. However, the current study also focuses on understanding the impact of imperfect CSIT application.

The channel matrix estimated as $Hhat$ ($\widehat{\mathbf{H}}$) differs from the actual channel matrix **H**. An imperfect channel matrix is defined as:

$$\widehat{\mathbf{H}} = \mathbf{H} + \varepsilon \tag{39}$$

Where **H** denotes the actual channel matrix. $\mathcal{E}$ is the error matrix whose entries are i.i.d zero-mean unit-variance complex Gaussian variables which are independent of **H.** Therefore, the precoding design at the BS is obtained from $\widehat{\mathbf{H}}$.

3.6 Channel Estimation

Channel estimation is a crucial aspect of wireless communication systems, and imperfections in CSI estimation can significantly impact system performance. Section 3.2 modelled the system under the assumption of perfect CSI. Here, the model for channel estimation in the presence of imperfections is as follows:
Assuming a perfect channel model **H** and an imperfectly estimated channel $\widehat{\mathbf{H}}$ at the received signal r can be derived as:

$$r = \widehat{\mathbf{H}}\, x + n \tag{40}$$

Where, $\widehat{\mathbf{H}}$ defines the estimated channel response, $\boldsymbol{x}$ is the transmitted signal and the variable n denotes the additive white Gaussian noise.

The estimation error $\mathcal{E}$ is specified as the deviation between the true channel, given as **H** and the estimated channel denoted by $\widehat{\mathbf{H}}$ **:**

$$\mathcal{E} = \mathbf{H} - \widehat{\mathbf{H}} \tag{41}$$

Less common yet important matrices and mathematics tools that can provide deeper insight in the analysis of M-MIMO systems, include the covariance matrix of channel estimates and effective channel matrix. Covariance matrix of channel estimates captures the uncertainty in channel estimates due to pilot contamination or noise and effective channel matrix combines the effects of channel estimation errors and the actual channel state. The combination of covariance matrix of channel estimates and the effective channel matrix contribute in understanding the estimation error, optimising pilot sequences and important for analysing the performance degradation due to imperfect CSI.

Covariance matrix of channel estimates can be expressed as**:**

$$\boldsymbol{C}_{\hat{H}} = \sigma^2 \boldsymbol{I} + \boldsymbol{\zeta} \tag{42}$$

Where σ^2 is the noise variance, **I** is the identity matrix and $\boldsymbol{\zeta}$ is the spatial correlation matrix of the channel, expressed as $\boldsymbol{\zeta} = \mathbb{E}[\mathbf{h}\mathbf{h}^{\mathrm{H}}]$, as **h** is the channel vector. The effective channel matrix can be modelled as (39):

$$\boldsymbol{H}_{\boldsymbol{eff}} = \boldsymbol{H} + \boldsymbol{\mathcal{E}} \tag{42}$$

Where $\mathcal{E}$ represents the estimation error, which can be modeled as a zero-mean Gaussian random variable with covariance $\boldsymbol{C}_{\hat{H}}$**.** The estimated channel $\widehat{\mathbf{H}}$ can be obtained through Least Squares (LS) Minimum Mean Square Error (MMSE) or channel estimation procedures.The LS channel estimator, also referred to as a zero-forcing estimator, is a straightforward and conventional channel estimator that assumes a Gaussian distribution. For MMSE estimation, use the covariance matrix $\boldsymbol{C}_{\hat{H}}$ to improve the accuracy of the channel estimates:

$$\widehat{\mathbf{H}}_{\mathrm{MMSE}} = \mathbf{H} + \boldsymbol{C}_{\hat{H}} \boldsymbol{H}^{H} (\mathbf{H}\mathbf{H}^{\mathrm{H}} + \sigma^2 \boldsymbol{I})^{-1} \tag{43}$$

Now, we can model the estimation error as the difference between the true channel and the estimated channel:

$$\mathcal{E}_{\mathrm{MMSE}} = \mathbf{H} - \widehat{\mathbf{H}}_{\mathrm{MMSE}} \tag{44}$$

3.7 Bit-Error-Rate

Modelling BER for an imperfect CSI in a wireless transmission system with 16-QAM and 64-QAM modulation involves considering both the estimation error and the noise in the system. The model assumes additive white Gaussian noise.

Let r be the received signal and $\boldsymbol{s}$ is the transmitted signal. In addition, $\boldsymbol{n}$ denotes the noise, $\widehat{\mathbf{H}}$ represents the estimated channel, and finally the estimation error is defined by $\boldsymbol{\mathcal{E}}$. The received signal can be expressed as in Eq. (40). For 64-QAM, the BER can be modelled using similar approach as 16-QAM in [145], but with different coefficients and arguments for the complementary error function (erfc). Eq, (44) is the general form of the BER for 64-QAM:

$$\mathrm{BER}_{64-\mathrm{QAM}} = \frac{7}{24}\mathrm{erfc}\left(\sqrt{\frac{1}{42}SINR_K}\right) + \frac{1}{4}erfc\left(\sqrt{\frac{9}{42}SINR_K}\right) + \frac{1}{8}erfc\left(\sqrt{\frac{25}{42}SINR_K}\right) \tag{45}$$

Here, the first term accounts for the probability of error for one set of signal points in the 64-QAM constellation. The second term represents the probability of error for another set of signal points. The third term adjusts the overall error probability by considering another set of signal points. The $erfc(x) = \frac{2}{\sqrt{\pi}}\int_x^{\infty} e^{-j^2}\, dj$ is the complementary error function used to model the probability of bit errors based on the SINR [9]

$$\mathrm{SINR}_{\mathrm{dB}} = 10\log_{10}\left(\frac{\mathbf{P_S}}{\mathbf{P}_{\boldsymbol{i}} + \mathbf{P}_{\boldsymbol{n}}}\right) \tag{46}$$

Where $(\mathbf{P_S})$ is the power of the desired signal, $(\mathbf{P}_{\boldsymbol{i}})$ is the total power of the interfering signals and $(\mathbf{P}_{\boldsymbol{n}})$ is the power of the background noise.

3.8 Spectral Efficiency

Spectral Efficiency (SE) is a critical over-the-air (OTA) system metric, representing the data rate achievable per unit bandwidth. Due to estimation errors and noise, affecting the CSI, the theoretical formula for SE can be modelled as follows:

$$\mathrm{SE} = \frac{R}{Bw} \tag{47}$$

where **R** is the data rate or throughput and Bw is the bandwidth. The data rate can be expressed in terms of the modulation scheme (16-QAM or 64-QAM) and the channel conditions, considering estimation errors and noise. The Shannon-Claude theorem (47) is often used for this purpose [56]

$$\mathbf{R} = Bw \log_2(1 + \mathrm{SNR}) \quad \text{(bits/s/Hz)} \tag{48}$$

The SNR in the presence of channel estimation errors can be modified as:

$$\mathrm{SNR} = \left(\frac{\mathbf{P_S}}{\mathbf{P_i} + \mathbf{P_n}}\right) \tag{50}$$

Where, $\mathbf{P_S}$ is the true channel power, $\mathbf{P_i}$ is the power of the channel estimation error and $\mathbf{P_n}$ is the noise power. The SE expression now becomes:

$$\mathrm{SE} = \frac{Bw\, log_2\left(1 + \frac{\boldsymbol{P_S}}{\boldsymbol{P_i} + \boldsymbol{P_n}}\right)}{Bw} \tag{51}$$

Simplifying, the bandwidth Bw cancels out, and the final expression for SE is:

$$SE = \log_2\left(1 + \frac{\boldsymbol{P_S}}{\boldsymbol{P_i} + \boldsymbol{P_n}}\right) \tag{49}$$

This formula gives the SE of the wireless communication system considering both channel estimation errors and noise, and it can be applied for both 16-QAM and 64-QAM modulation schemes.

3.9 Conclusion

In conclusion, we have established a robust framework for investigating precoding schemes in M-MIMO systems. This chapter has been instrumental in laying the groundwork for the subsequent analysis of system models, channel behaviours, and the impact of imperfections on precoding schemes. We initiated our exploration by defining a comprehensive system model, outlining the essential components of our M-MIMO communication system. The subsequent section in the chapter delved into the intricacies of channel modelling, providing a detailed analysis of various precoding schemes under consideration. We carefully examined the mathematical aspects of each precoding scheme, in the context of M-MIMO. The model of imperfect channels using precoding schemes aligns with simulation scenarios, allowing us to evaluate the robustness of precoding methods in the presence of these imperfections. In the subsequent chapters, we will leverage this methodological foundation to conduct simulations and analyses that deepen our insights into the performance of precoding schemes.

4 Results and Analysis

4.1 Introduction

This chapter presents a thorough performance comparison and analysis of the precoding algorithms under study to ensure a thorough understanding. The simulation is conducted using various methodologies depending on the specific performance metric. Three performance metrics are utilised: bit error rate (BER), spectral efficiency (SE), and achievable sum rate (ASR). The sum capacity that can be achieved is determined by calculating the average capacity attained by each user in the cell. Meanwhile, the BER represents the likelihood of receiving an incorrect bit. This investigation focuses on a system previously defined in Chapter 3. The simulation utilised both 16-QAM and 64-QAM modulation, with signal-to-interference-plus-noise ratio (SINR) results range from 0 dB to 40 dB. The MATLAB® code listing is shown in Appendix B.

To examine the efficacy of the PiC on the defined performance metrics, a network scheme is evaluated under two scenarios. The first scenario assumes that the channel state information at the transmitter (CSIT) is free from corruption. The second scenario considers the corruption of CSIT due to pilot signals transferred by user equipment (UE) in the co-channel cells. In addition, we analyse the impact of PiC when the UE in the target cell is distributed throughout the cell.

The area throughput is an essential performance measure for modern cellular networks. The measurement is expressed in $bit/s/km^2$ and can be represented using Eq. (52) from [39]

$$\begin{aligned} &Area\ throughput\ [bit/s/km^2\ ] \\ &\qquad = Bw\ [Hz]\ \cdot\ De\ [cells/km^2\ ]\ \cdot\ SE\ [bit/s/Hz/cell] \end{aligned} \tag{50}$$

Given the variables Bw, De, and SE, we can determine the relationship between bandwidth, average cell density (De), and spectral efficiency per cell. The SE represents the quantity of data transmitted within a one second (1s) across a bandwidth of 1 Hz. The area throughput

in future cellular networks can be increased by focusing on these three main components. By improving these components, higher area throughput can be achieved. Maximising the attainable SE is crucial for the development of communication systems. The channel capability establishes the utmost SE, as defined by Claude Shannon [146], [147].
The ergodic achievable rate is given in [56]

$$\mathbf{R}_{j,m} = \log_2\left(1 + \mathrm{SINR}_{j,m}\right) \tag{51}$$

after manipulations the $SINR_{j,m}$ achieved by each user, k, is given by:

$$SINR_{j,m} = \frac{\left|E\left(h_{j,j,m}^{T}\, w_{j,m}\right)\right|^2}{\sum_{l,k} E\left[\left|\left(h_{l,j,m}^{T}\, w_{l,k}\right)\right|^2\right] - \left|E\left(h_{j,j,m}^{T}\, w_{j,m}\right)\right|^2 + \sigma^2} \tag{52}$$

- where w is the precoding vector at the mth user in the jth cell and the noise power at the receiver is represented as σ^2. Finally, the BER is computed using Eq. (55) for the 64-QAM (64-ary quadrature amplitude modulation), and 16-QAM modulation in (54). 64-QAM is ideal for high-data-rate applications where the channel conditions are favourable. But requires more complex receivers and higher SNR to decode the signal accurately. 64-QAM is applicable where channel conditions are relatively good, such as in LTE, cable modems and Wi-Fi standards. While, 16-QAM is a good choice when you need a balance between data rate and robustness. 16-QAM is more robust to noise and interference, making it suitable for more challenging environments such as some Wi-Fi standards and digital Television broadcasting [110].

$$\begin{aligned}\mathrm{BER}_{16-\mathrm{QAM}} = \frac{3}{8}\mathrm{erfc}\left(\sqrt{\frac{1}{10}SINR_K}\right) + \frac{1}{4}erfc\left(\sqrt{\frac{9}{10}SINR_K}\right) \\ -\frac{1}{8}erfc\left(\sqrt{\frac{5}{2}SINR_K}\right)\end{aligned} \tag{55}$$

4.2 Channel estimation error

The computation involves evaluating the Normalised Mean-Square Error (NMSE) of the estimate to analyse the impact of PiC on channel estimation. The NMSE quantifies the level of accuracy in channel estimation.

The calculation is performed using:

$$NMSE = \frac{E\left[\left|\mathbf{H} - \widehat{\mathbf{H}}\right|^2\right]}{E[|\mathbf{H}|^2]} \tag{53}$$

Where $\boldsymbol{H}$ and $\widehat{\boldsymbol{H}}$ are previously defined in Section 3.6. The decrease in NMSE value indicates an improvement in the accuracy of channel estimation.

4.3 Results for BER

This section will compare several precoders' Bit Error Rate (BER) performance in a M-MIMO system. Specifically, we will analyse the fundamental linear precoder MMSE. Further analyses will be conducted on the precoder based on matrix inversion approximation (NSA), the nonlinear LLL-aided ZF, and finally on the optimal Tomlinson-Harashima (TH) precoder. Our focus will be on a 16×16 and 32×32 system configuration. Analysis regarding signal-to-noise (SNR) ratios within a single cell as conducted in MATLAB® simulation environment. A channel known as additive white Gaussian noise (AWGN) is employed for the modulation techniques of 16-QAM and 64-QAM. The BER is determined by averaging the results from 10,000 Monte-Carlo trials and 100 iterations.

Figure 4.1 compares BER performance in Rayleigh fading channels. The effectiveness of different precoding strategies in reducing the BER is significantly affected by the limited number of antennas available at the base station. In practical scenarios, this limitation leads to a noticeable drop in performance. Essentially, with fewer antennas, the base station has less flexibility and capability to optimize signal transmission, resulting in higher error rates. However, the nonlinear precoders LLL aided ZF, and the TH precoder exhibited superior performance compared to the linear precoders, with NSA showcasing pronounced overall

system deterioration. Enhanced operation is achieved through increased computational complexity. The THP algorithm shows its resilience as the LLL-aided Zero Forcing technique gradually catches up with the SNR improvement. When comparing linear precoders, it is evident that MMSE outperforms NSA in performance. The NSA algorithm is computationally efficient, but it trades off optimality. Additionally, it is susceptible to interference and imprecision in the process of determining the characteristics of the communication channel. The NSA converges under certain conditions, such as when the norm of the operator is less than one. These conditions are not strictly met, therefore the series may diverge or show increasing behavior before stabilizing.

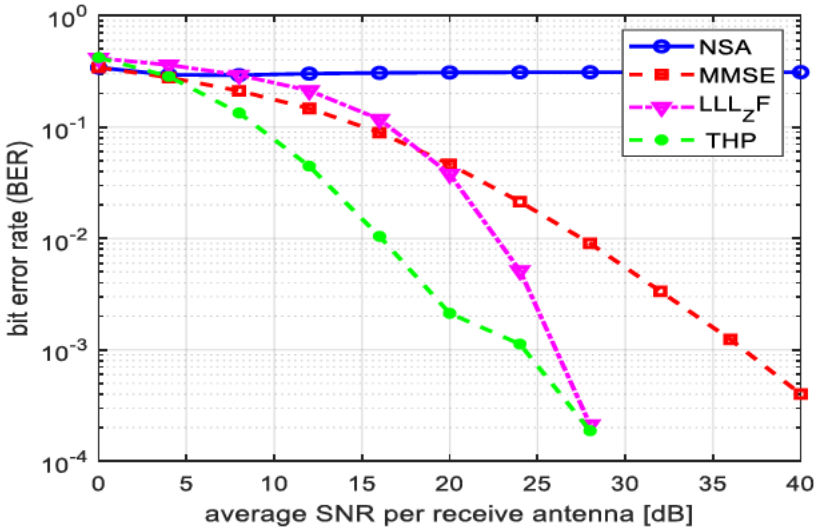

Figure 4.1 BER Comparison

Figure 4.2 and Figure 4. depicts the BER performance with 16 BS antennas and 16 User Equipment (UEs). The performance of the LLL-aided ZF nonlinear precoder in (16-QAM) modulation surpasses that of MMSE and NSA, resulting in a significant gain. The lattice reduction technique helps to mitigate the effects of noise and channel estimation errors, providing a more robust solution for interference suppression. LR, specifically using the Lenstra-Lenstra-Lovász (LLL) algorithm, can enhance the performance of ZF precoding and helps in making the channel matrix more well-conditioned, making the ZF precoder more adaptable to a wider range of channel conditions. Regarding 64-QAM, utilising LLL-aided ZF can result in an approximate 8 dB increase in gain compared to MMSE

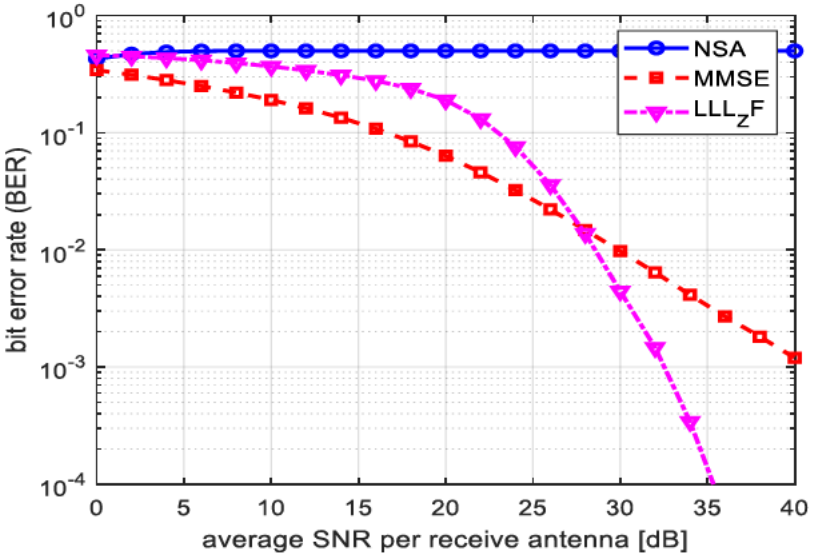

Figure 4.2 16 Transmit Antennas, 16 UEs at 16-QAM

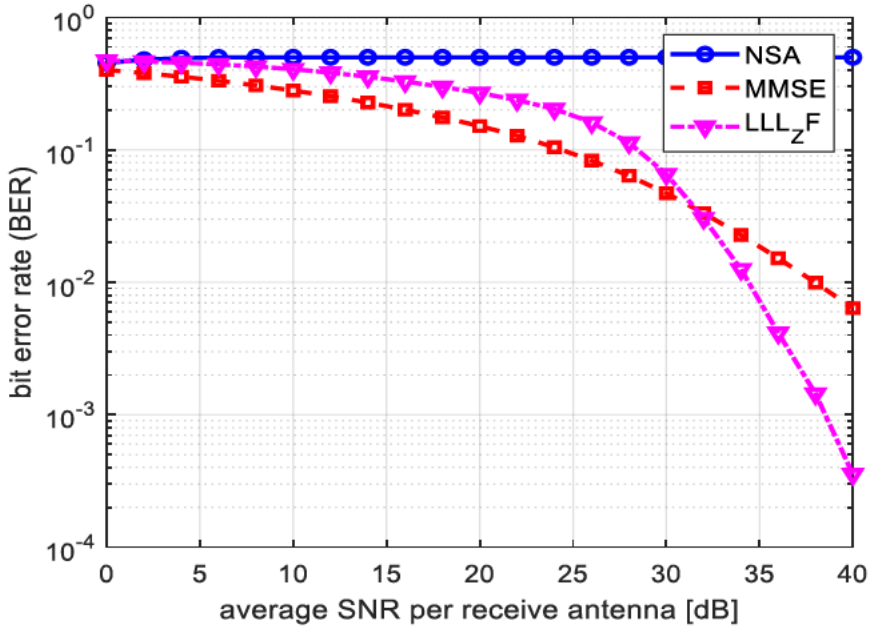

Figure 4.3 16 Transmit Antennas, 16 UEs at 64-QAM

Figure 4. and Figure 4. depict the simulation of transceivers in 32-user massive MIMO systems. In this case, the nonlinear LLL-aided ZF precoder demonstrates significant improvement compared to the linear MMSE and NSA for both systems, regardless of whether lower or higher-order modulations are used. LLL-aided ZF enhances the effective channel condition by reducing the channel matrix's condition number. In scenarios with fewer antennas, the channel matrix might be more ill-conditioned, and the LR technique helps make it more favourable for precoding. The behaviour of the BER curve observed between MMSE and LLL-ZF as the number of antennas varies demonsrate that the system performance is near optimal. As the number of transmit antennas increase from 16 to 32, the SNR increase from 28 dB to 38 dB. Thi means that as the transmitting antennas increses, MMSE can better manage interference, resulting to a gradual improvement in BER. While the LLL-ZF can effectively reduce interference leading to noticeable improvement in BER.

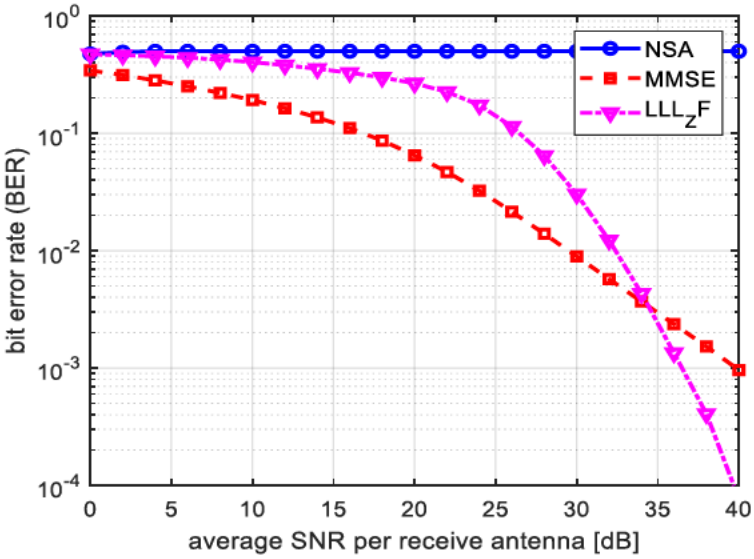

Figure 4.4 32 Transmit Antennas, 32 UEs at 16-QAM

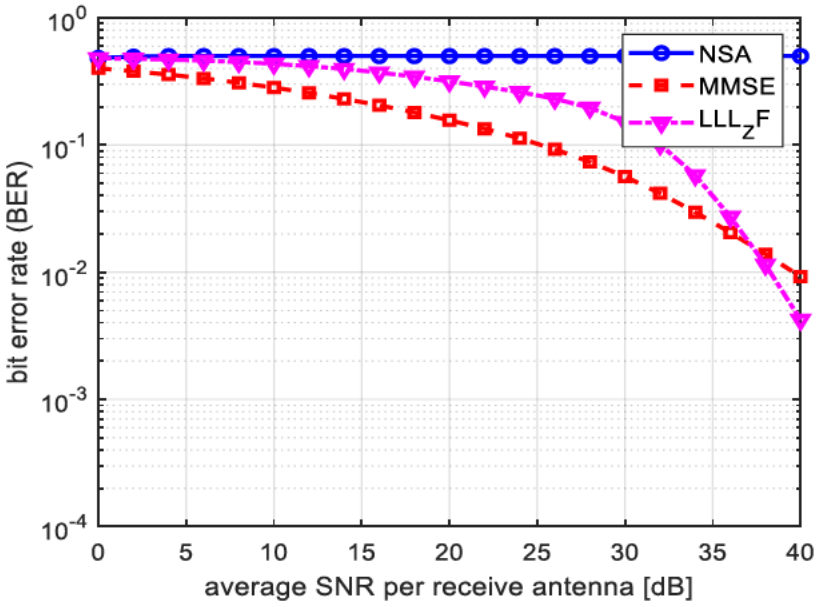

Figure 4.5 32 Transmit Antennas, 32 UEs at 64-QAM

The BER performance across various SNR thresholds for different antenna configurations using 16-QAM and 64-QAM modulation schemes is illustrated in **Error! Reference source not found.**. As the SNR increases, the BER decreases significantly for all configurations. Higher SNR values indicate

better performance and lower BER values signify fewer errors and higher reliability. A reference summary table showing the expected BER values per SNR thresholds for different numbers of antennas:

A more detailed breakdown of the BER values for different SNR thresholds and antenna configurations is elaborated in Table 4. below. For instance, with 16 antennas using 16-QAM, the BER drops from 0.45 at 0 dB SNR to near zero at 30 dB SNR. Similarly, with 32 antennas using 64-QAM, the BER reduces from 0.50 at 0 dB SNR to 0.000005 at 40 dB SNR. The data highlights that higher SNR values and more antennas generally result in lower BER, indicating improved communication reliability and performance.

Table 4.1: Detailed breakdown of athe BER values

SNR (dB)	16 Antennas (16-QAM)	16 Antennas (64-QAM)	32 Antennas (16-QAM)	32 Antennas (64-QAM)
0	0.45	0.55	0.40	0.50
5	0.30	0.45	0.25	0.40
10	0.15	0.30	0.10	0.25
15	0.05	0.15	0.02	0.10
20	0.01	0.05	0.005	0.02
25	0.001	0.01	0.0005	0.005
30	0.0001	0.001	0.00005	0.0005
35	0.00001	0.0001	0.000005	0.00005
40	0.000001	0.00001	0.0000005	0.000005

SNR assess the clarity and quality of the received signals and BER is calculated to determine the accuracy of the data transmission. The simulations were designed to mimic real-world scenarios as closely as possible, ensuring the results are both relevant and applicable.These findings support the potential for real-world implementation and further development. Performance under deffernt channel conditions are presented in section 4.4.

4.4 Results for Achievable sum rate with Conditioned CSI

In this section, we compare the linear precoding regarding the average per-user terminal rate and average SNR employing simulation. A single-cell M-MIMO system with M=256 antennas, K=32 user equipment, TPE order of J=4 and three different quality levels of CSI at the BS, $\tau \in \{0.15, 0.45, 0.75\}$ with an imperfect CSI at $(\tau = 0.75)$ defines the default model. The comparison is amongst RZF precoding, MMSE precoding, CSM-based precoding and TPE precoding.

From Figure 4. and Figure 4., RZF, MMSE, CSM, and TPE achieve the same average UT execution when a corrupted channel estimate is existing at $\boldsymbol{\tau = 0.75}$. Furthermore, RZF, MMSE, CSM and TPE performance is similar at low SNR values for any $\boldsymbol{\tau}$. At low SNR, the performance of communication systems is often dominated by the presence of noise, and the subtle differences in precoding schemes may not be as pronounced. The performance convergence at low SNR is attributed to the fact that, in such conditions, the impact of interference, noise, and channel imperfections becomes more prominent, minimizing the distinctions between these precoding techniques. It's worth considering that the efficacy of precoding schemes often varies across different SNR regimes. The anticipated observation is that the rate deviation becomes more significant at high SNRs and when $\boldsymbol{\tau}$ is low (namely, channel knowledge well defined).

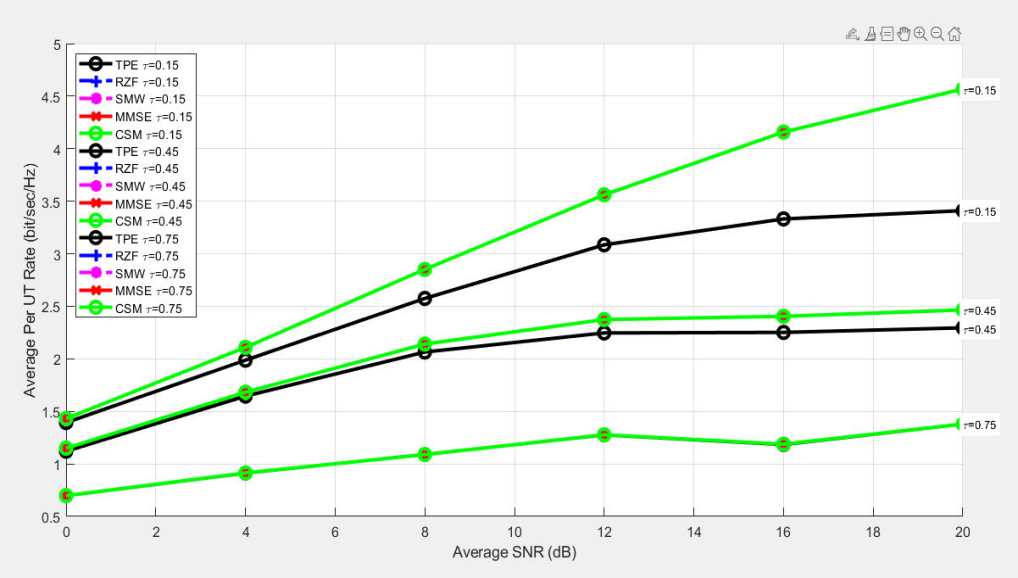

Figure 4.6 Average per UT rate vs SNR, varying CSI (M=126, K=32, J=4)

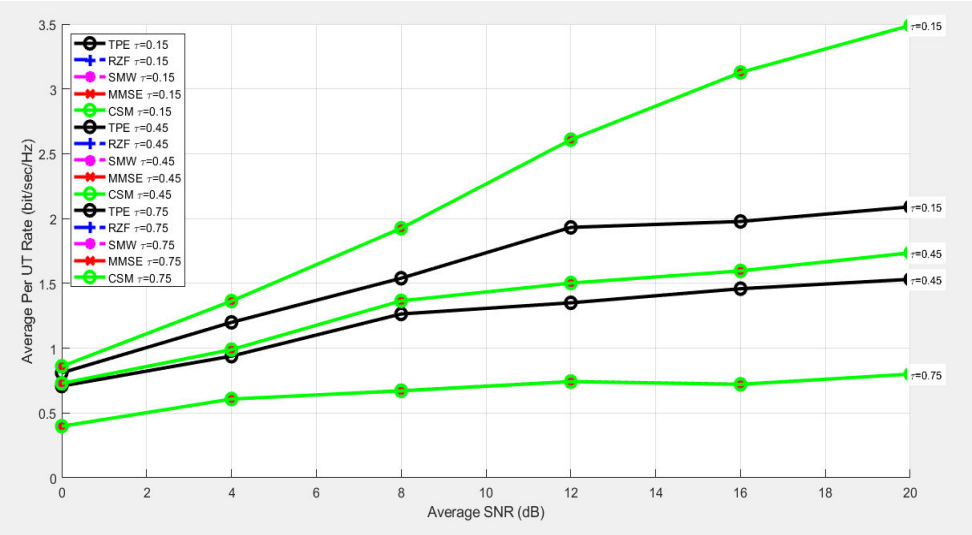

Figure 4.7 Average per UT rate vs SNR, varying CSI (M=126, K=64,J=4)

Figure 4. compares the RZF precoding, MMSE precoding, CSM-based, and TPE precoding. The RZF precoding, MMSE precoding, CSM-based, and TPE precoding offer the same bit rates for a semi-corrupted and full corrupted channels. The calculated bit rates were found to be close as observed at lower SNRs, notwithstanding of the value of $\boldsymbol{\tau}$**.**

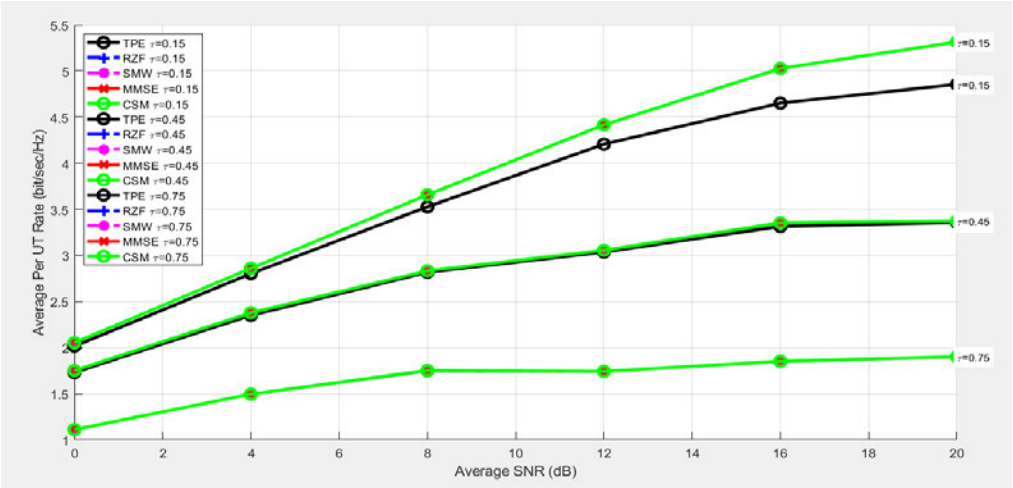

Figure 4.8 Average per UT rate vs SNR, varying CSI (M=256, K=32, J=4)

This precoding exhibits a degree of robustness to channel imperfections and errors. In the presence of semi-corrupted or fully corrupted channels, these precoding schemes are designed to mitigate the impact of channel impairments.

Figure 4. shows the correlation between the average attainable UT rates and the TPE order J. We consider the case $\tau = 0.1$, $M = 256$, and $K = 64$ to be in a system whereby TPE displays relatively poorly performance and the resulting precoding complexity is negatively affected. By choosing a more significant value for J results in a TPE performance similar to RZF. However, doing so will require additional hardware. The proposed TPE precoding does not surpass the RZF performance. This is especially noteworthy since TPE has J degrees of freedom that can be enhanced while RZF only has one design parameter. Hence, in a single-cell condition, the RZF precoding can be regarded as an upper bound to TPE precoding.

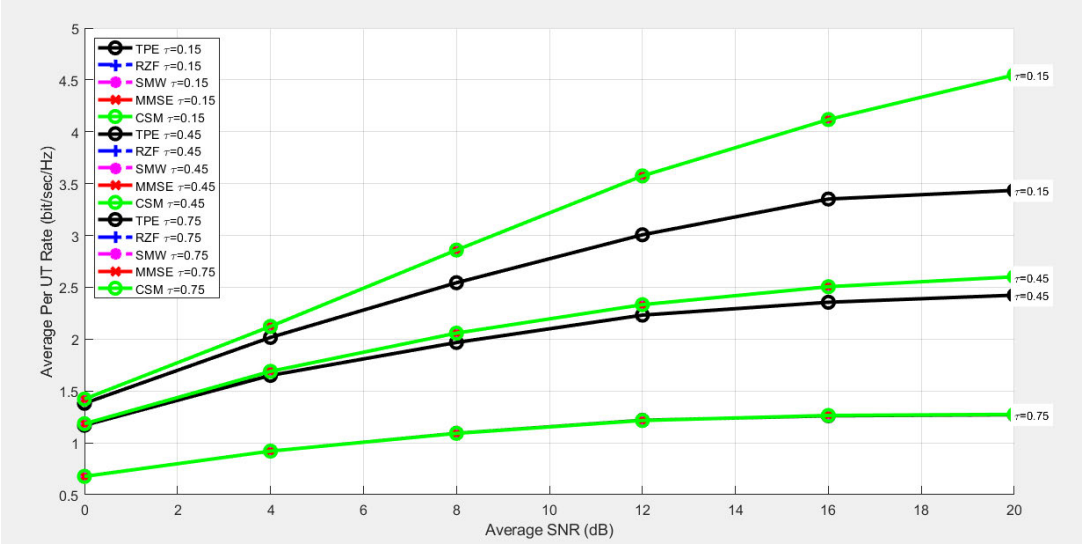

Figure 4.9 Average per UT rate vs SNR, varying CSI errors at the BS (M=256, K=64, J=4)

4.5 Results for SE with varying SNR (0, 5, 20) dB

This section presents spectral efficiencies obtained as the number of a BS antennas (M) varies from 10 to 1000, user equipment (k) were kept at 10 and increasing the SNR (0 dB, 5dB, 20 dB). The results of spectral efficiency for different precoding methods are depicted in Figure 4. and Figure 4.. Three different precoding schemes have been analysed, the two linear precoders ZF and MR, along with the hybrid precoder PZF. When M is approximately equal to K, linear processing results in a significant loss, which diminishes rapidly with increasing number of antennas. As the value of M increases to twice the number of users, a trade-off is observed between ZF and hybrid PZF. All precoding schemes exhibited a consistent increase in spectral efficiency as the ratio of antennas to users increased. PZF demonstrates superior performance compared to linear precoders ZF and MR. These precoding are compared at SNR = 0 dB in Figure 4., it is noted that the SE of PZF is just under 70 bps/Hz, with a marginal rise in Figure 4.12 as power SNR = 5dB. The SE is superior in the high SNR region, as shown in Figure 4., where at 20 dB, the SE is approximately 75 bps/Hz.

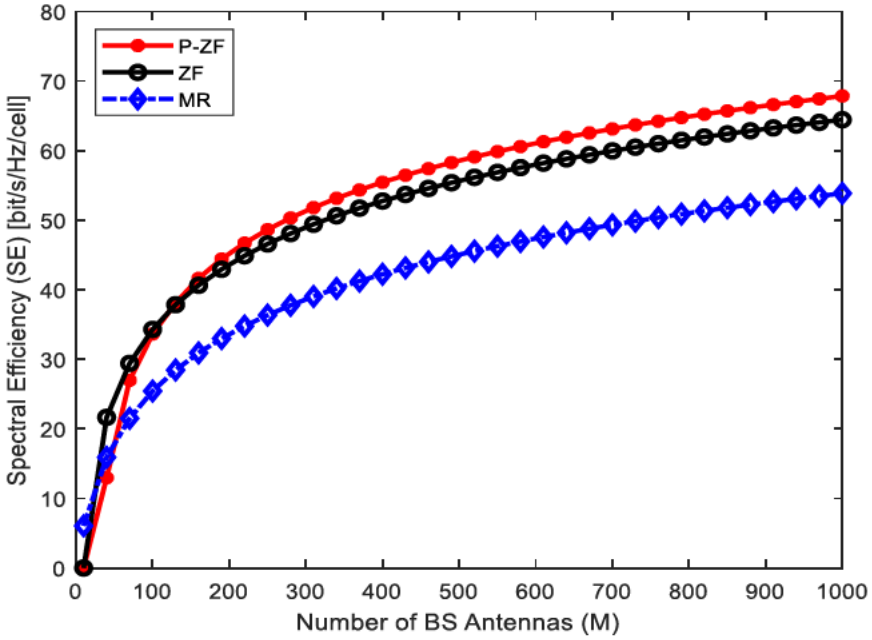

Figure 4.10 Spectral Efficiency versus number of BS antennas (M) for k=10 at 0 dB

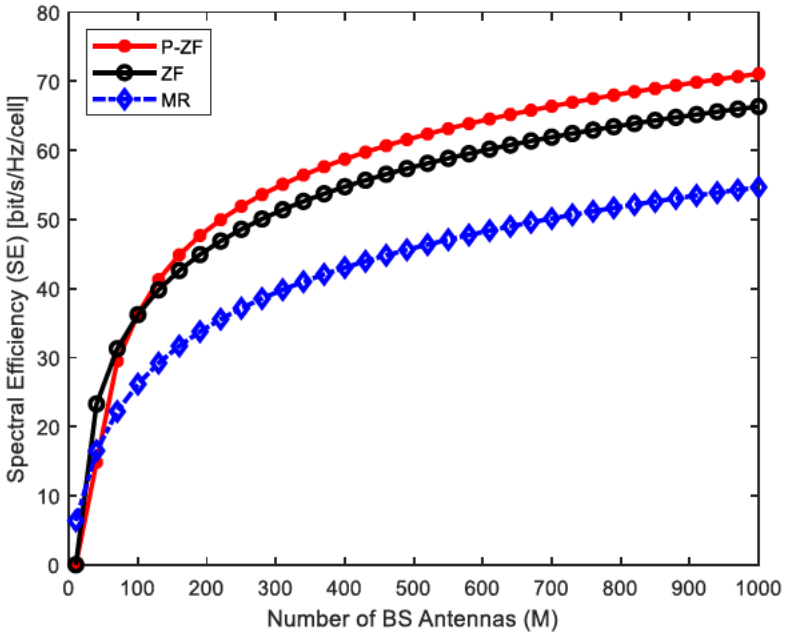

Figure 4.11 Spectral Efficiency versus number of BS antennas (M) for k=10 at 5 dB

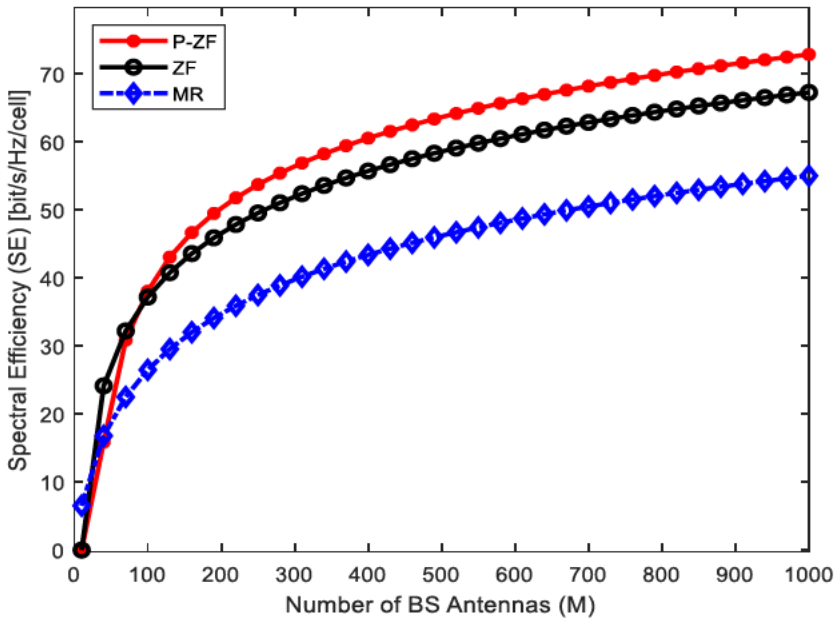

Figure 4.3 Spectral Efficiency versus number of BS antennas (M) for k=10 at 20 dB

Figure 4.13 displays the BER vs SNR for Thomlinson-Harashima precoder. The system is engineered to achieve a BER for most communication systems. The BER obtained in this case is utilised for determining the data rate for Figure 4.14. Figure 4.14 shows that the increase in the number of transmit antennas leads to a corresponding increase in SE.

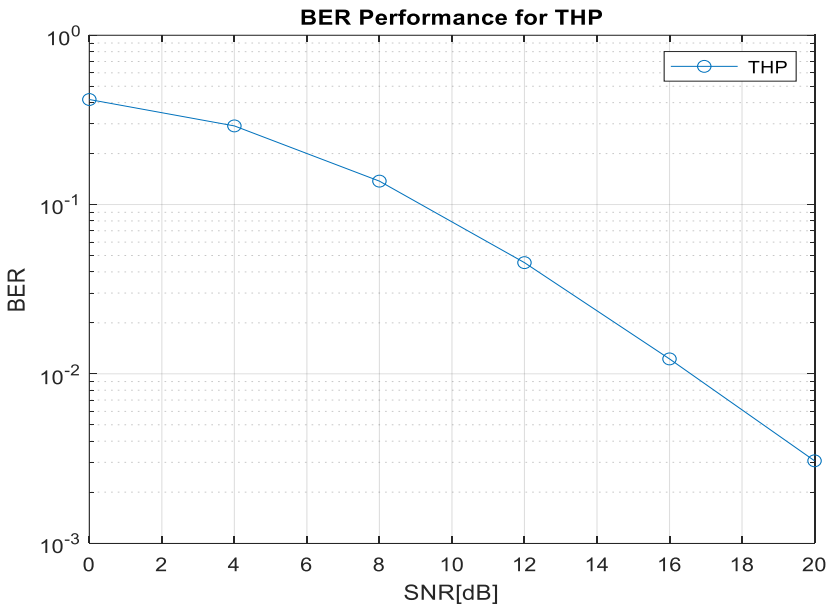

Figure 4.5 BER versus SNR [dB] for THP

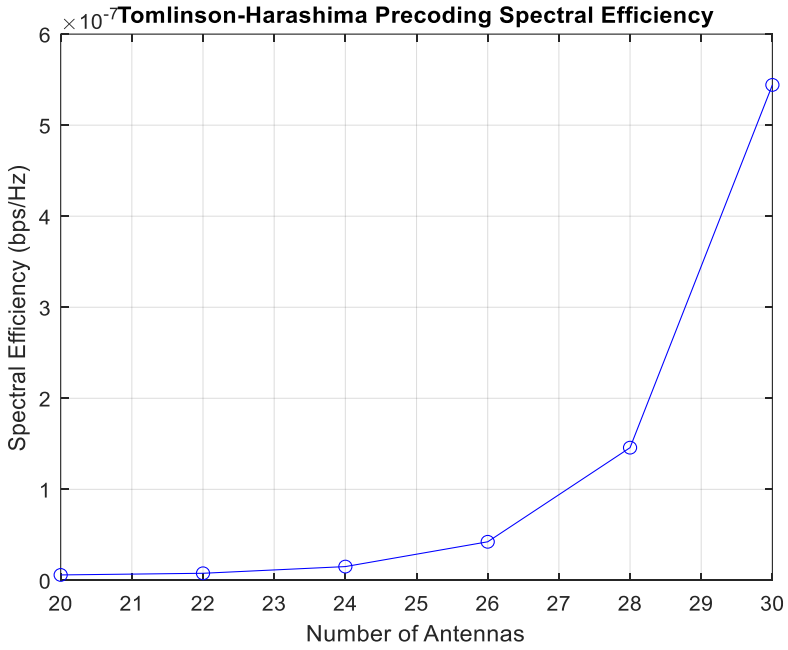

Figure 4.4 Spectral Efficiency versus number of antennas (M) for THP. M varies from 20 to 30

4.6 Conclusion

This chapter discussed the impact of channel estimation errors and presented a comprehensive analysis of BER versus SNR, and the results for ASR and SE. Our investigation into channel estimation errors has provided valuable insights into the robustness of precoding schemes under conditions where accurate channel state information is difficult to obtain. The BER versus SNR analysis is a critical benchmark for evaluating the error resilience of different precoding strategies. The analysis of error rates under varying signal-to-noise ratios unveils the trade-offs and performance differentials between the precoding schemes. These findings assist in selecting precoding strategies which demonstrate resilience in varying channel conditions.

Furthermore, the exploration of ASR reveals insights into the capacity and effectiveness of the communication system. By quantifying the system's ability to transmit data at higher rates while optimizing spectral resources, we develop the practical implications of each precoding scheme in real-world scenarios. The interplay between these diverse metrics provides a holistic view of precoding scheme performance. The nuanced trade-offs between error rates, achievable sum rates, and spectrum efficiency inform our understanding of the strengths and limitations inherent in each precoding strategy. The findings presented herein contribute towards understanding M-MIMO precoding and offers insights for designing and implementing robust communication systems in dynamic and challenging environments.

5 Conclusion

5.1 Dissertation Conclusion

As indicated in the introduction to this thesis, the main aim of the study was to analyse the performance of precoding schemes for M-MIMO. We conducted a thorough study of various precoding schemes, which encompassed both linear and nonlinear techniques. The optimum linear precoding schemes with the least amount of complexity were selected, and their results were compared with those of the nonlinear precoding schemes. A comparison was drawn between the performance of different scenarios, focusing on the BER and SE metrics. The evaluation was conducted on a Rayleigh fading channel. Next, the analysis was carried out for both perfect and imperfect CSI.

Based on the literature analyses, it was determined that ZF, MMSE, and NSA are linear precoding techniques that offer optimal performance. In this research, we also considered the nonlinear precoding techniques THP and LR-LLL, known for their robustness to varying channel conditions and ability to balance performance. Performance metrics like Achieving Sum Rate, SE, BER, and SINR were utilised to assess the system's performance. Nonlinear precoders frequently strive to achieve optimality under certain performance trade-off, yet this pursuit results in heightened complexity. Achieving optimality might require intricate algorithms and computations, making them less practical for real-time implementation, especially in resource-constrained environments.

In the current study, the nonlinear LLL-ZF algorithm exhibited superior performance compared to the linear precoders, as evidenced by the severe degradation in performance observed with NSA. The LR technique helps to mitigate the impact of noise and inaccuracies in channel estimation, providing a more robust solution for interference suppression. The following conclusions can be drawn:

- The THP algorithm shows its resilience as the LLL-aided Zero-Forcing technique gradually catches up with the SNR improvement.

- The performance of the LLL-aided ZF nonlinear precoder in 16-QAM modulation surpasses that of MMSE and NSA, resulting in a significant gain. Regarding the immence modulation 64-QAM, utilising LLL-aided ZF can result in an approximate 8 dB increase in gain compared to MMSE.

- When comparing linear precoders, it is evident that MMSE outperforms NSA, as NSA algorithm is computationally efficient, but it trades off optimality. Additionally, it is susceptible to interference and imprecision in the process of determining the characteristics of the communication channel.

- Linear precoders were compared regarding the average per-user terminal rate and average SNR employing simulation. The simulation model is categorised into three quality stages of CSI at the BS defined as, $\tau \in \{0.15, 0.45, 0.75\}$ with an imperfect CSI at $(\tau = 0.75)$. Linear precoders displayed identical performance results at low SNR values for any $\boldsymbol{\tau}$. Our investigation into channel estimation errors has provided valuable insights into the robustness of precoding schemes under conditions where accurate channel state information is difficult to acquire. The BER versus SNR analysis is a critical benchmark for evaluating the error resilience of different precoding strategies.

- The performance convergence at low SNR is attributed to the fact that, in such conditions, the impact of interference, noise, and channel imperfections becomes more prominent, minimizing the distinctions between these precoding techniques.

Nonlinear precoders might require accurate and up-to-date channel state information (CSI) for optimal performance. Obtaining and maintaining such CSI might be challenging in dynamic and practical scenarios, making the nonlinear precoders sub-optimal in certain practical contexts.

In conclusion, the main goal for this work has been successfully achieved.

5.2 Research Challenges and Limitations

Research on the performance analysis of precoding schemes in Massive MIMO encounters various challenges and limitations due to the complexity of the systems and the intricate nature of wireless communication. These challenges impact the accuracy, and generalisability of research findings. Here are some key challenges:

- The research was conducted through simulations in MATLAB®. Analysed simulated results for various linear and nonlinear signal processing techniques and different assumed antenna array sizes provided valuable insights into massive MIMO. Due to the unavailability of measurement equipment, this study was confined to simulations as realistic wireless channels could not be accessed.

- Extensive computational resources were needed to simulate and analyse the performance of precoding approaches, which limited the scalability of the investigation.

- The investigation utilised up to 512 BS antennas, requiring extensive computational resources that were not feasible on a standard laptop. Then, the number of antenna elements assumed was always equal to or larger than the expected number of users in a given cell. The machine used was unable to handle massive antenna computation, therefore the number of transmitting and receiving antennas was reduced to 16x16 and 32x32.

- Different precoding schemes have distinct trade-offs in complexity, performance, and robustness under varying channel conditions. Identifying the optimal precoding scheme under diverse scenarios is challenging since each requires unique solutions.

5.3 Future directions for the research

The evolving landscape of wireless communication and the continued advancements in M-MIMO systems present numerous avenues for future research in the performance analysis of precoding schemes. Critical directions for advancing the understanding and optimization of precoding techniques in M-MIMO include:

- Leveraging machine learning and artificial intelligence techniques for precoding schemes in M-MIMO is promising. Future research may explore adaptive precoding algorithms that learn and adapt to dynamic channel conditions, enabling efficient and adaptable precoding strategies.

- This work did not simulate Energy Efficiency (EE). Addressing EE is crucial for sustainable communication networks. Future studies may focus on developing EE precoding techniques that balance performance and power consumption, paving the way for greener communication systems.

- Hybrid beamforming architectures have gained attention for their ability to address hardware constraints in Massive MIMO. Future research may optimise hybrid precoding designs, efficiently combining analogue and digital precoding to achieve better performance gains.

- Investigating security and privacy aspects of precoding in Massive MIMO systems is a crucial yet less explored area. Future research may explore precoding techniques that address security vulnerabilities, ensure confidentiality, and to enhance user privacy.

- To address the computational challenges encountered with the use of up to 512 BS antennas, future research should focus on optimizing computational resources and developing more efficient algorithms. This will enable the handling of a larger number of antenna elements, which is crucial for supporting the expected number of users in a given cell. Additionally, exploring advanced hardware solutions and parallel processing techniques could mitigate the limitations faced by standard laptops. By enhancing the

computational capabilities, it will be possible to fully leverage the benefits of massive MIMO systems with configurations beyond the current 16x16 and 32x32 antenna setups.

References

[1] Cisco. "The COVID recovery: How tech can drive an Inclusive Future | The Network." https://newsroom.cisco.com/feature-content?type=webcontent&articleId=2137844 (accessed 2022).

[2] Cisco, "Cisco Annual Internet Report (2018–2023)," in *White paper Cisco public*, ed, 2020.

[3] A. Nordrum, K. Clark, and C. Gorman, "Everything you need to know about 5g," ed: IEEE Spectrum, 2017.

[4] R. Chataut and R. Akl, "Massive mimo systems for 5g and beyond networks-overview, recent trends, challenges, and future research direction," *Sensors (Basel)*, vol. 20, no. 10, May 12 2020, doi: 10.3390/s20102753.

[5] E. G. Larsson, O. Edfors, F. Turfvesson, and T. L. Marzetta, "Massive MIMO for next generation wireless systems," *IEEE Communications Magazine*, 2014.

[6] H. Yin, D. Gesbert, M. C. Filippou, and Y. Liu, "Decontaminating pilots in massive MIMO systems," in *2013 IEEE International Conference on Communications (ICC)*, 2013: IEEE, pp. 3170-3175.

[7] A. Chehri and H. T. Mouftah, "Phy-mac mimo precoder design for sub-6 ghz backhaul small cell," in *2020 IEEE 91st Vehicular Technology Conference (VTC2020-Spring)*, 25-28 May 2020 2020, pp. 1-5, doi: 10.1109/VTC2020-Spring48590.2020.9128733.

[8] N. C. Giri, A. Sahoo, J. R. Swain, P. Kumar, A. Nayak, and P. Debogoswami, "Capacity & performance comparison of SISO and MIMO system for next generation network (NGN)," *International Journal of Advanced Research in Computer Engineering & Technology (IJARCET)* vol. 3, no. 9, 2014.

[9] L. Lu, G. Y. Li, A. L. Swindlehurst, A. Ashikhmin, and R. Zhang, "An overview of massive MIMO: benefits and challenges," *IEEE Journal of Selected Topics in Signal Processing*, vol. 8, no. 5, pp. 742-758, 2014, doi: 10.1109/jstsp.2014.2317671.

[10] S. V. Panchami and M V Sathyanarayana, "A review on MIMO systems with antenna," *International Journal of Engineering Research & Technology (IJERT)*, vol. 5, no. 22, 2017.

[11] D. Bala, G. M. Waliullah, Mst A Hena, M. I. Abdullah, and M. A. Hossain, "Study the performance of capacity for siso, simo, miso and mimo in wireless communication," *Journal of Network and Information Security*, vol. 8, no. 1&2, 2020.

[12] Felipe A. P. de Figueiredo, "An overview of massive mimo for 5g and 6g," *IEEE Latin America Transactions*, vol. 20, no. 6, pp. 931-940, 2022.

[13] F. Jameel, M. A. A. Haider, and A. A. Butt, "Massive MIMO: A survey of recent advances, research issues and future directions," *2017 International Symposium on Recent Advances in Electrical Engineering (RAEE), Islamabad, Pakistan, ,* 2017, doi: 10.1109/RAEE.2017.8246040.

[14] K.-Y. Lian, S.-J. Hsiao, and W.-T. Sung, "Mobile monitoring and embedded control system for factory environment," *Sensors*, vol. 13, no. 12, pp. 17379-17413, 2013.

[15] T. M. Fernández-Caramés, M. González-López, C. J. Escudero, and L. Castedo, "Performance evaluation of multiple-antenna IEEE 802.11 p transceivers using an FPGA-based MIMO vehicular channel emulator," *EURASIP Journal on Wireless Communications and Networking*, vol. 2012, pp. 1-22, 2012.
[16] P. Pan, H. Wang, L. Shen, and C. Lu, "Equivalence of joint ML-decoding and separate MMSE-ML decoding for training-based MIMO systems," *IEEE Access*, vol. 7, pp. 178862-178869, 2019.
[17] B. Aouadi and J. B. Tahar, "Enhancement of characteristics of antenna arrays employing s-shaped resonators," *Journal of Electromagnetic Analysis and Applications*, vol. 4, no. 8, 2012, doi: 10.4236/jemaa.2012.48045.
[18] O. Bilenne, P. Mertikopoulos, and E. V. Belmega, "Derivative-free optimization over multi-user mimo networks," in *International Conference on Network Games, Control and Optimization*, 2021: Springer, pp. 17-24.
[19] S. Kaur and A. Sharma, "Performance estimation of SISO and MIMO Ro-FSO link under atmospheric turbulence," *Optical and Quantum Electronics*, vol. 56, no. 1, 2023, doi: 10.1007/s11082-023-05667-y.
[20] S. Sanwal, A. Kumar, M. Arib Faisal, and M. I. Hassan, "Performance of MIMO System—A Review," *Advances in Communication and Computational Technology: Select Proceedings of ICACCT 2019*, pp. 655-676, 2021.
[21] L. Desclos, S. Rowson, and J. Shamblin, "Antenna system optimized for SISO and MIMO operation," San Diego, United State Patent Appl. 13/621,811 2017.
[22] R. Muthalagu, "A novel nonlinear and non-iterative precoding technique for single and Multi User MIMO systems," *Wireless Personal Communications*, vol. 106, no. 4, pp. 2359-2373, 2019, doi: 10.1007/s11277-019-06321-1.
[23] A.-A. Lu, X. Gao, W. Zhong, C. Xiao, and X. Meng, "Robust transmission for massive MIMO downlink with imperfect CSI," *IEEE Transactions on Communications*, vol. 67, no. 8, pp. 5362-5376, 2019.
[24] D. W. Yue, "Specular component-based beamforming for broadband massive MIMO systems with doubly-ended correlation," *Electronics Letters*, vol. 52, no. 12, pp. 1082-1084, 2016.
[25] L. Song, X. Wang, Y. Zhang, and H. Zhou, "Separated horizontal and vertical transmission methods in massive mimo systems," in *2015 IEEE 81st Vehicular Technology Conference (VTC Spring)*, 2015: IEEE, pp. 1-5.
[26] N. Akbar, S. Yan, A. M. Khattak, and N. Yang, "On the pilot contamination attack in multi-cell multiuser massive mimo networks," *IEEE Transactions on Communications*, vol. 68, no. 4, pp. 2264-2276, 2020, doi: 10.1109/tcomm.2020.2967760.
[27] W. Zhang *et al.*, "Distributed structured compressive sensing-based time-frequency joint channel estimation for massive MIMO-OFDM systems," *Mobile Information Systems*, vol. 2019, 2019.
[28] T. L. Marzetta, "Massive MIMO: An Introduction," *Bell Labs Technical Journal*, vol. 20, 2015.
[29] J. Yang, L. Zhang, C. Zhu, X. Guo, and J. Zhang, "Energy Efficiency Optimization of Massive MIMO Systems Based on the Particle Swarm Optimization Algorithm," *Wireless Communications and Mobile Computing*, vol. 2021, pp. 1-11, 11/08 2021, doi: 10.1155/2021/6622830.

[30] E Bjornson, J Hoydis, M Kountouris, and M Debbah, "Massive mimo systems with non-ideal hardware: Energy efficiency, estimation, and capacity limits," *arXiv:1307.2584v3*, 2014.
[31] O. Elijah, C. Y. Leow, A. R. Tharek, S. Nunoo, and S. Z. Iliya, "Mitigating pilot contamination in massive MIMO system 5G_An overview," presented at the IEEE Xplore, 2015.
[32] H. Xie, F. Gao, S. Zhang, and S. Jin, "A unified transmission strategy for TDD/FDD massive MIMO systems with spatial basis expansion model," *IEEE Transactions on Vehicular Technology*, vol. 66, no. 4, pp. 3170-3184, 2016.
[33] B. Zhang, H. Li, X. Liang, X. Gu, and L. Zhang, "Fully connected layer-shared network architecture for massive MIMO CSI feedback," *Electronics Letters*, vol. 58, no. 6, pp. 255-257, 2022.
[34] X. Lu, D. Niyato, H. Jiang, P. Wang, and H. V. Poor, "Cyber insurance for heterogeneous wireless networks," *IEEE Communications Magazine*, vol. 56, no. 6, pp. 21-27, 2018.
[35] S. Jo, J. Lee, and J. So, "Deep learning-based massive multiple-input multiple-output channel state information feedback with data normalisation using clipping," *Electronics Letters*, vol. 57, no. 3, pp. 151-154, 2021.
[36] M. H. Siddiqui, K. Khurshid, I. Rashid, A. A. Khan, and K. Ahmed, "Optimal massive MIMO detection for 5G communication systems via hybrid n-bit heuristic assisted-VBLAST," *IEEE Access*, vol. 7, pp. 173646-173656, 2019.
[37] J. Jose, A. Ashikhmin, T. L. Marzetta, and S. Vishwanath, "Pilot contamination and precoding in multi-cell TDD systems," (in English), *IEEE Transactions on Wireless Communications*, vol. 10, no. 8, pp. 2640-2651, Aug 2011, doi: 10.1109/Twc.2011.060711.101155.
[38] M. Kawambwa, "Pilot contamination mitigation techniques in massive MIMO systems: A precoding approach," 2016.
[39] E Björnson, J Hoydis, and L Sanguinetti, *Massive MIMO Networks: Spectral, Energy, and Hardware Efficiency*. Hanover: Now Publishers Inc., 2018.
[40] H. Zhi and X. Ding, "Pilot allocation scheme based on coalition game for TDD massive MIMO systems," *EURASIP Journal on Wireless Communications and Networking*, vol. 2019, no. 1, p. 60, 2019.
[41] A. A. I. Ayidh, Y. Sambo, and M. A. Imran, "Mitigation pilot contamination based on matching technique for uplink cell-free massive MIMO systems," *Scientific Reports*, vol. 12, no. 1, p. 16893, 2022.
[42] N. N. Moghadam, H. Shokri-Ghadikolaei, G. Fodor, M. Bengtsson, and C. Fischione, "Pilot precoding and combining in multiuser MIMO networks," *IEEE Journal on Selected Areas in Communications*, vol. 35, no. 7, pp. 1632-1648, 2017.
[43] T. L. Marzetta, E. G. Larsson, H. Yang, and H. Q. Ngo, *Fundamentals of Massive MIMO*. 2015.
[44] Z. Gong, C. Li, and F. Jiang, "Pilot contamination mitigation strategies in massive MIMO systems," *IET Communications*, vol. 11, no. 16, pp. 2403-2409, 2017.
[45] S. S. Ioushua and Y. C. Eldar, "Pilot sequence design for mitigating pilot contamination with reduced RF chains," *IEEE Transactions on Communications*, vol. 68, no. 6, pp. 3536-3549, 2020.
[46] X. Yan, H. Yin, M. Xia, and G. Wei, "Pilot sequences allocation in TDD massive MIMO systems," in *2015 IEEE Wireless Communications and Networking Conference (WCNC)*, 2015: IEEE, pp. 1488-1493.

[47] O. Dikmen and S. Kulaç, "Power allocation algorithms for massive MIMO system," *Avrupa Bilim ve Teknoloji Dergisi*, no. 28, pp. 444-452, 2021.
[48] M Mandloi, D Gurjar, P Pattanayak, and H Nguyen, *5G and beyond wireless systems phy layer perspective* (Springer Series in Wireless Technology). Aalborg, Denmark, 2021.
[49] P. Jayanthi, S. Rachana, and M. Ramya, "Linear precoding techniques for MIMO systems," in *Proceeding of Fifth International Conference on Microelectronics, Computing and Communication Systems: MCCS 2020*, 2021: Springer, pp. 371-382.
[50] J. Li, Z. Wu, P. Zhu, D. Wang, and X. You, "Scalable pilot assignment scheme for cell-free large-scale distributed MIMO with massive access," *IEEE Access,* vol. 9, pp. 122107-122112, 2021.
[51] A. Li *et al.*, "A tutorial on interference exploitation via symbol-level precoding: overview, state-of-the-art and future directions," *IEEE Communications Surveys & Tutorials,* vol. 22, no. 2, pp. 796-839, 2020.
[52] H. Yang and T. L. Marzetta, "Performance of conjugate and zero-forcing beamforming in large-scale antenna systems," *IEEE Journal on Selected Areas in Communications,* vol. 31, no. 2, pp. 172-179, 2013, doi: 10.1109/jsac.2013.130206.
[53] M. A. Albreem, A. H. A. Habbash, A. M. Abu-Hudrouss, and S. S. Ikki, "Overview of precoding techniques for massive mimo," *IEEE Access,* vol. 9, pp. 60764-60801, 2021, doi: 10.1109/access.2021.3073325.
[54] T. Omar, T. Ketseoglou, O. Naffaa, A. Marzvanyan, and C. Carr, "A precoding real-time buffer based self-healing solution for 5g networks," *Journal of Computer and Communications,* vol. 9, no. 06, pp. 1-23, 2021.
[55] M. Vu and A. Paulraj, "MIMO wireless linear precoding," *IEEE Signal Processing Magazine,* vol. 24, no. 5, pp. 86-105, 2007.
[56] N. Fatema, G. Hua, Y. Xiang, D. Peng, and I. Natgunanathan, "Massive MIMO linear precoding: A survey," *IEEE systems journal,* vol. 12, no. 4, pp. 3920-3931, 2017.
[57] R. P. Ketcham, J. Verdyck, and M. Moonen, "Joint beamforming and power allocation for multiuser MISO broadcast channel SWIPT employing OFDM," *Ieee Access,* vol. 9, pp. 165154-165172, 2021.
[58] L. Han, B. Shi, and W. Zou, "Performance analysis and power control for full-duplex relaying with large-scale antenna array at the destination," *EURASIP Journal on Wireless Communications and Networking,* vol. 2017, no. 1, pp. 1-9, 2017.
[59] L. Sanguinetti, E. Bjornson, and J. Hoydis, "Toward massive MIMO 2.0: Understanding spatial correlation, interference suppression, and pilot contamination," *IEEE Transactions on Communications,* vol. 68, no. 1, pp. 232-257, 2020, doi: 10.1109/tcomm.2019.2945792.
[60] A. Israr, Z. Rauf, J. Muhammad, and F. Khan, "Performance analysis of downlink linear precoding in massive MIMO systems under imperfect CSI," *Wireless Personal Communications,* vol. 96, pp. 2603-2619, 2017.
[61] G. M. Waliullah, D. Bala, M. A. Hena, M. I. Abdullah, and M. A. Hossain, "Performance analysis of Zero Forcing and MMSE equalizer on MIMO system in wireless channel," *Journal of Network and Information Security,* vol. 8, no. 1&2, 2020.

[62] Y Li, J Wang, and Z Gao, "Performance analysis of precoding based on massive mimo system," presented at the MATEC Web of Conferences, China, 2015.
[63] N. Hassan and X. Fernando, "Massive MIMO wireless networks: An overview," *Electronics,* vol. 6, no. 3, 2017, doi: 10.3390/electronics6030063.
[64] M. Wang, F. Wang, and Z. Zhong, "Wireless MIMO switching: distributed zero-forcing and MMSE relaying using network coding," *EURASIP Journal on Advances in Signal Processing,* vol. 2013, no. 1, pp. 1-10, 2013.
[65] Z. Quan, J. Luo, H. Zhang, and L. Jiang, "Efficient massive MIMO detection for m-QAM symbols," *Entropy,* vol. 25, no. 3, p. 391, 2023.
[66] B. Peng *et al.,* "Reconfigurable intelligent surface enabled spatial multiplexing with fully convolutional network," *arXiv preprint arXiv:2201.02834,* 2022.
[67] M. Ding, S. Liu, H. Luo, and W. Chen, "MMSE based greedy antenna selection scheme for af MIMO relay systems," *IEEE Signal Processing Letters,* vol. 17, no. 5, 2010, doi: 10.1109/LSP.2010.2042531.
[68] L. Mroueh, S. Rouquette-Léveil, and J.-C. Belfiore, "Reduced feedback for selective fading MIMO broadcast channels," *EURASIP Journal on Wireless Communications and Networking,* vol. 2011, pp. 1-17, 2011.
[69] S. Hashima and O. Muta, "Fast matrix inversion methods based on Chebyshev and Newton iterations for zero forcing precoding in massive MIMO systems," *EURASIP Journal on Wireless Communications and Networking,* vol. 2020, no. 1, pp. 1-12, 2020.
[70] H. Weingarten, Y. Steinberg, and S. S. Shamai, "The capacity region of the gaussian multiple-input multiple-output broadcast channel," *IEEE Transactions On Information Theory,* vol. 52, no. 9, pp. 1-6, 2006.
[71] N. J. Juyul Lee. "Dirty Paper Coding vs. Linear Precoding for MIMO Broadcast Channels." (accessed.
[72] B. Song and M. Haardt, "Effects of Imperfect Channel State Information on Achievable Rates of Precoded Multi-user MIMO Broadcast Channels with Limited Feedback," IEEE ICC, Germany, 2009.
[73] Jinxing Li and Youping Zhao. "Channel Characterization and Modeling for Large Scale Antenna Systems." International Symposium on Communications and Information Technologies. (accessed.
[74] A. Li, F. Liu, C. Masouros, Y. Li, and B. Vucetic, "Interference exploitation 1-bit massive MIMO precoding: A partial branch-and-bound solution with near-optimal performance," *IEEE Transactions on Wireless Communications,* vol. 19, no. 5, pp. 3474-3489, 2020.
[75] S. Zarei, W. Gerstacker, and R. Schober, "Low-complexity hybrid linear/Tomlinson-Harashima precoding for downlink large-scale MU-MIMO systems," in *2016 IEEE Globecom Workshops (GC Wkshps)*, 2016: IEEE, pp. 1-7.
[76] S. Yang *et al.,* "Security situation assessment for massive MIMO systems for 5G communications," *Future Generation Computer Systems,* vol. 98, pp. 25-34, 2019.
[77] M. Sarajlić, F. Rusek, J. R. Sánchez, L. Liu, and O. Edfors, "Fully decentralized approximate zero-forcing precoding for massive MIMO systems," *IEEE Wireless Communications Letters,* vol. 8, no. 3, pp. 773-776, 2019.
[78] J. Yang, X. Wang, S. Chen, and Z. Zhong, "Design of low-complexity vector perturbation precoding technique for multiuser MIMO systems," in *2016 8th International Conference on Wireless Communications & Signal Processing (WCSP)*, 2016: IEEE, pp. 1-5.

[79] C. Masouros, M. Sellathurai, and T. Ratnarajah, "Computationally efficient vector perturbation precoding using thresholded optimization," *IEEE Transactions on Communications*, vol. 61, no. 5, pp. 1880-1890, 2013.
[80] M. Barrenechea, M. Mendicute, and E. Arruti, "Fully Pipelined implementation of tree-search algorithms for vector precoding," *International Journal of Reconfigurable Computing*, vol. 2013, p. 496013, 2013/02/21 2013, doi: 10.1155/2013/496013.
[81] J.-C. Chen, C.-K. Wen, S. Jin, and K.-K. Wong, "A low complexity pilot scheduling algorithm for massive MIMO," *IEEE Wireless Communications Letters*, vol. 6, no. 1, pp. 18-21, 2016.
[82] X. Nie and F. Zhao, "Joint pilot allocation and pilot sequence optimization in massive MIMO systems," *IEEE Access*, vol. 8, pp. 60637-60644, 2020.
[83] X. Liu, "Low-complexity unsupervised learning-based hybrid precoding for massive MIMO systems," *IET Communications*, vol. 17, no. 15, pp. 1773-1779, 2023.
[84] J. Xu, Y. Wang, W. Xu, S. Jin, H. Shen, and X. You, "On uplink performance of multiuser massive MIMO relay network with limited RF chains," *IEEE Transactions on Vehicular Technology*, vol. 69, no. 8, pp. 8670-8683, 2020.
[85] P. Uthansakul and A. Ahmad Khan, "On the energy efficiency of millimeter wave massive MIMO based on hybrid architecture," *Energies*, vol. 12, no. 11, p. 2227, 2019.
[86] Z. Lv and Z. Xi, "Radio frequency link and user selection algorithm for 5g mobile communication system," *Complexity*, vol. 2021, pp. 1-10, 2021.
[87] S. N. Sur, D. Kandar, A. Silva, N. D. Nguyen, S. Nandi, and D. T. Do, "Hybrid precoding algorithm for millimeter-wave massive mimo-noma systems," *Electronics*, vol. 11, no. 14, 2022. [Online]. Available: https://www.mdpi.com/2079-9292/11/14/2198.
[88] N. Li, Z. Wei, H. Yang, X. Zhang, and D. Yang, "Hybrid precoding for mmWave massive MIMO systems with partially connected structure," *IEEE Access*, vol. 5, pp. 15142-15151, 2017.
[89] O. S. Faragallah, H. S. El-Sayed, and G. Mohamed, "Performance enhancement of mmWave MIMO systems using deep learning framework," *IEEE Access*, vol. 9, pp. 92460-92472, 2021.
[90] W. X. Le Liang and X. Dong, "Low-complexity hybrid precoding in massive multiuser MIMO systems," *IEEE Wireless Communications Letters*, vol. 3, no. 6, pp. 653-656, 2014.
[91] O El Ayach, S Rajagopal, S Abu-Surra, Z Pi, and R W Heath, "Spatially sparse precoding in millimeter wave MIMO systems," *IEEE Transactions on Wireless Communications*, vol. 13, no. 3, pp. 1499 - 1513, 2014, doi: 10.1109/TWC.2014.011714.130846.
[92] S. Zarei, W. Gerstacker, and R. Schober, "A low-complexity linear precoding and power allocation scheme for downlink massive MIMO systems," presented at the Asilomar Conference on Signals, Systems and Computers, 2013.
[93] P. D. Arapoglou, K. Liolis, M. Bertinelli, A. Panagopoulos, P. Cottis, and R. De Gaudenzi, "MIMO over satellite: A review," *IEEE communications surveys & tutorials*, vol. 13, no. 1, pp. 27-51, 2010.

[94] M. Han, J. Du, Y. Zhang, X. Li, K. M. Rabie, and G. Nauryzbayev, "Efficient hybrid beamforming design in mmWave massive MU-MIMO DF relay systems with the mixed-structure," *IEEE Access,* vol. 9, pp. 66141-66153, 2021.
[95] M. Noor-A-Rahim *et al.*, "Wireless communications for smart manufacturing and industrial IoT: Existing technologies, 5G and beyond," *Sensors,* vol. 23, no. 1, p. 73, 2022.
[96] N. Fang, X. Su, J. Zeng, and Y. Kuang, "Effective user selection algorithm for quantized precoding in massive MIMO," in *2013 8th International Conference on Communications and Networking in China (CHINACOM)*, 2013: IEEE, pp. 353-357.
[97] F. Hu, K. Wang, S. Li, and L. Jin, "Energy efficiency-oriented resource allocation for massive MIMO systems with separated channel estimation and feedback," *Electronics,* vol. 9, no. 4, p. 582, 2020.
[98] J. R. Pérez *et al.*, "Empirical characterization of the indoor radio channel for array antenna systems in the 3 to 4 GHz frequency band," *IEEE Access,* vol. 7, pp. 94725-94736, 2019.
[99] E. N. Tominaga, O. L. López, H. Alves, R. D. Souza, and J. L. Rebelatto, "Performance analysis of MIMO-NOMA iterative receivers for massive connectivity," *IEEE Access,* vol. 10, pp. 46808-46822, 2022.
[100] M. LI and Y.-f. GUO, "An improved three-dimensional MIMO channel model based on GBSBEM," *Journal of Engineering Science and Technology Review,* vol. 6, no. 5, pp. 76-81, 2013.
[101] J. Liu, J. Dai, J. Wang, X. Yin, Z. Jiang, and J. Wang, "Achievable rates for full-duplex massive MIMO systems with low-resolution ADCs/DACs under imperfect CSI environment," *EURASIP Journal on Wireless Communications and Networking,* vol. 2018, no. 1, pp. 1-12, 2018.
[102] Z. Tang and A. S. Mohan, "An investigation of MIMO performance in the indoor ricean environment," *Wireless Personal Communications,* vol. 39, pp. 99-113, 2006.
[103] Y. Xuefeng and C. Xiang, "Geometry-based Stochastic Channel Modeling," in *Propagation Channel Characterization, Parameter Estimation, and Modeling for Wireless Communications*: IEEE, 2016, pp. 77-105.
[104] J. Dang *et al.*, "A geometry-based stochastic channel model and its application for intelligent reflecting surface assisted wireless communication," *IET Communications,* vol. 15, no. 3, pp. 421-434, 2021/02/01 2021, doi: https://doi.org/10.1049/cmu2.12075.
[105] R. Feng, C.-X. Wang, J. Huang, X. Gao, S. Salous, and H. Haas, "Classification and comparison of massive MIMO propagation channel models," *IEEE Internet of Things Journal,* vol. 9, no. 23, pp. 23452-23471, 2022.
[106] J.-H. Ro, W.-S. Lee, J.-G. Ha, and H.-K. Song, "An efficient precoding method for improved downlink massive MIMO system," *IEEE Access,* vol. 7, pp. 112318-112326, 2019.
[107] N. A. Malik and M. Ur-Rehman, "Green communications: Techniques and challenges," 2017.
[108] M. Zhou, Q. Wang, F. He, and J. Meng, "Impacts of phase noise on the anti-jamming performance of power inversion algorithm," *Sensors,* vol. 22, no. 6, 2022.

[109] Electrical4U. "Quadrature Amplitude Modulation (QAM): What is it?" https://www.electrical4u.com/quadrature-amplitude-modulation-qam/#google_vignette (accessed.
[110] R. W. World. "16 QAM modulation vs 64 QAM modulation vs 256 QAM modulation." https://www.rfwireless-world.com/Terminology/QAM.html (accessed.
[111] W. Jiang and H. D. Schotten, "Deep learning for fading channel prediction," *IEEE Open Journal of the Communications Society*, vol. 1, pp. 320-332, 2020.
[112] S. Singh, P. Singh, and K. Vasudevan, "Uplink sum rate analysis of multi-user massive MIMO–OFDM/OQAM systems in Ricean fading," *IET Communications*, vol. 14, no. 11, pp. 1773-1782, 2020.
[113] C. Zhang, "Channel state information acquisition method of internet of things based on deep learning," *The Journal of Engineering*, vol. 2021, no. 12, pp. 838-848, 2021.
[114] M. Mahmood, A. Koc, and T. Le-Ngoc, "Energy-efficient MU-massive-MIMO hybrid precoder design: Low-resolution phase shifters and digital-to-analog converters for 2D antenna array structures," *IEEE Open Journal of the Communications Society*, vol. 2, pp. 1842-1861, 2021.
[115] N. Jindal, J. G. Andrews, and S. Weber, "Rethinking MIMO for wireless networks: Linear throughput increases with multiple receive antennas," in *2009 IEEE International Conference on Communications*, 2009: IEEE, pp. 1-6.
[116] B. Q. Vuong, R. Gautier, H. Q. Ta, L. L. Nguyen, A. Fiche, and M. Marazin, "Joint semi-blind self-interference cancellation and equalisation processes in 5g qc-ldpc-encoded short-packet full-duplex transmissions," *Sensors*, vol. 22, no. 6, p. 2204, 2022.
[117] N. Katiran, S. M. Shah, N. Abdullah, A. S. A. Ghaffar, and F. A. Saparudin, "Investigation on the BER performance of downlink JT-CoMP-NOMA with different modulation schemes," *Indonesian Journal of Electrical Engineering and Computer Science*, vol. 20, no. 3, pp. 1309-1314, 2020.
[118] N. T. Phuong, V. V. Son, and P. T. Hiep, "Combining precoding and equalization for interference cancellation in MU-MIMO systems with high density users," *EURASIP Journal on Wireless Communications and Networking*, vol. 2022, no. 1, p. 34, 2022.
[119] G. Liu, H. Deng, X. Qian, W. Wang, and G. Peng, "Joint pilot allocation and power control to enhance max-min spectral efficiency in TDD massive MIMO systems," *IEEE Access*, vol. 7, pp. 149191-149201, 2019.
[120] H.-S. Hwang, J.-H. Ro, C.-Y. Park, Y.-H. You, and H.-K. Song, "Efficient gauss-seidel precoding with parallel calculation in massive MIMO systems," *Computers Materials & Continua*, vol. 70, no. 1, pp. 491-504, 2022.
[121] L. Xin, Y. Li, S. Zhe, and X. Zhang, "On over-the-air testing for devices with directional antennas," *IEEE Access*, vol. 8, pp. 121821-121832, 2020.
[122] T.-N. Tran and M. Voznak, "Switchable coupled relays aid massive non-orthogonal multiple access networks with transmit antenna selection and energy harvesting," *Sensors*, vol. 21, no. 4, p. 1101, 2021.
[123] Y. Xiao, Y. J. Zhu, and Z. G. Sun, "Linear precoding designs for MIMO VLC using multi-color leds under multiple lighting constraints," *Crystals*, vol. 8, no. 11, p. 15, 2018, doi: 10.3390/cryst8110408

[124] Y. Chen, X. Wen, and Z. Lu, "Achievable spectral efficiency of hybrid beamforming massive MIMO systems with quantized phase shifters, channel non-reciprocity and estimation errors," *IEEE Access,* vol. 8, pp. 71304-71317, 2020, doi: 10.1109/ACCESS.2020.2987613.
[125] A. S. Alwakeel and A. Elzanaty, "Semi-blind channel estimation for intelligent reflecting surfaces in massive MIMO systems," *IEEE Access,* vol. 10, pp. 127783-127797, 2022.
[126] M. Hmila, M. Fernández-Veiga, M. Rodríguez-Pérez, and S. Herrería-Alonso, "Non-orthogonal multiple access for unicast and multicast D2D: Channel assignment, power allocation and energy efficiency," *Sensors,* vol. 21, no. 10, p. 3436, 2021.
[127] Y. Xu, W. Zou, and L. Du, "A fast and low-complexity matrix inversion scheme based on CSM method for massive MIMO systems," *EURASIP Journal on Wireless Communications and Networking,* vol. 2016, no. 1, 2016, doi: 10.1186/s13638-016-0749-3.
[128] A. Neumaier and D. Stehlé, "Faster LLL-type Reduction of Lattice Bases," presented at the Proceedings of the ACM on International Symposium on Symbolic and Algebraic Computation, 2016.
[129] F. Rusek, D. Persson, L. Buon Kiong, E. G. Larsson, T. L. Marzetta, and F. Tufvesson, "Scaling Up MIMO: Opportunities and Challenges with Very Large Arrays," *IEEE Signal Processing Magazine,* vol. 30, no. 1, pp. 40-60, 2013, doi: 10.1109/msp.2011.2178495.
[130] M A M Albreem, "Approximate matrix inversion methods for massive MIMO detectors," presented at the 019 IEEE 23rd International Symposium on Consumer Technologies (ISCT), 2019.
[131] H Prabhu, J Rodrigues, O Edfors, and F Rusek, "Approximative matrix inverse computations for very-large MIMO and applications to linear pre-coding systems," *Host publication title missing,* pp. 2710-2715, 2013.
[132] D. Wübben, D. Seethaler, J. Jalden, and G. Matz, "Lattice reduction," *IEEE Signal Processing Magazine,* vol. 28, no. 3, pp. 70-91, 2011.
[133] Z. Tian and S. Qiao, "A hybrid method for lattice basis reduction," Technical Report CAS-14-01-SQ, Department of Computing and Software, McMaster University 2014.
[134] S. A. Khwandah, J. P. Cosmas, P. I. Lazaridis, Z. D. Zaharis, and I. P. Chochliouros, "Massive MIMO systems for 5G communications," *Wireless Personal Communications (2021),* 2021, doi: 10.1007/s11277-021-08550-9.
[135] M. A. Albreem, M. Juntti, and S. Shahabuddin, "Massive MIMO detection techniques: A survey," *IEEE Communications Surveys & Tutorials,* vol. 21, no. 4, pp. 3109-3132, 2019, doi: 10.1109/comst.2019.2935810.
[136] M. A. Albreem, M. H. Alsharif, and S. Kim, "A low complexity near-optimal iterative linear detector for massive mimo in realistic radio channels of 5g communication systems," *Entropy (Basel),* vol. 22, no. 4, Mar 28 2020, doi: 10.3390/e22040388.
[137] Z. Wang and W. Chen, "Regularized Zero-Forcing for multiantenna broadcast channels with user selection," *IEEE Wireless Communications Letters,* vol. 1, no. 2, pp. 129-132, 2012, doi: 10.1109/wcl.2012.022012.110206.
[138] C. Pan, H. Ren, M. Elkashlan, Nallanathan, and L. Hanzo, "Robust beamforming design for ultra-dense user-centric C-RAN in the face of realistic pilot

contamination and limited feedback," *IEEE Transactions on Wireless Communications,* vol. 18, no. 2, pp. 780-795, 2019, doi: 10.1109/twc.2018.2882442.
[139] K Zu, R C de Lamare, and M Haardt, "Multi-Branch Tomlinson-Harashima Precoding design for MU-MIMO systems: Theory and algorithms," *IEEE Transactions On Communications,* vol. 64, no. 3, pp. 939-951, 2014.
[140] E. Björnson, L. Sanguinetti, and M. Debbah, "Massive MIMO with imperfect channel covariance information," in *2016 50th Asilomar Conference on Signals, Systems and Computers*, 2016: IEEE, pp. 974-978.
[141] A. Alqahtani, "Rateless space-time block codes for 5g wireless communication systems," in *The Fifth Generation (5G) of Wireless Communication*, 2019, ch. Chapter 3.
[142] W. Zhang, S. Qiao, and Y. Wei, "Practical HKZ and minkowski lattice reduction algorithms," *Dept. Comput. Software, McMaster Univ., Hamilton, ON, Canada,* 2011.
[143] A. K. Lenstra, H. W. Lenstra, and L. Lovász, "Factoring polynomials with rational coefficients," *Mathematische annalen,* vol. 261, no. ARTICLE, pp. 515-534, 1982.
[144] L. Babai, "On Lovász'lattice reduction and the nearest lattice point problem," *Combinatorica,* vol. 6, pp. 1-13, 1986.
[145] E. Jorswieck and E. Björnson, "Optimal resource allocation in coordinated multi-cell systems," *Foundations and Trends® in Communications and Information Theory,* vol. 9, no. 2–3, pp. 113-381, 2013, doi: 10.1561/0100000069.
[146] F. M. Reza, *An introduction to information theory*. Courier Corporation, 1994.
[147] I. H. Ahmed and A. A. Abdulkafi, "Energy efficient operation for next generation massive mimo network," *Telecommunications and Radio Engineering,* vol. 83, no. 2, pp. 49-64, 2024, doi: 10.1615/TelecomRadEng.2023049046.

Nompumelelo Chili, Emmanuel Mukubwa and Nelendran Pillay, "Performance comparison of Linear and Nonlinear Precoding for massive MIMO." 3rd International Conference on Electrical, Computer and Energy Technologies (ICECET2023), November 16-17, 2023, Cape Town, South Africa. DOI: 10.1109/ICECET58911.2023.1038932

APPENDICES

APPENDIX A ALGORITHM 1

Algorithm 1 The Lenstra-Lenstra and Lovász algorithm

1. **Input:** B, δ
2. **Output:** LLL reduced basis**,** $\boldsymbol{T}$
3. Compute $\boldsymbol{B}^*$and ∪ with the Gram-Schmidt algorithm
4. $\mathbf{T} = \mathrm{I}_m$, $\mathrm{k} = 2$
5. **while** $\mathrm{k} \leq m$ **do**
6. *SIZEREDUCTION(k, k - 1)*
7. **if** $\|\mathrm{b}_k^*\|^2 < (\delta - \mu_{k,k-1}^2)\|\mathrm{b}_{k-1}^*\|^2$ **then**
8. SWAP(k)
9. K= max(2, *k -1*)
10. **else**
11. **for** $l = k - 2 \longrightarrow 1$ **do**
12. $SIZEREDUCTION(k, I)$
13. **end for**
14. *k=k+1*
15. **end if**
16. **end while**
17. **procedure** $SIZEREDUCTION(k, I)$
18. **if** $\left|\mu_{k,l}\right| > \frac{1}{2}$ **then**
19. $\mu = \left|\mu_{k,l}\right|, b_k = b_{k-\mu}.b_l, t_k = t_k - \mu t_l, \mu_{k,l} = \mu_{k,l} - \mu$
20. **for** $j = 1 \rightarrow l - 1$ **do**
21. $\mu_{k,j} = \mu_{k,j} - \mu.\mu_{l,j}$
22. **end for**
23. **end if**
24. **end procedure**
25. **Procedure** $SWAP(k)$
26. $SWAP$ b_k with b_{k-1}
27. $SWAP$ t_k with t_{k-1}
28. **for** $j = 1 \rightarrow k - 2$ **do**

29. $SWAP\ \ \mu_{k,j}$ with $\mu_{k-1,j}$

30. **end for**

31. $b_{k-1}^{*'} = b_k^* + \mu_{k,k-1} b_{k-1}^*$

32. $\mu_{k,k-1}^{'} = \left(b_{k-1}^* b_{k-1}^{*'}\right) \Big/ \left\| b_{k-1}^{*'} \right\|^2$

33. $b_k^{*'} = b_{k-1}^* - \mu_{k,k-1}^{'} b_{k-1}^{*'}$

34. **for** $i = k+1 \rightarrow m$ **do**

35. $\mu'_{i,k-1} = \mu_{i,k-1}.\mu'_{k,k-1} + \mu_{i,k}.\|b_k^*\|^2 / \|b_{k-1}^{*\prime}\|^2$

36. $\mu'_{i,k} = \mu_{i,k-1}.-\mu'_{i,k}.\mu_{k,k-1}$

37. $\mu_{i,k} = \mu_{i,k}^{'}, \mu_{i,k-1} = \mu_{i,k-1}^{'}$

38. **end for**

39. $b_{k-1}^* = b_{k-1}^{*'}, \quad b_k^* = b_k^{*'}, \quad \mu_{k,k-1} = \mu_{k,k-1}^{'}$

40. end procedure

APPENDIX B MATLAB CODE FOR ZF,MMSE,NSA AND LR-LLL

```
function simpleMIMOsimulation(var)
% -- set up default/custom parameters

  if isempty(var)

    disp('using default simulation settings and parameters...')

    % set default simulation parameters
    par.simName = 'ERR_4x4_16QAM'; % simulation name (used for saving results)
    par.runId = 0; % simulation ID (used to reproduce results)
    par.MR = 16; % receive antennas
    par.MT = 16; % transmit antennas (set not larger than MR!)
    par.mod = '16QAM'; % modulation type: 'BPSK','QPSK','16QAM','64QAM'
    par.trials = 10000; % number of Monte-Carlo trials (transmissions)
    par.SNRdB_list = 0:2:40; % list of SNR [dB] values to be simulated
    par.detector = {'ZF','NSA','MMSE','LLL_ZF'}; % define detector(s) to be
simulated
    % algorithm specific
    par.alg.maxiter = 3;

  else
    disp('use custom simulation settings and parameters...')
    par = varargin{1}; % only argument is par structure

  end
  % -- initialization

  % use runId random seed (enables reproducibility)
  rng(par.runId);
  % set up Gray-mapped constellation alphabet (according to IEEE 802.11)
  switch (par.mod)
    case 'BPSK'
      par.symbols = [ -1 1 ];
    case 'QPSK'
      par.symbols = [ -1-1i,-1+1i, ...
                      +1-1i,+1+1i ];
    case '16QAM'
      par.symbols = [ -3-3i,-3-1i,-3+3i,-3+1i, ...
                      -1-3i,-1-1i,-1+3i,-1+1i, ...
                      +3-3i,+3-1i,+3+3i,+3+1i, ...
                      +1-3i,+1-1i,+1+3i,+1+1i ];
    case '64QAM'
      par.symbols = [ -7-7i,-7-5i,-7-1i,-7-3i,-7+7i,-7+5i,-7+1i,-7+3i, ...
                      -5-7i,-5-5i,-5-1i,-5-3i,-5+7i,-5+5i,-5+1i,-5+3i, ...
                      -1-7i,-1-5i,-1-1i,-1-3i,-1+7i,-1+5i,-1+1i,-1+3i, ...
                      -3-7i,-3-5i,-3-1i,-3-3i,-3+7i,-3+5i,-3+1i,-3+3i, ...
                      +7-7i,+7-5i,+7-1i,+7-3i,+7+7i,+7+5i,+7+1i,+7+3i, ...
                      +5-7i,+5-5i,+5-1i,+5-3i,+5+7i,+5+5i,+5+1i,+5+3i, ...
                      +1-7i,+1-5i,+1-1i,+1-3i,+1+7i,+1+5i,+1+1i,+1+3i, ...
                      +3-7i,+3-5i,+3-1i,+3-3i,+3+7i,+3+5i,+3+1i,+3+3i ];

  end
```

```
 % -- start simulation

  % initialize result arrays (detector x SNR)
  res.BER = zeros(length(par.detector),length(par.SNRdB_list)); % bit error rate

  % generate random bit stream (antenna x bit x trial)
  bits = randi([0 1],par.MT,par.Q,par.trials);
  % trials loop
  tic
  for t=1:par.trials

    % generate transmit symbol
    idx = bi2de(bits(:,:,t),'left-msb')+1;
    s = par.symbols(idx).';
    s_real = [real(s);imag(s)]; % converting s from complex to real.
    % generate iid Gaussian channel matrix & noise vector
    n = sqrt(0.5)*(randn(par.MR,1)+1i*randn(par.MR,1));
    n_real = [real(n);imag(n)]; % converting n from complex to real.

    H = sqrt(0.5)*(randn(par.MR,par.MT)+1i*randn(par.MR,par.MT));
    H_real = [real(H),-imag(H);imag(H),real(H)];  % converting H from complex to
real.

    % Calculations needed for lattice reduction
    T = LLL(H_real,par.MT);
    s_LR = inv(T)*s_real;
    H_LR = H_real*T;

    % Fixed LLL
    T_fixed = MLLL(H,par.MT);
    s_fixed = inv(T_fixed)*s;
    H_fixed = H*T_fixed;

    % transmit over noiseless channel (will be used later)
    x = H*s;
    x_real = [real(x);imag(x)];
    x_LR = H_LR*s_LR;
    x_fixed = H_fixed*s_fixed;

    % SNR loop
    for k=1:length(par.SNRdB_list)

      % compute noise variance (average SNR per receive antenna is: SNR=MT*Es/N0)
      N0 = par.MT*par.Es*10^(-par.SNRdB_list(k)/10);

      % transmit data over noisy channel
      y = x+sqrt(N0)*n;
      y_real = x_real + sqrt(N0)*n_real;
      y_LR = x_LR + sqrt(N0)*n_real;

      y_fixed = x_fixed + sqrt(N0)*n;

      % algorithm loop
      for d=1:length(par.detector)

        switch (par.detector{d}) % select algorithms
```

```
            case 'ZF' % zero-forcing detection
                 [idxhat,bithat] = ZF(par,H,y,x,n);
            case 'MMSE' % zero-forcing detection
            [idxhat,bithat] = MMSE(par,H,y,N0);
          case 'LLL_ZF' % zero-forcing detection
            [idxhat,bithat] = LLL_ZF(par,H_LR,y_LR,T);
            case 'NSA' % Neumann-Series Application
             [idxhat,bithat] = Neumann(par,H,y,N0);
%             case 'THP'% Tomlinson-Harashima Precoding
%               G_thp =Precoder_Thomlinson_Harashima();
            otherwise
            error('par.detector type not defined.')
        end
        % -- compute error metrics
        err = (idx~=idxhat);
        res.BER(d,k)               =               res.BER(d,k)               +
sum(sum(bits(:,:,t)~=bithat))/(par.MT*par.Q);

      end % algorithm loop

    end % SNR loop

    % keep track of simulation time
    if toc>10
      time=toc;
      time_elapsed = time_elapsed + time;
      fprintf('estimated      remaining      simulation      time:      %3.0f
min.\n',time_elapsed*(par.trials/t-1)/60);
      tic
    end

  end % trials looP

  % normalize results
  res.BER = res.BER/par.trials;
  res.time_elapsed = time_elapsed;

  % -- save final results (par and res structure)

  save([ par.simName '_' num2str(par.runId) ],'par','res');

  %% -- show results (generates  Matlab plot)

  marker_style = {'bo-','rs--','mv-.','kp:','g*-','c>--','yx:'};
  figure(1)
  for d=1:length(par.detector)
    if d==1

      semilogy(par.SNRdB_list,res.BER(d,:),marker_style{d},'LineWidth',2)
%       semilogy(SNR,BER,'-o');
      hold on
    else
      disp(res.BER(d,:));
      semilogy(par.SNRdB_list,res.BER(d,:),marker_style{d},'LineWidth',2)
%        semilogy(SNR,BER,'-o');
    end
%     semilogy(SNR,BER','-o')
```

```
  end
  hold off
  grid on
  xlabel('average SNR per receive antenna [dB]','FontSize',12)
  ylabel('bit error rate (BER)','FontSize',12)
  axis([min(par.SNRdB_list) max(par.SNRdB_list) 1e-4 1])
  legend(par.detector,'FontSize',12)
  set(gca,'FontSize',12)

end

% -- set of detector functions
%% zero-forcing (ZF) detector
 function [idxhat,bithat] = ZF(par,H,y,x,n)
 xhat = H\y;     inv(H)*y;
   xhat = pinv(H)*y;
   [~,idxhat]            =            min(abs(xhat*ones(1,length(par.symbols))-
ones(par.MT,1)*par.symbols).^2,[],2);
  bithat = par.bits(idxhat,:);
 end

%% MMSE detector (MMSE)
function [idxhat,bithat] = MMSE(par,H,y,N0)
xhat = (H'*H+(N0/par.Es)*eye(par.MT))\(H'*y);
[~,idxhat]              =              min(abs(xhat*ones(1,length(par.symbols))-
ones(par.MT,1)*par.symbols).^2,[],2);
bithat = par.bits(idxhat,:);
end

%% lattice reduced zero-forcing (LR_ZF) detector
function [idxhat,bithat] = LLL_ZF(par,H_LR,y_LR,T)
  xhat_real = H_LR\y_LR; % inv(H)*y
  xhat_quan = MyQuan_LR(xhat_real,2*par.MT,T,length(par.symbols));
  xhat =  xhat_quan(1:par.MT,:)+1i*xhat_quan((par.MT+1):2*par.MT,:);
  [~,idxhat]              =              min(abs(xhat*ones(1,length(par.symbols))-
ones(par.MT,1)*par.symbols).^2,[],2);
  bithat = par.bits(idxhat,:);
end

%% Neumann-Series Approximation based massive MIMO detection
function [idxhat,bithat] = NSA(par,H,y,N0)
A = H'*H+(N0/par.Es)*eye(par.MT);
MF = H'*y;
D = diag(diag(A));
E = triu(A,1)+tril(A,-1);
Ainv = 0;
for i = 0:par.alg.maxiter
    Ainv = Ainv+((-inv(D)*E)^i)*inv(D);
end
xhat = Ainv*MF;
[~,idxhat]              =              min(abs(xhat*ones(1,length(par.symbols))-
ones(par.MT,1)*par.symbols).^2,[],2);
bithat = par.bits(idxhat,:);
end
```

APPENDIX C THP PSEUDO CODE

```
EbNo← [0:4:20]
for all (i) do
   SNR← EbNo(i)
    std← 10^(-SNR/20)
    Generate infor bit 0 or 1 randomly for each BS
    do modulation for the data bits transmitted by each BS(16 QAM AND 64 QAM)
to     generate x
    Generate channel matrix H using Rayleigh distribution
   Using LQ decomposition of H, Find L and Q matrices
   Find S and inv(S)
   Multiply L with inv  (s) to get B matrix values
   Find transmitted signal x1 by solving the equation :mod(x-(B-1)*x1)=x1 where
mod implies modulo operation for the signal from each BS
   Pre-multiply  the signal x1 with Q*
   Find the received signal whose value is H*Q**x1 and noise added to it
   Pre-multiply the received signal with inv (S)
   do modulo operation for the received signal for each UE
   do demodulation
   Calculate BER for each iteration
End for
```